Dahlin, David Clyde

MECHANISMS OF OXIDATION OF ACETAMINOPHEN

University of Washington PH.D. 1984

MECHANISMS OF OXIDATION OF ACETAMINOPHEN

by

David Clyde Dahlin

A dissertation submitted in partial fulfillment
of the requirements for the degree of

Doctor of Philosophy

University of Washington

1984

Approved by Sidney D. Nelson
(Chairperson of Supervisory Committee)

Program Authorized
to Offer Degree Department of Medicinal Chemistry

Date December 19, 1983

Doctoral Dissertation

In presenting this dissertation in partial fulfillment of the requirements of the Doctoral degree at the University of Washington, I agree that the Library shall make its copies freely available for inspection. I further agree that extensive copying of this dissertation is allowable only for scholarly purposes, consistent with "fair use" as prescribed in the U.S. Copyright Law. Request for copying or reproduction of this dissertation may be referred to University Microfilms, 300 North Zeeb Road, Ann Arbor, Michigan 48106, to whom the author has granted "the right to reproduce and sell (a) copies of the manuscript in microform and/or (b) printed copies of the manuscript made from microform.

Signature 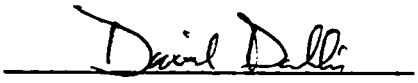

Date December 19, 1983

TABLE OF CONTENTS

LIST OF FIGURES

LIST OF TABLES

ACKNOWLEDGEMENTS

I would like to express my deepest gratitude to the people who have contributed to this effort.

Special thanks are due to Dr. Sidney D. Nelson, an exceptional scientist, teacher, and individual. And, to my much loved wife Sherry, who has shared in both the excitments and the frustrations of these several years, responding only with patience and understanding.

My parents, Clyde and Jean Dahlin, have been most important in the achievement of this goal, not only for providing encouragement, love, and a warm home, but also for financial support through a decade of college. The same appreciation is felt toward my wife's parents, Bob and Jeannine Bowles, who are like my own.

The following have aided in this project either through their expertise or their friendship: Dr. Michael Bartels, Dr. Thomas Baillie, Mr. Patrick Bednarski, Dr. Jim Christie, Dr. Gary Elmer, Mr. Todd Fast, Dr. Anthony Forte, Dr. Perry Gordon, Mr. Brad Greenway, Dr. Peter Harvison, Mr. William Howald, Dr. Lokanathan Iyer, Dr. Edward Krupski, Mr. James Omichinski, Mr. David Porubek, Dr. Rory Remmel, Dr. John Slattery, Dr. Anthony Streeter, Dr. William Trager, Mr. John Wilson, and Dr. Cheryl Zimmerman.

Important to my early college education was Dr. Eugene Schermer, who through his talent as an educator sparked my interest in chemistry.

Special thanks go to Mrs. Margret Kramer and Mr. Jay Craver for their essential help in the preparation of this manuscript.

And last but most, I want to acknowledge our Lord Jesus Christ for His guidance throughout this project and this life.

Dedicated to

Sherry and Katie

CHAPTER I

INTRODUCTION

Understanding the effects of xenobiotics (i.e. drugs, toxins, environmental contaminants) on biological systems has been a priority of medical researchers for a considerable time, indeed centuries. Clearly such knowledge is invaluable in the judicious use of therapeutic agents and in the enlightened administration of curative measures in cases of drug and chemical toxicity. More recently, the antithetical relationship, the effect of biological systems on xenobiotics, has been recognized as a significant determinant in the pharmacology and toxicology of drugs and other foreign compounds. Hence, investigations in the fields of medicinal chemistry, pharmacokinetics, toxicology, and pharmacology have yielded a wealth of information on the metabolic fate of biologically relevant compounds that has been useful to both clinicians and researchers.

The body's biochemical and physiological handling of xenobiotics does much to determine the efficacy of a given drug or the outcome of exposure to an undesirable chemical. Most compounds that enter the body are converted to chemically stable metabolites that are generally more polar and readily excreted into the urine or bile, or are expired. In the case of therapeutic agents, the rate, the chemical nature, and even the site of such molecular alterations influences the amount of drug reaching the target organs and tissues. This is commonly viewed as a protective mechanism and as such is exemplified in the metabolism of

harmful foreign compounds, allowing the removal of often nonpolar molecules that would otherwise be difficult to eliminate.

However, as a result of metabolism and toxicity studies in recent years it has been realized that the same enzyme systems which normally provide protection from foreign compounds can generate potent alkylating and arylating agents, a process that has been termed metabolic activation. It has been demonstrated in man and experimental animals that such reactive metabolites are capable of eliciting serious lesions including hepatic, renal and pulmonary necrosis, cancer, bonemarrow aplasia, and numerous other deleterious effects. For example, a number of chemically inert polycyclic aromatic hydrocarbons, such as benzo(a)pyrene, are enzymatically converted to reactive and mutagenic diol epoxides.[1,2,3] The anticancer agent adriamycin is reduced in the cell to a transitory semiquinone radical. This radical, through a recycling process with molecular oxygen, is thought to be responsible for superoxide and hydroxyl radical generation[4,5,6] resulting in an observed cardiac toxicity.[7] These are distinct from adverse drug reactions due to an excessive therapeutic effect or an untoward secondary effect caused by the parent compound or a stable metabolite.[8] Such toxic reactions can usually be correlated to drug or metabolite levels in the body. Highly reactive products of metabolic activation, on the other hand, may exist for seconds or less, and thus relationships between metabolite levels and tissue lesions can rarely be established.

Another example of a compound that can elicite this type of toxicity is the drug acetaminophen. Investigations of the mechanism of

its metabolic activation and the identification of a potent arylating product of its biological oxidation comprise much of this thesis.

Three p-aminophenol derivatives, acetaminophen, phenacetin, and acetanilide, were introduced into clinical use during the late nineteenth century.[9] All possessed analgesic-antipyretic properties similar to aspirin, and were used principally for the reduction of fever.[10] It was not long after this that clinicians realized acetanilide was too toxic for human administration, and phenacetin became the most widely used of the three derivatives.[11] But, it has more recently become apparent that interstitial nephritis and possibly renal pelvic tumors are associated with phenacetin abuse,[12,13,14] and prudently the compound has been removed from drug formulations. Therefore, of the three p-aminophenols acetaminophen is the only agent currently in use.

At therapeutic doses acetaminophen is a safe drug, devoid of appreciable side effects.[10] It possesses analgesic and antipyretic activities almost identical to aspirin yet does not have the gastrointestinal and hemorrhagic side effects of the salicylates. But unlike aspirin, it has little antiinflammatory activity and is therefore ineffective as an antirheumatic. In addition to it use as one of the more popular over-the-counter analgesics, acetaminophen is also present in over two hundred formulations for the relief of headaches, coughs, and colds.[11]

The first evidence that acetaminophen may be toxic came in 1966 when Boyd and Bereczky[15] observed acetaminophen-induced hepatic lesions in the rat. Later that same year the first report of acetaminophen-

related deaths in man appeared when Davidson and Eastham[16] described the demise of two patients in a Scottish mental institution who had taken massive doses of the drug. Extensive media coverage of this unfortunate event was considered[17] partially responsible for a dramatic rise in acetaminophen overdose cases reported in the United Kingdom during the ensuing years.[18-24] With "near epidemic proportions" acetaminophen had gained acceptance as a major method of suicide.[11] Fortunately, the frequency of acetaminophen overdose in the United States has not reached this magnitude.[25] However, some American clinicians have noted an increase in such cases,[11] and there have been growing numbers of reports in U.S. medical journals.[26-30] Whether or not this indicates an upward trend is not known, but it does serve to emphasize the importance of our mechanistic understanding of the events leading to acetaminophen overdose toxicity.

The most common cause of death in acetaminophen overdose is liver failure.[11] This is typically marked by fulminant hepatic necrosis in the centrilobular areas, but damage may extend toward the midzonal and periportal regions.[16] Examination of liver sections usually reveals eosinophilic degeneration of the cells and pyknosis of the nuclear material. Kidney tubule necrosis has also been observed in acetaminophen overdose, and while acute renal failure has occasionally been the primary cause of death, in clinical importance it is usually secondary to liver injury.[11,31,32]

The clinical course of acetaminophen overdose toxicity follows a consistent pattern.[31] Two to three hours after ingestion of a toxic dose (estimated 10-15 gm in humans)[33] the patient experiences nausea

and vomitting and may be moderately obtunded. This is followed by abdominal pain in the upper right quadrant. Within the first 24 hours after overdose these symptoms may subside and the patient appear to be fully recovered.[11] However, if the dose was sufficient to produce liver damage it becomes biochemically apparent within 48-72 hours.[23] Like other forms of necroinflammatory liver disease, acetaminophen-induced hepatotoxicity is evidenced by pronounced elevation in serum concentrations of alanine transaminase (GPT), aspartate transaminase (GOT), hydroxybutyrate dehydrogenase (HBD), and lactate dehydrogenase (LDH). Also observed are mild hyperbilirubenemia, prolonged clotting time, and lowered glucose and bicarbonate blood levels.

Following the initial reports of acetaminophen-induced liver damage in rats, toxicity studies were done in several other species. Whereas rats are not particularily disposed toward acetaminophen hepatotoxicity, mice and hamsters are more susceptible. A dose of 300 mg/kg in hamsters produced a 90% incidence of necrosis[34] while in mice 500 mg/kg yielded a 75% incidence.[35] This is contrasted to rats where necrosis was produced in only 2% of the animals administered 1000 mg/kg.[35] Importantly, acetaminophen was shown to cause a fulminant hepatic necrosis in mice, hamsters, and rats similar to that observed in man, thus providing acceptable animal models.[34]

Subsequent investigations of the pathogenesis of acetaminophen-induced liver injury provided a link between liver necrosis and liver metabolism of the drug. The metabolically derived toxicity of acetaminophen proved to be similar to that seen with other compounds previously studied. For example, Brodie et al.[36] determined

through radiolabel studies that a metabolite of the hepatotoxin bromobenzene bound irreversibly to cellular proteins. Pretreatment with the cytochrome P-450 inducer phenobarbital potentiated the observed liver necrosis, and this correlated well with an increase in protein binding of the metabolite. As with bromobenzene, acetaminophen-induced hepatic necrosis was found by Jollow et al.[37] to be accompanied by covalent binding of metabolite to liver proteins. Pretreatment with phenobarbital increased both binding and necrosis in a parallel manner. Additionally, both were dramatically reduced by pretreatment with the cytochrome P-450 inhibitor piperonyl butoxide. In the same study the cellular localization of the irreversibly bound metabolite was ascertained by autoradiography of mouse liver sections after a toxic dose of radiolabeled acetaminophen. While protein-bound radiolabel was present throughout the liver, it was most evident in the necrotic centrilobular region, the area containing the highest levels of cytochrome P-450. Again, both necrosis and autoradiographically determined binding increased with phenobarbital pretreatment and decreased with the preadministration of piperonyl butoxide. These experiments led investigators to believe the hepatotoxicity associated with large doses of acetaminophen may arise from cytochrome P-450 metabolism of the drug to a reactive species that binds to cellular proteins.

Verification of this came with the determination that reactive metabolite formation could be monitored *in vitro* by measuring radiolabeled metabolite binding to liver microsomal protein.[38] Since omission of NADPH or replacement of air with carbon monoxide reduced

covalent binding, it was concluded that formation of the reactive metabolite was a cytochrome P-450 mixed function oxidase-catalyzed process. Furthermore, the pretreatments previously used *in vivo* were effective in microsomes. Hence, treatment of hamsters with 3-methylcholanthrene, another inducer of cytochrome P-450, increased covalent binding and necrosis *in vivo*,[34] and raised the V_{max} for covalent binding *in vitro*.[34,39] Cytochrome P-450 inhibition by piperonyl butoxide pretreatment was reflected in reduced necrosis and protein binding *in vivo*[34] as well as a decrease in microsomal protein binding.[38] A similar relationship was seen in mice[37,38] and rats[38] both *in vivo* and *in vitro* with phenobarbital.[35]

The thiol-containing tripeptide glutathione(γ-L-glutamyl-L-cysteinylglycine) was determined to play a major role in the *in vivo* detoxification of the acetaminophen arylating metabolite. At nontoxic doses in mice[35] and hamsters[34] covalent protein binding of a radiolabeled acetaminophen metabolite did not occur, and hepatic glutathione levels were only marginally lowered. In contrast, covalent binding of radiolabel was observed with toxic doses of acetaminophen, and liver glutathione was diminished as much as 90%. Time course experiments in mice established that metabolite protein binding was not significant until approximately 80% of the hepatic glutathione had been depleted, and that lowering of the endogenous glutathione stores by diethylmaleate pretreatment markedly potentiated both binding and necrosis.[40] The addition of glutathione or cysteine to microsomal incubations of acetaminophen blocked *in vitro* protein binding with concomitant formation of the corresponding 3-S-glutathionyl or 3-S-cysteinyl

acetaminophen conjugates, indicating protection was mediated through thiol-scavenging of an electrophilic species. These conjugates observed *in vitro* had also been detected as metabolites *in vivo*. 3-S-Cysteinyl acetaminophen[42,43] and 3-S-(N-acetyl)cysteinyl acetaminophen[44] (mercapturic acid conjugate) were confirmed to be urinary metabolites, metabolically derived from 3-S-glutathionyl acetaminophen. And more recently, the glutathione conjugate of acetaminophen has been identified in the bile.[45] A more direct correlation *in vivo* between the thiol conjugates and detoxification of the arylating acetaminophen metabolite was made by Jollow et al.[46] who monitored urinary levels of the mercapturic acid conjugate in the hamster after toxic and nontoxic doses of acetaminophen. At a nontoxic dose of 25 mg/kg the acetaminophen mercapturate comprised 14% of the dose in unpretreated animals, and after 3-methylcholanthrene pretreatment this was elevated to 26% of the dose. With 500 mg/kg an increase in the amount of the mercapuric acid conjugate was seen, but this equalled only 6 to 7% of the dose in both 3-methylcholanthrene-pretreated and control animals. This percentage decrease in thiol conjugate with increasing acetaminophen dose paralleled the diminuation of hepatic glutathione previously observed with administration of larger amounts of the drug.[34,35,40]

All of the observations discussed above, i.e. necrosis and covalent binding potentiation with P-450 inducers and diethylmaleate pretreatment, decreased tissue injury and protein binding with P-450 inhibitors, and altered glutathione levels and thiol metabolite disposition with toxic and nontoxic doses, strongly implicated the role

of metabolic activation in the toxicity of acetaminophen. Many subsequent studies have been aimed at determining the structure of the toxic acetaminophen metabolite. Initially, it was proposed by Mitchell and co-workers[46-48] that acetaminophen was oxidized to N-hydroxyacetaminophen which would then dehydrate to the ultimate toxin, N-acetyl-p-benzoquinone imine (NAPQI), as shown in Figure 1.1. This postulate was based on several lines of indirect evidence. Specifically, a number of compounds structurally related to acetaminophen underwent cytochrome P-450-dependent N-hydroxylation, including acetanilide,[49] p-chloroacetanilide,[50] phenacetin,[51] and 2-acetylaminofluorine.[52] In addition, it was determined through induction and inhibition studies that acetaminophen is metabolized by the same cytochrome P-450 isozymes that N-hydroxylate p-chloroacetanilide[50] and phenacetin.[51] Thus, a logical correlation was made between the N-hydroxylation of these aromatic acetamides and acetaminophen metabolic activation.

While the N-hydroxylation proposal appeared to satisfy a number of criteria established through various studies of the arylating intermediate, more recent evidence has been produced which contradicts the role of N-hydroxyacetaminophen in acetaminophen toxicity. Significantly, N-hydroxyacetaminophen was found to have a much longer half life at physiological pH than anticipated from experimental observations,[53,54] and the compound was only slightly more toxic than acetaminophen, further detracting from its proposed role. More direct evidence was provided by colorometric assays[55] and carrier pool trapping experiments[56] (work contained in this dissertation) which demonstrated that N-hydroxyacetaminophen was not formed in microsomal

FIGURE 1.1: N-HYDROXYLATION MECHANISM FOR THE METABOLIC ACTIVATION OF ACETAMINOPHEN.

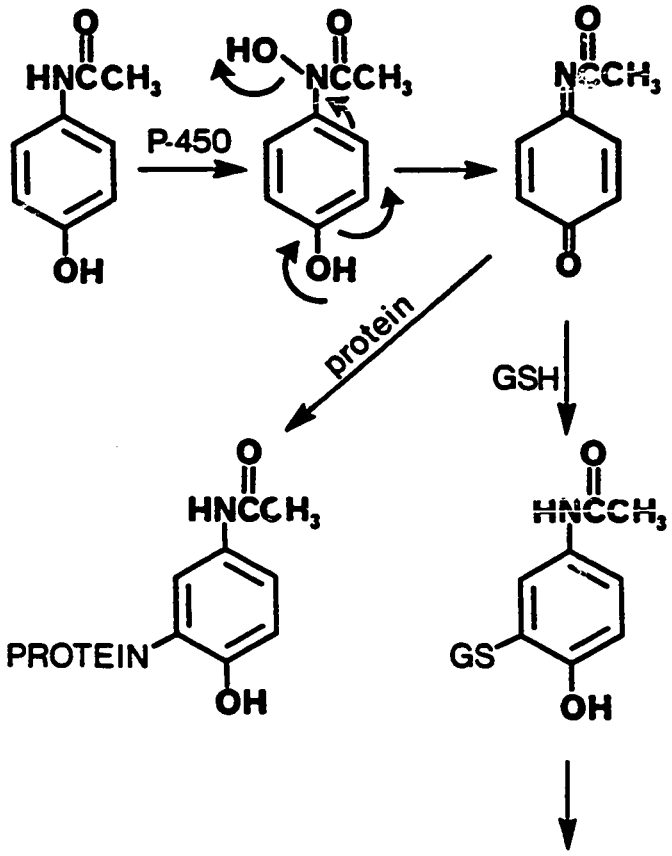

CYSTEINE, MERCAPTURIC ACID,

AND GLUTATHIONE CONJUGATES

incubations of acetaminophen to concentrations well below those required to account for the observed protein binding.

Although N-hydroxyacetaminophen is apparently not a metabolite of acetaminophen *in vivo*, NAPQI has characteristics that implicate it as the reactive species. Mulder et al.[57] provided evidence that synthetic N-hydroxyacetaminophen decomposed to NAPQI, and that the product quinone imine bound to proteins as well as conjugated with glutathione. Miner and Kissinger[58] were able to generate NAPQI electrochemically in buffer while Blair et al.[59,60] obtained stable benzene solutions of the purported intermediate by chemical means. Both groups demonstrated the formation of 3-S-glutathionylacetaminophen from NAPQI in the presence of glutathione. The synthesis and isolation of pure crystalline NAPQI was accomplished by Dahlin and Nelson[61] (work contained in this dissertation). These studies resulted in the direct detection of NAPQI as a product of acetaminophen oxidation in cumene hydroperoxide-supported incubations of purified cytochrome P-450. Additionally, evidence in the form of metabolite partitioning was provided for NAPQI formation from acetaminophen in microsomal incubations with an added cofactor regenerating system.[62] Thus, evidence accumulated from a number of laboratories indicates strongly that NAPQI is the metabolite responsible for acetaminophen protein binding and hepatotoxicity in overdose.

A schematic summary of current understanding of acetaminophen metabolism is presented in Figure 1.2. At therapeutic doses the drug undergoes phase II conjugation with glucuronic acid and sulfate. These two routes combined account for 60-80% of the dose in mammals, and

FIGURE 1.2: BIOTRANSFORMATION OF ACETAMINOPHEN.

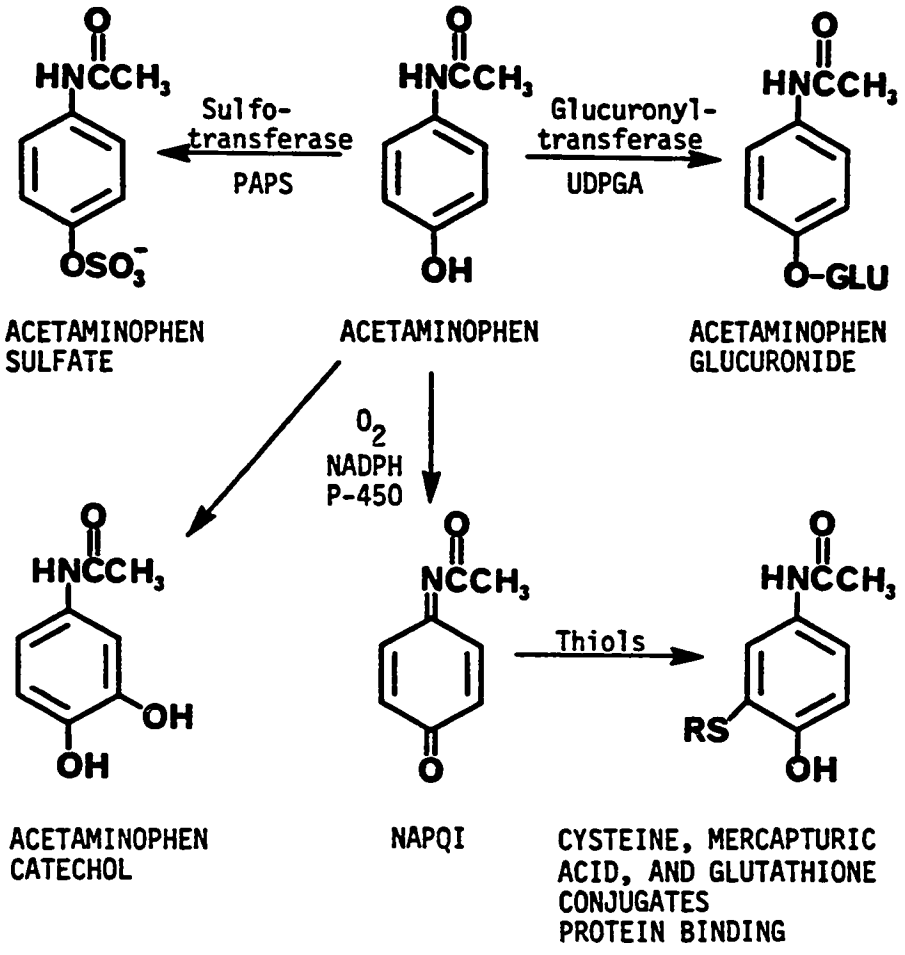
HNCCH3
O
Sulfo-
transferase
PAPS
Glucuronyl-
transferase
UDPGA
OSO3-
OH
O-GLU
ACETAMINOPHEN
SULFATE
ACETAMINOPHEN
ACETAMINOPHEN
GLUCURONIDE
O2
NADPH
P-450
NCCH3
Thiols
RS
ACETAMINOPHEN
CATECHOL
NAPQI
CYSTEINE, MERCAPTURIC
ACID, AND GLUTATHIONE
CONJUGATES
PROTEIN BINDING

approximately 80% in man.[63] A small percentage of the drug is excreted unchanged, and the balance is routed through oxidative pathways catalyzed by cytochrome P-450 yielding NAPQI and minor amounts of 3,4-dihydroxyacetanilide (acetaminophen catechol). The quinone imine is conjugated by glutathione and excreted in the bile (minor),[45] or further metabolized to the urinary 3-S-cysteinyl[42,43] and 3-S-mercapturic acid[44] conjugates, as well as small amounts of 3-methylthioacetaminophen. In overdose the phase II conjugations are saturated routing more drug through the oxidative pathways. Liver glutathione levels are depleted by the increased NAPQI production, and the excess quinone imine binds to tissue proteins and elicites cell injury.

Studies contained in this thesis have concentrated on the oxidative route responsible for production of the hepatotoxic arylating metabolite. In light of the previously discussed indications that N-hydroxylation was inconsistent with experimental observations, sensitive carrier pool trapping methods were utilized to provide strong evidence that N-hydroxyacetaminophen was not a product of acetaminophen metabolism _in vitro_.[56] These studies contributed to the rejection of the N-hydroxylation proposal and are the subject of Chapter II.

One of the more feasible alternatives to the intermediacy of N-hydroxyacetaminophen was one-electron oxidation of acetaminophen by cytochrome P-450 with subsequent release of the semiquinone imine radical from the enzyme-product complex. The radical could of itself be toxic, or alternatively undergo a disproportionation yielding acetaminophen and NAPQI. Experiments presented in Chapter III using horseradish peroxidase demonstrated that enzymatic production of the

acetaminophen radical resulted in protein binding with inhibition characteristics very similar to those observed in microsomal incubations of acetaminophen.[67]

The most extensive studies in this work are the subject of Chapter IV, and concern identification and characterization of the acetaminophen arylating metabolite. The key to these studies came with the synthesis of pure crystalline NAPQI.[61] Possession of a synthetic standard allowed the development of HPLC assays providing direct evidence for the cytochrome P-450-catalyzed formation of NAPQI from acetaminophen.[62] In addition, the interactions of NAPQI with protein, glutathione, NADH, NADPH, and NADPH cytochrome P-450 reductase were investigated yielding information relevant to the toxicity and metabolism of the intermediate.[68-71]

CHAPTER II

DETERMINATION OF THE ROLE OF N-HYDROXYACETAMINOPHEN IN ACETAMINOPHEN METABOLIC ACTIVATION, IN VITRO.

A. INTRODUCTION

As discussed in Chapter I, the chemical structure of the hepatotoxic acetaminophen metabolite has been sought by many laboratories. From the early work of Mitchell and co-workers[46-48] it was proposed that metabolic activation may occur through N-oxidation by liver cytochrome P-450 to N-hydroxyacetaminophen, yielding upon loss of water the electrophile NAPQI (Figure 1.1). This was supported by compelling indirect evidence, and indeed for several years was considered the favored hypothesis.[49-52]

However, subsequent investigations did not substantiate the N-hydroxylation proposal. The key leading to its rejection came with the development of procedures for the difficult synthesis of N-hydroxyacetaminophen in the laboratories of Healy[53] and Gemborys.[54] Significantly, N-hydroxyacetaminophen was found to be only slightly more toxic than acetaminophen in mice.[53] Since formation of the reactive intermediate was considered a minor pathway, N-hydroxylation could not account for the amount of protein binding and liver damage observed. Further, it was determined that while N-hydroxyacetaminophen indeed underwent dehydration to NAPQI, the half life of this process was approximately 15 minutes at physiological pH. This relatively long

existence was confusing in light of earlier experiments by McMurtry et al.[72] who studied the effects of pretreatments on renal toxicity of acetaminophen in rats. These investigators determined that while 3-methylcholanthrene pretreatment markedly increased liver necrosis and metabolite binding at 250 mg/kg acetaminophen, no evidence of kidney damage was observable. At a higher dose of 750 mg/kg pretreatment actually reduced renal necrosis and covalent binding relative to nonpretreated controls, presumably by increasing liver metabolism of the drug and thereby limiting the bioavailability of acetaminophen to the kidneys. But, it was expected that an intermediate with the apparent moderate stability of N-hydroxyacetaminophen should migrate to the well-perfused kidneys, especially with induction of hepatic cytochrome P-450 isozymes that activate acetaminophen. And while liver formation of the reactive metabolite was confirmed by hepatic necrosis and protein binding, no such evidence for renal involvement was found. Thus, the chemical characteristics of synthetic N-hydroxyacetaminophen were not in agreement with experimental observations of the reactive intermediate. It should be noted that while this evidence for a short-lived intermediate was not conclusive, it was in accordance with the centrilobular localization of acetaminophen-induced liver damage and protein binding, the reactive intermediate apparently too unstable to migrate any significant distance within the organ of formation.

More direct evidence that N-hydroxyacetaminophen was not a metabolite of acetaminophen was produced by Hinson et al.[55] using an HPLC-UV assay for the ferric-complexed hydroxamic acid in microsomal incubations of acetaminophen. No N-hydroxyacetaminophen was detected as

a metabolite of acetaminophen. In the same study N-hydroxyacetaminophen was detected in microsomal incubations of N-hydroxyphenacetin, thus indicating that if it were formed from acetaminophen, release from the enzyme active site would probably occur. More importantly, the incubations of N-hydroxyphenacetin yielding N-hydroxyacetaminophen produced far less protein binding than incubations of acetaminophen, thereby providing kinetic evidence that the reactive metabolite of acetaminophen was not formed from N-hydroxyacetaminophen. However, the limits of ferric N-hydroxyacetaminophen complex detection in the HPLC-UV assay were difficult to verify. While the assay itself was sensitive enough to determine N-hydroxyacetaminophen in the nanomolar range, if formed at very low levels its presence within the detection limits could not be ensured over the course of the incubations.

Concurrent with Hinson's studies, this laboratory was using sensitive carrier-trapping experiments to determine whether N-hydroxyacetaminophen was a metabolite of acetaminophen *in vitro*. These are the subject of this chapter.

B. RESULTS

Synthesis of N-hydroxyacetaminophen

Initial attempts using the method of Healy et al.[53] for the synthesis of N-hydroxyacetaminophen (N,4'-dihydroxyacetanilide) utilizing acetyl protection of p-nitrophenol were unsuccessful. However, benzyl protection of the phenolic oxygen allowed preparation of small quantities of the hydroxamic acid.[73] As can be seen from the

scheme in Figure 2.1, benzyl chloride was used to produce the benzyl ether of p-nitrophenol. Reduction of the nitro group to the hydroxylamine was accomplished with zinc and ammonium chloride in water and was followed by acetylation with acetyl chloride yielding the benzyl-protected hydroxamic acid. The protecting group was removed by hydrogenolysis over 5% palladium on carbon giving a low yield (5%) of N-hydroxyacetaminophen possessing spectral characteristics (proton NMR, IR, EIMS) virtually identical to those reported by others.[53,54]

Carrier-Trapping Experiments

The results of experiments designed to determine the intermediacy of N-hydroxyacetaminophen *in vitro* are presented in Figure 2.2. Approximately 13 nmoles of radiolabel from incubations of ^{3}H-acetaminophen were covalently bound to microsomal proteins in 15 minutes (Figure 2.2A). The addition of 0.5 μmoles of synthetic N-hydroxyacetaminophen as an unlabeled carrier pool did not significantly effect the amount of measured binding. Radiolabel incorporation into the carrier pool, isolated as the ferric complex by HPLC, was approximately 10^{3}-fold less than covalent binding (Figure 2.2B). Furthermore, the use of controls omitting cofactor demonstrated that this small carrier pool incorporation was not above background and was non-NADPH dependent.

Confirmation of the Presence of N-Hydroxyacetaminophen in HPLC Eluates

Samples of the ferric chelate of the N-hydroxyacetaminophen carrier pool isolated by HPLC from microsomal incubations were added to

FIGURE 2.1: SYNTHESIS OF N-HYDROXYACETAMINOPHEN.

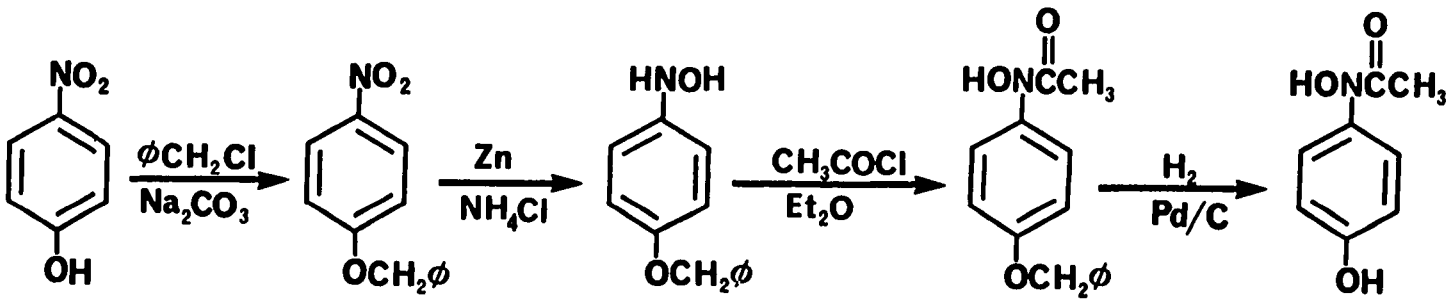
NO2
OH
φCH2Cl
Na2CO3
NO2
OCH2φ
Zn
NH4Cl
HNOH
OCH2φ
CH3COCl
Et2O
O
HONCCH3
OCH2φ
H2
Pd/C
O
HONCCH3
OH

FIGURE 2.2: TIME COURSE OF (A) THE IRREVERSIBLE BINDING OF RADIOLABEL FROM ^{3}H-ACETAMINOPHEN TO MICROSOMAL PROTEIN, AND (B) THE INCORPORATION OF RADIOLABEL INTO A CARRIER POOL OF N-HYDROXYACETAMINOPHEN.

● - ACETAMINOPHEN + N-HYDROXYACETAMINOPHEN + NADPH
o - ACETAMINOPHEN + N-HYDROXYACETAMINOPHEN - NADPH
■ - ACETAMINOPHEN - N-HYDROXYACETAMINOPHEN + NADPH
□ - ACETAMINOPHEN - N-HYDROXYACETAMINOPHEN - NADPH

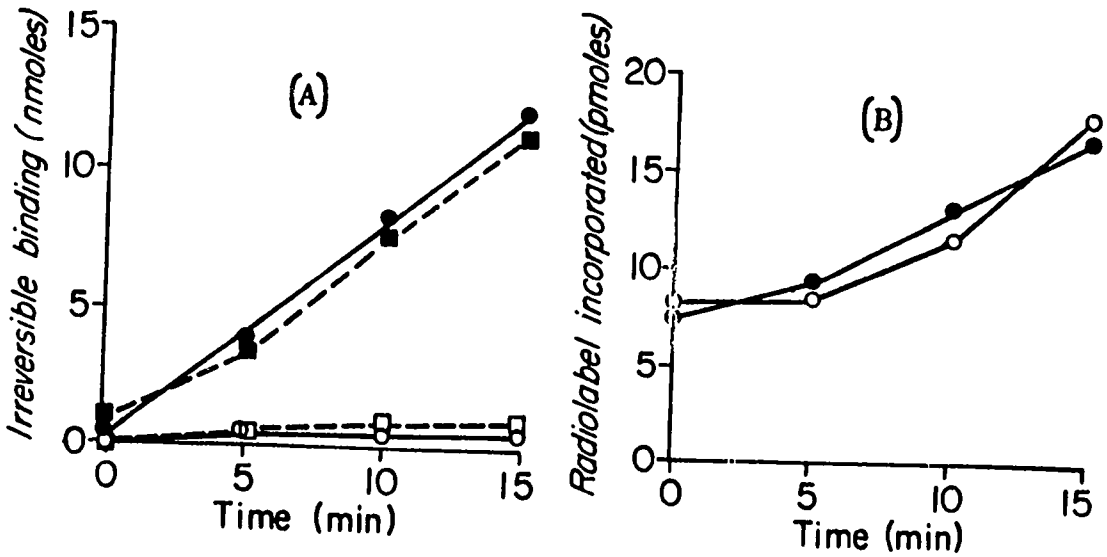
Irreversible binding (nmoles)
15
10
5
0
(A)
0
5
10
15
Time (min)
Radiolabel incorporated (pmoles)
20
15
10
5
0
(B)
0
5
10
15
Time (min)

solutions of EDTA. Chemical ionization mass spectrometry of ethyl acetate extractions of the uncomplexed hydroxamic acid produced spectra identical to authentic N-hydroxyacetaminophen (Figure 2.3).

C. DISCUSSION

The use of carrier-trapping techniques is common when measuring molecules that are unstable or at low concentrations. The addition of a carrier pool that is chemically identical to the determined compound yet isotopically distinguishable provides "protection" for the detected species, and thus enhances sensitivity and precision. The procedures used here were similar to those described by Jerina et al.[74] for determining the intermediacy of 1,2-naphthalene oxide in the microsomal oxidation of naphthalene to naphthol.

If N-hydroxyacetaminophen were produced in microsomal incubations of acetaminophen two observations should have been evident. First, radiolabel from the substrate would have been incorporated into the carrier pool, and second, the presence of the unlabeled carrier pool should have caused a decrease in levels of radiolabel covalently bound to microsomal proteins. Neither of these were observed. Therefore, under the conditions of these experiments N-hydroxyacetaminophen could only be formed as a metabolite of acetaminophen if it did not dissociate from the enzyme-product complex. Based on the findings of Hinson[55] that N-hydroxyphenacetin can be metabolized to detectable levels of N-hydroxyacetaminophen by microsomal oxygenases, a lack of dissociation of the acetaminophen-derived product from these enzymes is

FIGURE 2.3: (A) CHEMICAL IONIZATION MASS SPECTRUM OF SYNTHETIC N-HYDROXYACETAMINOPHEN, (B) CHEMICAL IONIZATION MASS SPECTRUM OF SYNTHETIC N-HYDROXYACETAMINOPHEN ISOLATED BY HPLC FROM INCUBATIONS OF MOUSE LIVER MICROSOMES AFTER A 15 MINUTE INCUBATION PERIOD.

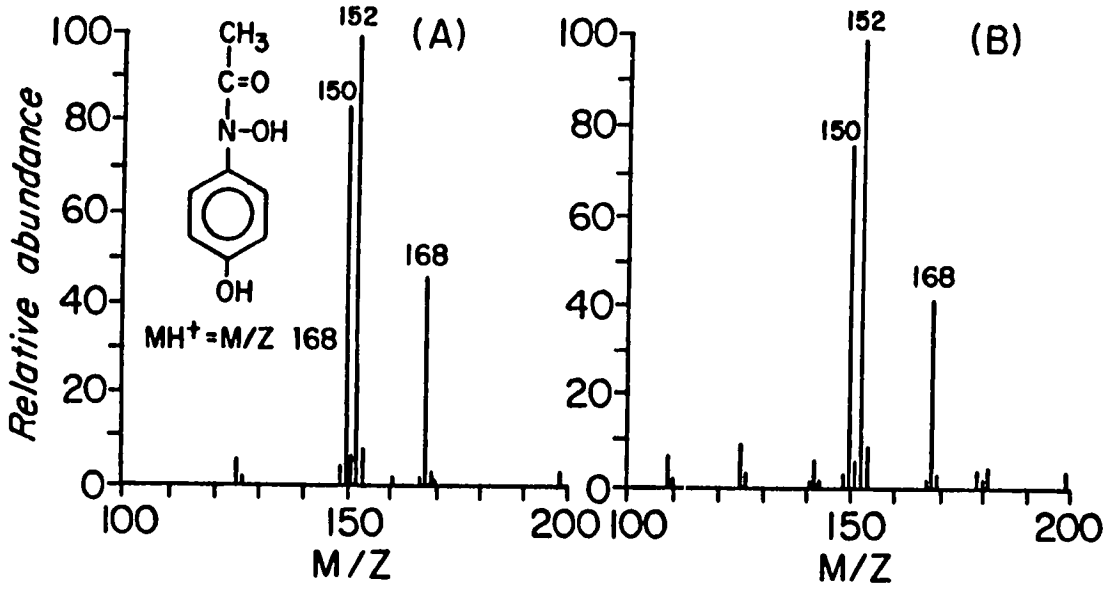
Relative abundance
100
80
60
40
20
0
100
150
200
M/Z
CH3
C=O
N-OH
OH
MH+=M/Z 168
152
150
168
(A)
(B)

highly unlikely. Thus, it was concluded that the electrophilic metabolite of acetaminophen which binds to microsomal protein is not formed from N-hydroxyacetaminophen. Further, since the evidence discussed in Chapter I implicates NAPQI as the ultimate toxin, activation mechanisms other than N-hydroxylation should be considered.

D. EXPERIMENTAL

1. MATERIALS

High pressure liquid chromatography (HPLC) used for analysis of incubation mixtures and purification of radiolabeled acetaminophen was accomplished on a Waters Associates (Milford, MA) liquid chromatograph equipped with a Model 440 absorbance detector, a 600A solvent delivery system, a U6K injector, and a μBondapak C-18 column. HPLC solvents were filtered through a Millipore Filtration Apparatus (Millipore Corporation, Bedford, MA) and degassed in a Branson-12 sonicator (Branson Company, Shelton, CT). Liquid scintillation was performed in Aquasol 2 scintillation cocktail (New England Nuclear Corporation, Boston, MA) with a Beckmann LS-7500 instrument (Beckmann Instruments Incorporated, Fullerton, CA). This microprocessor-controlled system utilized counting programs to correct for quench in all samples. Melting points (uncorrected) were obtained with a Thomas-Hoover capillary melting point apparatus (Arthur H. Thomas Company, Philadelphia, PA). NMR spectra were recorded on a Varian EM 360A spectrometer (Varian Associates, Instruments Division, Palo Alto, CA)

using tetramethylsilane as an internal standard. Direct probe chemical ionization mass spectra were obtained on a Biospect chemical ionization mass spectrometer (Scientific Research Corporation, Baltimore, MD). Using methane as a reagent gas, the source pressure was 0.5 torr at a temperature of 180°C. Infared spectra were taken on a Perkin Elmer 727B I.R. Spectrometer. Gas chromatography of the silyl derivative of synthetic N-hydroxyacetaminophen was performed on a Hewlett Packard Model 5840 gas chromatograph (Hewlett Packard, Avondale, PA) with a 1.8m x 2.0mm i.d. glass column containing 3% S.E.-30 packing (Applied Science, State College, PA). All pH measurements required in the preparation of buffers were made with an Orion Model 701A/Digital Ionalyzer (Orion Research Incorporated, Cambridge, MA).

Radiolabeled acetaminophen was purified by a combination of reverse phase HPLC and thin layer chromatography on 250μm Analtech Silca Gel GF Uniplates (Analtech Incorporated, Newark, DE) using diethyl ether as solvent.

Adult male Swiss-Webster mice (20-25 gm) were obtained from the Laboratory of Animal Medicine, Washington State University (Pullman, WA), and allowed food and water ad libitum.

Homogenization of liver samples in the preparation of microsomes was performed in a Potter-Elvehjem glass tube with a motor-driven teflon pestle having 0.10-0.15 mm clearance. Centrifugation of homogenates at 9000 g was carried out in a 4°C cold room with a Sorval Model NSE Angle Centrifuge (Ivan Sorval Incorporated, Norwalk, CT). A Beckmann L2-65B refrigerated ultracentrifuge (Beckmann Instruments Incorporated, Palo Alto, CA) fitted with a Model 42.1 rotor head was

used for 105,000 g spins of samples in polycarbonate tubes. Determinations of protein concentration by the method of Lowry were done with a Gilford Stasar II UV spectrophotometer (Gilford Instrument Laboratories, Oberlin, OH).

Microsomal incubations were done in Kimble Disposable Culture Tubes (VWR Scientific, San Fransisco, CA) in a Dubnoff Incu-Shaker water bath (Lab-Line Instruments Incorporated, Melrose Park, IL) at a constant 37°C. Precipitated liver protein samples were spun down using a Damon HN-SII table top centrifuge (International Equipment Company, Needham Heights, MA).

Chemicals purchased from Sigma Corporation (St. Louis, MO) included bovine serum albumin, NADP, glucose-6-phosphate, glucose-6-phospate dehydrogenase, 1.0 M $MgCl_2$ solution, and Trizma base. Phenol reagent (Folin-Ciocalteau) used in the Lowry protein assay was supplied by Fischer Scientific (Fair Lawn, NJ).

Tritium-labeled acetaminophen (general label, 5.6 mCi/mmole) was obtained from New England Nuclear Corporation. Organic HPLC solvents and heptane sulfonic acid were purchased from Waters Associates, and all other chemicals were of reagent grade from commercial suppliers.

2. METHODS

Preparation of Buffers and Miscellaneous Solutions

Buffers:

a) Tris/KCl buffer at pH 7.4 was made by combining 2.42 gm Trizma base and 11.5 gm KCl in a 1.0 liter volumetric flask. Distilled

and deionized water was added to volume, and concentrated HCl used to adjust to pH 7.4.

b) 0.05 M phosphate buffer at pH 7.4 was prepared by combining 400 ml of 0.1 M K_2HPO_4 (17.4 gm/l) and 100 ml of 0.1 M KH_2PO_4 (13.6 gm/l) with 500 ml distilled and deionized water. Final adjustment to pH 7.4 was made by addition of either 0.05 M KH_2PO_4 or K_2HPO_4.

Solutions:

a) 1.0 liter of mobile phase for HPLC separation of the ferric complex of N-hydroxyacetaminophen consisted of 500 ml methanol, 490 ml distilled and deionized water, and 10 ml acetic acid with 5.0 mM heptane sulfonic acid and 1.0 mM ferric chloride. The resulting solution was passed through a Millipore filtration apparatus using a 0.45μ filter and further degassed by sonication under vacuum.

b) Components used in the Lowry protein assay included bovine serum albumin standards, 2N phenol reagent (Folin-Ciocalteau), 10% sodium carbonate, 2% sodium potassium tartarate, and 1% copper sulfate. BSA standards were prepared by dissolving 0.05, 0.1, 0.2, and 0.3 mg protein/ml water. Phenol reagent was commercially supplied and used as a 1:20 dilution in water. A 10% sodium carbonate solution was made by combining 100 gm Na_2CO_3 and 20 gm NaOH in 1.0 liter of water. The copper sulfate solution was prepared by dissolving 1.56 gm $CuSO_4 \cdot 5H_2O$ in 100 ml water. And finally, 2.68 gm $NaKC_4H_4O_6 \cdot 4H_2O$ was mixed with 100 ml water to give the sodium potassium tartarate. 1.0 ml each of the copper

sulfate and tartarate solutions were combined with 20 ml of carbonate before addition to the protein samples.

In Vitro Trapping Experiments Using a Carrier Pool of Synthetic N-Hydroxyacetaminophen

The determination of acetaminophen-derived radiolabel incorporation into the synthetic carrier pool of N-hydroxyacetaminophen required isolation of the mouse liver microsomal fraction.[47,51,58,75] Adult male Swiss Webster mice (20-25 gm) were sacrificed by decapitation. The livers were quickly removed and placed in ice cold Tris/KCl buffer, pH 7.4. If possible all subsequent work was done on ice. The buffer was decanted, and the livers were weighed. Cold Tris/KCl buffer was added (3 ml/gm liver), the tissue was minced, and homogenation was performed with four vertical strokes of a motor-driven Potter-Elvehjem homogenizer. The homogenate was spun at 9000 g for 20 minutes at 4°C. After the supernanant was withdrawn it was centrifuged at 105,000 g for 60 minutes at 5-10°C. The resulting pellet was resuspended in 0.05 M sodium phosphate buffer, pH 7.4, to 10-20 mg microsomal protein/ml (based on the approximation of 30 mg mirosomal protein/gm liver weight). Microsomal protein concentration was determined by a modification of the Lowry method.[76,77] In triplicate, 0.01 ml aliquots of the microsomal suspension were added to 1.0 ml of water. To these and each of a series of protein standards (duplicates of: 0, 0.05, 0.1, 0.2, and 0.3 mg BSA/ml water) 1.0 ml Lowry reagent (1.0 ml copper sulfate, 1.0 ml tartarate, 20 ml carbonate) was added.

After 10 minutes, phenol reagent (3.0 ml) was included, and the solutions were placed in a 55°C water bath for 10 minutes. Colorometric determination of the samples and standards following Beer's Law was made at 540 nm. Based on these results, microsomal protein was adjusted to 6.0 mg/ml by dilution with phosphate buffer.

Microsomal incubations, performed at a volume of 3.0 ml, contained microsomal protein (6.0 mg), NADPH (6.0 mg), EDTA (3.0 µmoles), ^{3}H-acetaminophen (3.0 µmoles, 120 dpm/nmole) purified by TLC (silca, diethyl ether) and reverse phase HPLC (86.5/12.5/1.0 methanol-water-acetic acid), and N-hydroxyacetaminophen (0.5 µmoles) in phosphate buffer (0.05 M, pH 7.4). Reaction mixtures were shaken in a 37°C water bath for 15 minutes then terminated by protein precipitation with cold methanol (4.0 ml) and placed on ice. The precipitated proteins were removed by centrifugation in 15 ml centrifuge tubes. The synthetic carrier pool was removed from the reaction supernatants by extraction with ethyl acetate, and the organic phase was then dried over anhydrous sodium sulfate, and evaporated under a stream of nitrogen. N-Hydroxy-acetaminophen was reconstituted in 0.05 ml HPLC mobile phase which included 1.0 mM ferric chloride. Isolation of the ferric hydroxamic acid complex was accomplished by reverse phase HPLC using a UV absorbance detector fitted with a 546 nm filter. With a solvent flow of 1.0 ml/minute (50/49/1 methanol-water-acetic acid) on a µBondapak C-18 column the ferric chelate of N-hydroxyacetaminophen eluted at 3-4 minutes. The ferric-complexed N-hydroxyacetaminphen was collected and combined with 10.0 ml Aquasol 2 scintillation cocktail, and radioactivity was determined by liquid scintillation spectroscopy.

Proteins precipitated by cold methanol from the microsomal incubations were subjected to succesive washes to remove noncovalently bound radiolabel. The procedure involved suspension of the protein in the solvent, thorough mixing, re-centrifugation, and removal of solvent. Washes were done three times with 80% methanol (4.0 ml), once with trichloroacetic acid (4.0 ml), twice with 3/1 ethanol-diethyl ether (4.0 ml), and once more with 80% methanol. After the last centrifugation supernatants were checked for radioactivity above background (30-45 dpm) by counting 1.0 ml as previously described, and the 80% methanol wash repeated if necessary. Washed protein pellets were then dissolved in 1.0 M NaOH (0.25 ml), and 0.20 ml of this solution was counted by liquid scintillation. Of the remainder, 0.01 ml was used to determine the protein concentration by the method of Lowry.

Mass Spectral Determination of the N-Hydroxyacetaminophen Ferric Chelate Isolated by HPLC

As a verification that the compound collected from reverse phase HPLC was N-hydroxyacetaminophen, samples of the eluted chelate were combined with 10 ml of 1.0 mM EDTA. Uncomplexed N-hydroxyacetaminophen was then extracted into ethyl acetate, dried over anhydrous sodium sulfate, evaporated to a small volume with nitrogen, and analyzed by direct insertion probe chemical ionization mass spectroscopy.

3. SYNTHESIS

4-Benzyloxynitrobenzene

p-Nitrophenol (10.0 gm, 72 mmole), sodium carbonate (20.0 gm, 185 mmole), and benzyl chloride (7.48 gm, 59 mmole) were vigorously stirred in refluxing ethanol overnight (200 ml). Upon cooling long colorless needles appeared which were collected by suction filtration and washed with dilute HCl (25 ml, 0.5 N) followed by water (100 ml). The collected material was recrystallized from hot ethanol to give product (9.98 gm, 61% yield) with melting point of 105°C (literature[73] 105°C). NMR ($CDCl_3$, 60 MHz): δ 5.10 (s, 2H, benzylic H), 6.98 (d, 2H, $J_{3,2}$= 9 Hz, 3,5 aromatic H), 7.35 (s, 5H, benzyl aromatic H), 8.17 (d, 2H, $J_{2,3}$= 9 Hz, 2,6 aromatic H).

N-Hydroxy-4'-benzyloxyacetanilide

4-Benzyloxynitrobenzene (5.0 gm, 0.02 mole) was suspended in 7/1 ethanol-water (40 ml). Aqueous NH_4Cl (4%, 10.0 ml) was then combined with vigorous stirring followed by the slow addition of zinc (4.0 gm) dust. The reaction mixture was heated to 67°C and maintained at this temperature for 3 minutes, then filtered through Celite. After cooling by addition of cold water (60 ml) and placing on ice, product hydroxylamine precipitated and was filtered and washed with water (20 ml). The entire yield (approximately 1 gm) was carried through the acetylation step immediately due to decomposition upon storage.

4-Benzyloxyphenylhydroxylamine (approximately 1 gm, 0.005 mole) was dissolved in diethyl ether (100 ml) and cooled to 0°C. A

bicarbonate slurry (7.0 gm $NaHCO_3$, 12 ml H_2O) was added followed by acetyl chloride (3.0 gm, 0.04 mole in 5.0 ml ether) dropwise over the course of 2 hours and stirred for another 2 hours. At the end of this period water (10 ml) and 3N NaOH (20 ml) were added, and the aqueous phase neutralized with solid NaH_2PO_4 and water. With the final volume at approximately 90 ml the benzyl-protected hydroxamic acid was extracted with two portions of diethyl ether (140 ml), and dried over anhydrous Na_2SO_4. Filtration and evaporation of the solvent yielded an orange residue (0.99 gm) which was treated with activated charcoal and recrystallized twice from 2/5 ethyl acetate-hexane. The buff-colored product, N-hydroxy-4'-benzyloxyacetanilide, was in approximately 6% yield (0.3 gm) and melted at 103°C (literature[73] 105°C). Thin layer chromatography gave a single spot (R_f= 0.55, silica, diethyl ether). NMR ($CDCl_3$, 60 MHz): δ 2.0 (s, 3H, acetyl H), 5.00 (s, 2H, benzylic H), 6.90 (d, 2H, $J_{3',2'}$= 9 Hz, 3',5' aromatic H), 7.25 (d, 2H, $J_{2',3'}$= 9 Hz, 2',6' aromatic H), 7.31 (s, 5H, benzyl aromatic H), 8.30 (s, 1H, exchangeable H).

N-4'-Dihydroxyacetanilide

N-Hydroxy-4'-benzyloxyacetanilide (250 mg, 0.97 mmole) was dissolved in 15 ml ethanol containing 1 drop of concentrated HCl and 5% Pd/charcoal (2.0 mg). Hydrogenolysis at 30 psi H_2 was carried out for 1 hour, followed by filtration through Celite. Evaporation yielded a brown residue which was recrystallized from 3/1 tetrahydrofuran-ethyl acetate to give a 3% (4 mg) of N-hydroxyacetaminophen with a melting point of 121-123°C (literature[53] 122°C). Chemical ionization mass

spectra (methane) showed m/e 168 (M+1), and 152 (M-16), while proton NMR and IR characteristics were virtually indentical to those reported by others.[53,54] Gas chromatography (3% S.E.-30) of the silyl derivative showed the presence of 1-2% acetaminophen.

CHAPTER III

PEROXIDASE-MEDIATED FORMATION OF REACTIVE METABOLITES OF ACETAMINOPHEN

A. INTRODUCTION

The study presented in Chapter II provided strong evidence against the formation of N-hydroxyacetaminophen *in vitro*, and thereby contributed to the rejection of the N-hydroxylation proposal for metabolic activation of acetaminophen. Therefore, alternative mechanisms for the formation of the arylating metabolite were considered.[67]

Other postulates that have been suggested include the formation of acetaminophen N-[78] or O-[41] hydroperoxides, the arylating species, NAPQI, being formed through loss of the elements of hydrogen peroxide or water, respectively. However, there is neither supporting evidence for these proposals, nor any known precedent in cytochrome P-450-catalyzed reactions.

Two other possible mechanisms for acetaminophen activation do not involve oxygen incorporation, both invoking one-electron oxidations of acetaminophen to the semiquinone imine radical. In one postulate the free radical oxidation product is released from the enzyme active site, whereas in the second mechanism radical recombination and site-mediated dehydration yield NAPQI directly. The abstraction-recombination mechanism is consistent with current understanding of P-450-mediated reactions from the work of Groves et al.[79] and Ortiz de Montellano,[80]

whereas a one-electron oxidation with release of the radical product from the enzyme has not been observed in P-450-mediated reactions. However, peroxidases are enzymes that do catalyze such one-electron oxidation reactions,[81,82] and therefore studies were undertaken to characterize acetaminophen oxidation by horseradish peroxidase to determine if there are any similarities between the products of acetaminophen oxidation by this enzyme and by cytochrome P-450.

B. RESULTS

Covalent Binding Studies

In the presence of horseradish peroxidase and hydrogen peroxide radiolabel from ^{3}H-acetaminophen was irreversibly bound to an acceptor protein, bovine serum albumin (BSA, Figure 3.1). Covalent binding was not measureable upon omission of either the peroxidase or the peroxide, indicating an enzyme-mediated process. The binding reaction was almost totally inhibited in the presence of either 0.2 µg/ml catalase or 1.5 mM L-ascorbic acid, whereas the addition of 20 µg/ml superoxide dismutase had no effect (Figure 3.2). Glutathione at a concentration of 0.1 mM inhibited binding by approximately 50% with concomitant formation of a glutathione conjugate. This conjugate had the same retention time on reverse phase HPLC as that isolated from P-450 incubations of acetaminophen containing glutathione. Radiolabeled acetaminophen analogs, N-methylacetaminophen and phenacetin, were not measurably activated by horseradish peroxidase to metabolites that bind to BSA.

FIGURE 3.1: HORSERADISH PEROXIDASE/H_2O_2-MEDIATED BINDING OF [^{3}H]-ACETAMINOPHEN TO BSA. RESULTS SHOW THE MEANS ± S.D. OF AT LEAST FOUR DETERMINATIONS FOR COMPLETE INCUBATIONS (●), MINUS PEROXIDASE (■), AND MINUS H_2O_2 (▲).

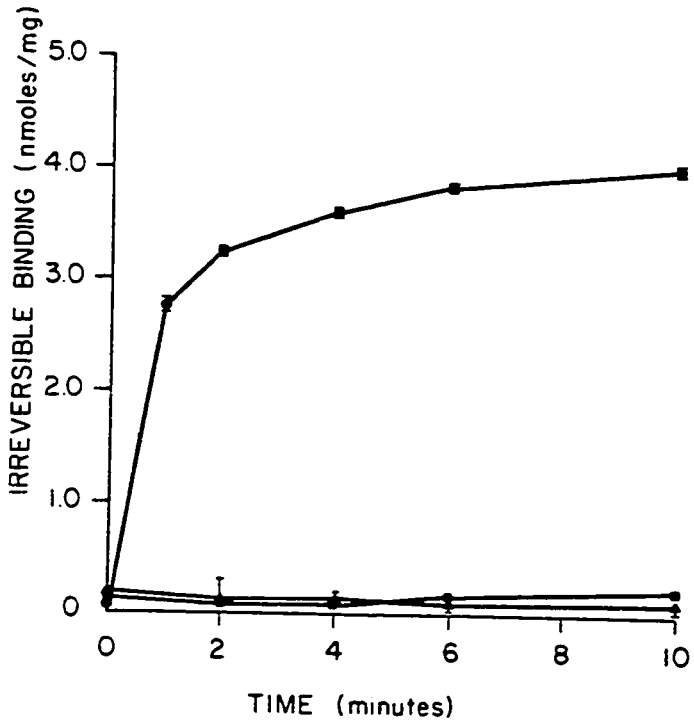
IRREVERSIBLE BINDING (nmoles/mg)
5.0
4.0
3.0
2.0
1.0
0
0
2
4
6
8
10
TIME (minutes)

FIGURE 3.2: HORSERADISH PEROXIDASE/H_2O_2-MEDIATED BINDING OF [^{3}H]-ACETAMINOPHEN TO BSA. RESULTS SHOW THE MEANS ± S.D. OF AT LEAST FOUR DETERMINATIONS FOR COMPLETE INCUBATIONS (●), AND THE EFFECTS OF THE ADDITION OF 1.0 mM GLUTATHIONE (■), 1.5 mM ASCORBIC ACID (▲), 0.02 GM/ML SOD (⊙), AND 0.2 MG/ML CATALASE (□).

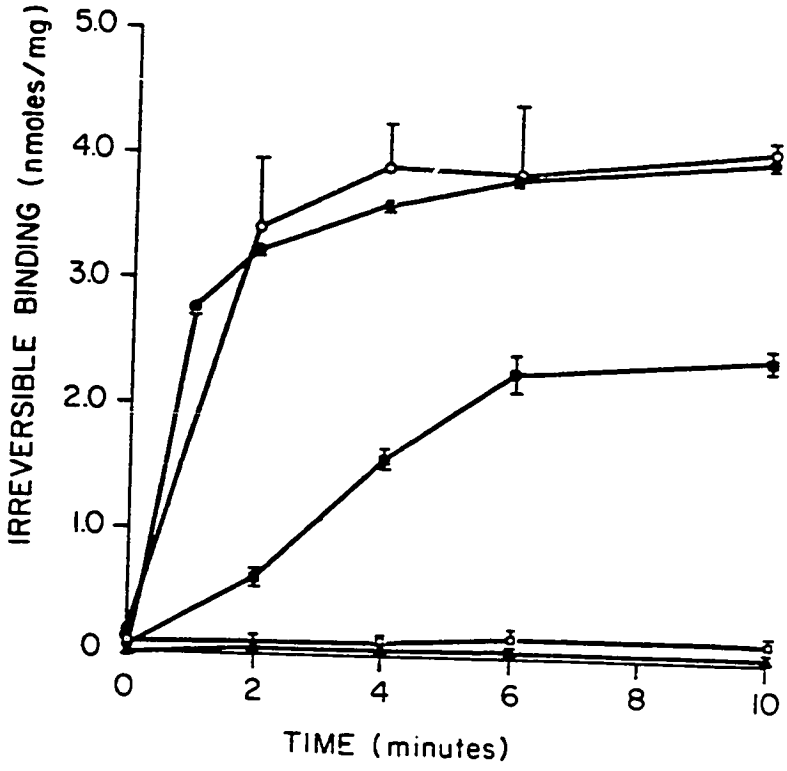
IRREVERSIBLE BINDING (nmoles/mg)
5.0
4.0
3.0
2.0
1.0
0
0
2
4
6
8
10
TIME (minutes)

Studies on Acetaminophen Free Radical Formation in Peroxidase Incubations

Electron spin resonance (ESR) measurements were used to determine that a free radical was generated in the acetaminophen-horseradish peroxidase incubations. This radical appeared immediately after addition of the enzyme to the reaction mixture and reached maximum levels within 16 minutes, followed by a slow decay with a half life of two hours (Figure 3.3). Since the free radical signal was not observed in the absence of acetaminophen, peroxidase, or hydrogen peroxide, enzymatic formation of the species was indicated. The radical was not formed from the superoxide-generating system of xanthine-xanthine oxidase and was diminished in the presence of glutathione or L-ascorbic acid, producing the ascorbate radical in the latter case. When mouse liver microsomes were added to the acetaminophen-peroxidase system the free radical disappeared rapidly.

Since it was not apparent whether the radical was centered on carbon, oxygen, or nitrogen, spin trapping studies were undertaken. The radical was generated by UV photolysis of acetaminophen solutions in the presence of the spin trap 5,5-dimethyl-1-pyrroline-N-oxide (DMPO). Spectra of the DMPO-trapped radical possessed hyperfine splitting constants of A_H^β = 18.7 G and A_N = 15.2 G (Figure 3.4). It had been previously demonstrated that carbon-centered radicals spin trapped with DMPO result in hyperfine splitting constants of $A_H^\beta > A_N$, whereas oxygen-centered radicals produce constants of $A_N > A_H^\beta$.[83] Nitrogen radicals, with a spin number of one, add to DMPO giving additional hyperfine splittings that were not observed with the acetaminophen

FIGURE 3.3: ESR SPECTRUM OF THE ACETAMINOPHEN FREE RADICAL PRODUCED IN THE PRESENCE OF HORSERADISH PEROXIDASE AND H_2O_2.

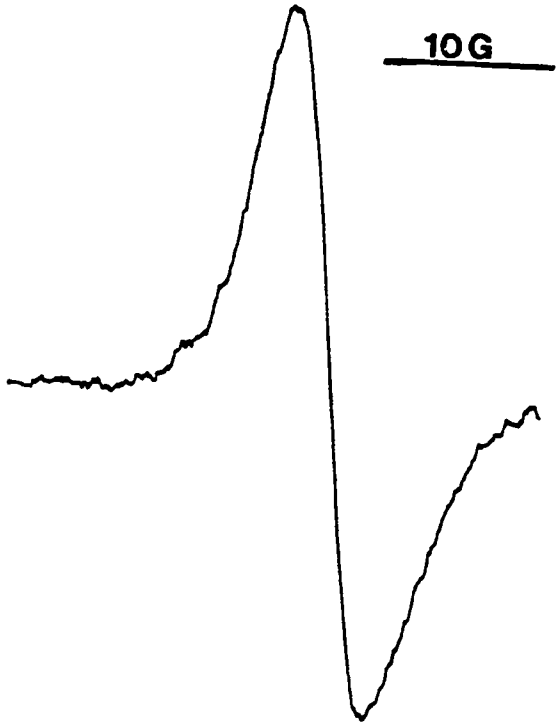
10 G

FIGURE 3.4: ESR SPECTRUM OF THE DMPO SPIN-ADDUCT OF THE ACETAMINOPHEN FREE RADICAL. OBTAINED BY UV PHOTOLYSIS OF ACETAMINOPHEN IN AQUEOUS SOLUTION IN THE PRESENCE OF DMPO.

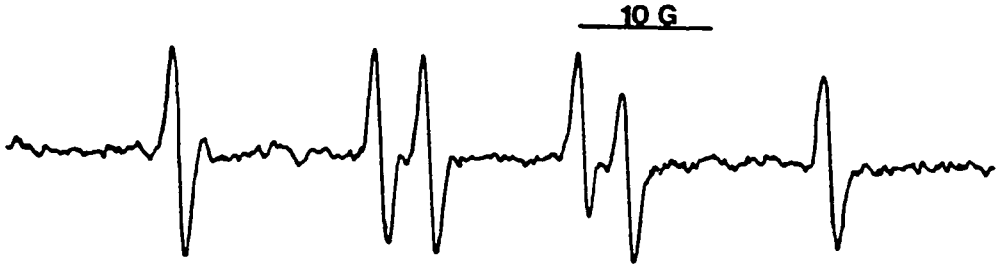
10 G

radical. Hence, it appeared from the spectrum in Figure 3.4 that the DMPO-trapped radical was carbon-centered.

C. DISCUSSION

The covalent binding of radiolabel from ^{3}H-acetaminophen to BSA in the horseradish peroxidase system was an enzymatic process, as indicated by a lack of significant binding in the absence of hydrogen peroxide or peroxidase (Figure 3.1). Consistent with the requirement for hydrogen peroxide was the inhibition of binding by the inclusion of catalase (Figure 3.2). In contrast, superoxide dismutase (SOD) had no effect on the binding reaction. SOD has similarly been shown to have no effect on cytochrome P-450-mediated binding of acetaminophen to liver microsomes isolated from mice.[84] Furthermore, in the peroxidase-mediated reactions, as with cytochrome P-450-mediated reactions,[39,85] covalent binding of acetaminophen to proteins was inhibited by both glutathione and L-ascorbic acid. The same glutathione conjugate of acetaminophen was formed by both enzymes in incubations containing glutathione, whereas ascorbic acid appeared to act as a reductant of the reactive species. These results imply that a similar arylating species is formed from acetaminophen by horseradish peroxidase and cytochrome P-450.

The radiolabeled analogs of N-methylacetaminophen and phenacetin were not activated by the peroxidase at substrate concentrations equivalent to those at which acetaminophen binding reached approximately 4 nmoles/mg BSA. The lack of binding of these compounds

implies that both the amide nitrogen and the phenolic oxygen must be devoid of alkyl sustituents. Microsome-mediated covalent binding of N-methylacetaminophen has also been found to be much less extensive than that of acetaminophen[86] while phenacetin binds to about the same extent as acetaminophen under the same conditions; however, the mechanisms are different.[87]

One intermediate that was detected in the peroxidase-mediated reactions was an acetaminophen free radical (Figure 3.3). From the hyperfine splitting constants of the acetaminophen radical generated by UV photolysis and trapped with DMPO (Figure 3.4), the radical was primarily carbon-centered. While it is recognized that the conditions used to generate the DMPO adduct were quite different from the peroxidase incubations, the untrapped acetaminophen radical generated by UV photolysis did produce the same ESR signal observed in the peroxidase system. Further, the spin trap was used not so much to identify the regiochemistry of the unpaired electron, but rather to determine the structure of the detected species, an aryl radical. The acetaminophen analogs N-methylacetaminophen and phenacetin appeared to generate unstable radicals at rates considerably slower than acetaminophen radical formation. Because of their apparent instability, no characterization of these species could be made.

From these data it is not possible to establish whether the free radical is responsible for protein binding in the peroxidase system. Whereas the rate of covalent binding was maximal during the first 2-3 minutes (Figure 3.1), steady state levels of the radical were maximal at approximately 16 minutes. But, since these results were obtained in

separate incubations under slightly different conditions, the discrepency in maxima may be artifactual, simply reflecting the effects of adding a large amount of exogenous protein (BSA for the binding study) on radical formation. Or alternatively, it may represent quinone imine scavenging by protein from a semiquinone imine/quinone imine couple. Another possibility is that covalent binding was limited by destruction of protein binding sites by the peroxidase/H_2O_2 system or by the reactive metabolite itself. In support of this was the prolonged period of linear binding in the presence of glutathione (Figure 3.2). Regardless of the answer to this question, these experiments have established that acetaminophen activation to a reactive species can occur through a radical process, and that the resulting metabolite has characteristics very similar to that formed in microsomal incubations of acetaminophen.

It is intriguing to spectulate whether horseradish peroxidase and cytochrome P-450 activate acetaminophen by a common mechanism. Indeed, attention has been given to the possibility that in the presence of certain supportive oxidants cytochrome P-450 may function as a peroxidase, independent of NADPH and oxygen.[88-90] However, current evidence does not support this proposal.[91] Rather it appears there are significant differences between the two oxidative mechanisms.

The peroxidases as a class catalyze the oxidation of secondary substrates (electron donor molecules) at the expense of the primary substrates (peroxides).[81,82] This is shown below:

$$ROOH + 2AH_2 \longrightarrow ROH + H_2O + A + AH_2 \qquad \text{Equation 3.1}$$

where ROOH represents H_2O_2, or a number of alkyl hydroperoxides or peroxyacids. The donor molecule, AH_2, can be any of a wide range of compounds[92] able to undergo free radical oxidations, such as hydroquinone, ascorbic acid, catechols, indole acetic acid, or in this case acetaminophen. From spectral and kinetic data the catalytic cycle shown in Figure 3.5 has been proposed.[82] The heme-containing enzyme at the resting ferric state rapidly and stoichiometrically binds peroxide. Depending upon the peroxide used, water, an alcohol, or an acid is released with concomitant formation of a green complex at the oxidation state of a ferric oxene. This complex, designated as compound I, possesses the same characteristic UV spectrum with maximal absorbance at 395 nm regardless of the particular peroxidase or peroxide employed. Resonace stabilization occurs, probably including a positively charged electron hole in the porphyrin. Compound I is reduced by a secondary substrate molecule by one electron producing a red compound II at the oxidation state of a ferryl hydroxide. The secondary substrate is released as a free radical, usually undergoing a dismutation to the parent molecule plus the two-electron oxidized product (NAPQI in these studies) as shown below.

$$2AH^{\cdot} \longrightarrow AH_2 + A \qquad \text{Equation 3.2}$$

Compound II is then reduced by a second electron donor molecule, again releasing a radical product, and returning to the resting state. It is significant that the definative characteristics of the enzymes have been found consistent for all peroxidases and peroxides studied.

FIGURE 3.5: CATALYTIC CYCLE OF THE PEROXIDASES.

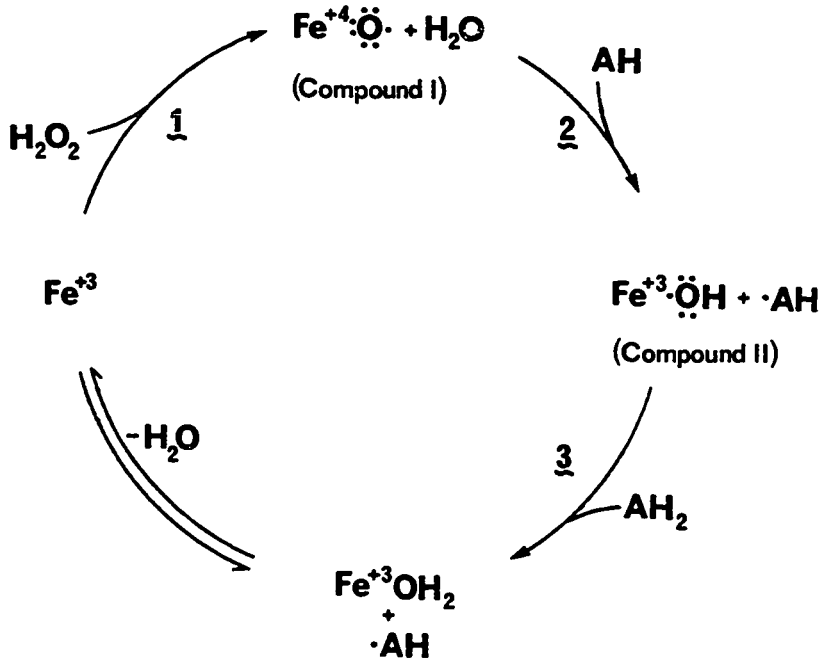
Fe+4:Ö· + H2O
(Compound I)
AH
2
H2O2
1
Fe+3
Fe+3·ÖH + ·AH
(Compound II)
-H2O
3
AH2
Fe+3OH2
+
·AH

Specifically, interaction between the enzyme and peroxide has one-to-one stoichiometry producing compound I, which is identifiable by a distinct UV spectrum. Both kinetic and spectral similarities seen in all compound I complexes studied have led investigators to believe they share a common activated oxygen species.

The possibility that cytochrome P-450 may function as a peroxidase under specific conditions was first suggested after the discovery that P-450 oxidations of some organic substrates can be supported by hydroperoxides as well as NADPH and oxygen, as illustrated below.[89,90]

$$ROOH + R'H_2 \xrightarrow{P\text{-}450} ROH + H_2O + R'OH \qquad \text{Equation 3.3}$$

Moreover, peroxidases had been shown to mediate N-dealkylation reactions, thus inducing speculation that the mechanism of oxidative N-dealkylations by P-450 and peroxidases were similar. [93]

However, several lines of evidence have ruled out a peroxidase mechanism for hydroperoxide-supported cytochrome P-450 reactions. Significantly, no peroxidase is known to carry out oxygen insertion reactions similar to the aliphatic hydroxylations mediated by cytochrome P-450.[91] Also, the regioselectivity of oxidant-supported P-450 hydroxylations vary with different hydroperoxides, and these all differ from NADPH/O_2-supported reactions.[94] In other studies, both ESR and stopped-flow UV data demonstrated that spectral characteristics of the initial P-450-peroxide complex are strongly influenced by the alkyl moiety of the hydroperoxide[95] which is not characteristic of true peroxidase reactions.[96] These data indicate that alkyl functionalities

of the employed oxidants were retained, and therefore the initial P-450-peroxide complex was unlike peroxidase compound I.

Even more convincing evidence against the P-450 peroxidase mechanism came from studies by Blake and Coon.[97] In contrast to the one-to-one stoichiometry of the peroxidase compound I formation, cytochrome P-450 titrations with various peroxy compounds resembled substrate binding curves, indicating reversible formation of an initial complex. The kinetics of this process were consistent with the following model:

$$\text{P-450} + \text{ROOH} \rightleftharpoons \text{C} \rightleftharpoons \text{D} \qquad \text{Equation 3.4}$$

where C represented an enzyme-substrate complex and D was the species spectrally observed. The ratio k_1/k_2 was treated as an association constant for peroxide binding since it correlated well with the hydrophobicity of the peroxy compound. In addition, the magnitude of k_3 and k_4, as well as the spectra of D, were functions of the peroxide structure. Thus, the reaction of P-450 with hydroperoxides seems to differ from the corresponding reactions of the peroxidases.

An alternative mechanism for the peroxide-dependent activity of cytochrome-P450 was proposed by White and Coon.[91] This involved homolytic cleavage of the peroxide oxygen-oxygen bond as shown in Figure 3.6. Step 1 consisted of peroxide and substrate binding in an unspecified order yielding a complex probably corresponding to C in Equation 3.4. Enzyme-substrate complexation would be mediated by hydrophobic interactions with the peroxide binding at the sixth ligand

FIGURE 3.6: PROPOSED MECHANISM OF HOMOLYTIC PEROXIDE-DEPENDENT ALIPHATIC HYDROXYLATION BY CYTOCHROME P-450.

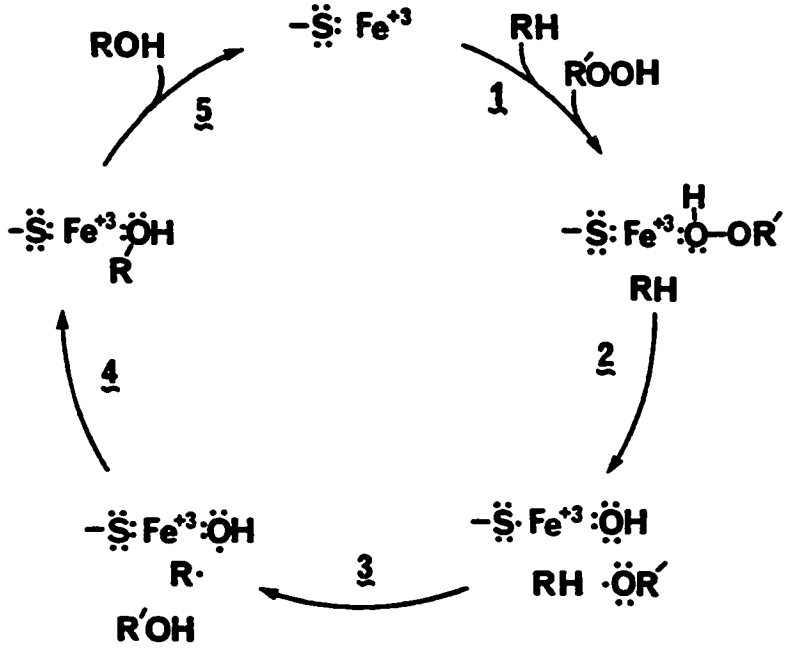
–S: Fe+3
RH
ROOH
1
–S: Fe+3 :O–OR´
H
RH
2
–S· Fe+3 :OH
RH ·OR´
3
–S: Fe+3 :OH
R·
R´OH
4
–S: Fe+3 :OH
R
5
ROH

position through the terminal oxygen. The first departure from the classical peroxidase mechanism is shown in step 2 of Figure 3.6 where homolytic cleavage of the peroxide oxygen-oxygen bond was invoked in a manner analogous to the Fenton reaction shown below.

$$Fe^{+2} + H_2O_2 \longrightarrow Fe^{+3} + OH^- + OH^{\cdot} \qquad \text{Equation 3.5}$$

This could be accomplished on the enzyme by an initial reduction of ferric iron to ferrous by the thiolate fifth ligand followed by the Fenton-type reaction producing a thiyl ferric hydroxide and alkoxy radical. While the electron distribution of this complex, shown below, could only be speculated, White and Coon noted similarities to the oxidation state of the peroxidase compond II, one-electron-reduced over the ferric oxene.

$$S^{\cdot}Fe^{II}OH^{\cdot} \longleftrightarrow S^{\cdot}Fe^{III}OH^{-} \longleftrightarrow S^{-}Fe^{III}OH^{\cdot} \longleftrightarrow S^{-}Fe^{IV}OH^{-} \qquad \text{Equation 3.6}$$

Step 3 involved abstraction of an available hydrogen atom of the substrate by the homolytically derived alkoxy radical. This accounted for the variable product distributions observed with the different peroxides, each producing a different alkoxy hydrogen atom abstractor with distinctive steric and electrophilic properties. In step 4 the substrate radical in close proximity collapsed with the oxygen of "compound II" forming a transient iron-coordinated product, followed by release of both product alcohols.

This mechanism, termed a peroxygenase rather than a peroxidase,

explained several phenomena observed with hydroperoxide-dependent hydroxylation. The different regioselectivity patterns observed with various peroxides and the absence of the uniform activated oxygen seen with peroxidases were accomodated by participation of the peroxide-derived alkoxy radical.

Cytochrome P-450 supported by NADPH and oxygen is currently thought to catalyze alkane C-H oxidation through a two step process involving hydrogen atom abstraction with subsequent radical recombination to produce the oxygen-incorporated product. This has been favored by the work of Groves[79] on norborane hydroxylation, and of Ortiz de Montellano[80] who trapped radicals formed during the P-450 oxidative metabolism of dihydropyridines. Two prominent hypotheses exist to explain these steps, differing primarily in the manner of oxygen-oxygen bond cleavage.[91] They are shown in Figure 3.7 and are the heterolytic oxenoid mechanism (A) and the homolytic quasi-Fenton (B). Both paths as postulated involve acylation (steps 5A, 5B) of the ferric iron-coordinated peroxide, and are represented as a peroxy acid for the oxenoid and as a peroxyimidic acid in the quasi-Fenton.

Considering first the oxenoid route (Figure 3.7, A), Hamilton[98] has suggested that the peroxy acid is capable of hydrocarbon oxidation while Coon[91] has proposed that further activation through heterolysis is necessary. This would result in free carboxylate and an oxygen atom coordinated to ferric iron (step 6A). Formally, the complex would be at the state of a thiyl ferric oxylide, but would undoubtably be resonace stabilized.

FIGURE 3.7: PROPOSED MECHANISMS OF O_2/NADPH-DEPENDENT ALIPHATIC HYDROXYLATION BY CYTOCHROME P-450. (A) HETEROLYTIC OXENOID ROUTE, (B) HOMOLYTIC QUASI-FENTON.

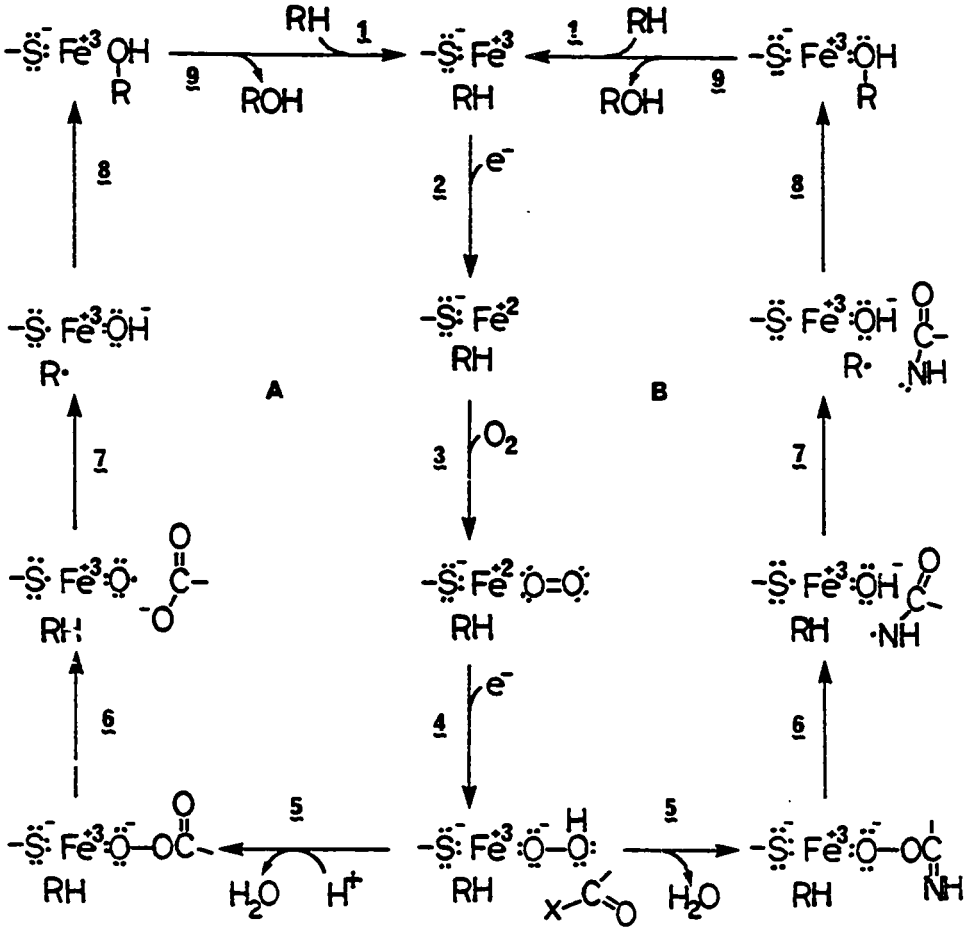
RH
1
ROH
9
e⁻
2
O₂
3
e⁻
4
5
H₂O
H⁺
6
7
8
A
B

$$S\cdot Fe^{III}O^{-} \longleftrightarrow S^{-}Fe^{III}O \longleftrightarrow S^{-}Fe^{IV}O^{-} \longleftrightarrow S^{-}Fe^{V}O^{-2} \qquad \text{Equation 3.7}$$

The thiyl ferric oxylide could perform oxygen insertions in accordance with the work of Groves et al.[79] by initially abstracting a hydrogen atom from the substrate molecule (step 7A). The activated oxygen, then at the state of an iron-bound hydroxy radical, would combine with the nascent substrate radical (step 8A). Dissociation of the hydroxylated product then would complete the catalytic cycle (step 9A).

The quasi-Fenton route (Figure 3.7, B) differs from the oxenoid postulate in the manner of oxygen-oxygen bond cleavage. Homolytic peroxide scission (step 6B) would produce an amidyl radical and a thiyl ferric hydroxide complex, distributing the oxidizing equivalents to two separate enzyme sites. In this proposal the amidyl radical would serve as the hydrogen atom abstractor (step 7B), and the resulting substrate radical would collapse with the enzyme-bound oxygen to form product (step 8B) followed by release (step 9B).

Both proposed mechanisms are consistent with the apparent radical mechanism of cytochrome P-450. And, both conveniently accomodate the role of the thiolate fifth ligand in oxygen activation, the thiolate serving as either an electron reservoir or an electron sink as required, with iron acting as a charge conduit. It is believed that in NADPH/O_2-supported P-450 reactions the oxenoid route may be more likely while the quasi-Fenton scheme better accounts for the characteristics of the peroxide-supported P-450 reactions.[91]

Returning again to the original question of cytochrome P-450 activation of acetaminophen, either the heterolytic or the homolytic

mechanism can be envisioned. Indeed, each may operate under appropriate conditions, the oxenoid in NADPH/O_2-supported reactions, and the quasi-Fenton in the presence of hydroperoxides. As will be discussed in Chapter IV, acetaminophen is oxidized to NAPQI by purified cytochrome P-450 and cumene hydroperoxide. Strong evidence against the intermediacy of N-hydroxyacetaminophen in acetaminophen activation was presented in Chapter II, and it also appears that other oxygen-incorporated metabolites, such as the acetaminophen catechol or epoxides, do not have a significant role in the observed hepatotoxicity. Since evidence has implicated NAPQI as the ultimate toxin (Chapter I), mechanistic proposals for acetaminophen oxidation to the arylating metabolite should accomodate quinone imine formation exclusive of oxygen incorporation.

Such a scheme is presented in Figure 3.8 for the cytochrome P-450 catalyzed oxidation of acetaminophen to NAPQI.[67] While the hydrogen atom abstractor is shown as an oxenoid intermediate (structure A), the quasi-Fenton acyl radical would be expected to serve equally well. Whichever initial enzyme complex is invoked hydrogen abstraction would produce a radical cage complex of ferric cytochrome-hydroxyl radical and substrate radical (structure B). The one-electron-oxidized substrate would be in the form of a resonance-stabilized semiquinone imine that theoretically could escape from the radical cage, resulting in tissue binding and necrosis. However, the acetaminophen radical, as will be dicussed in Chapter IV, is an excellent reductant (E_7^1 = -0.251 V) and probably would undergo further oxidation through a rapid second electron transfer producing NAPQI and the hydrated ferric cytochrome

FIGURE 3.8: HYPOTHETICAL SCHEME FOR THE CYTOCHROME P-450 OXIDATION OF ACETAMINOPHEN TO AN ELECTROPHILIC METABOLITE VIA SEMIQUINONE IMINE FREE RADICAL INTERMEDIATES.

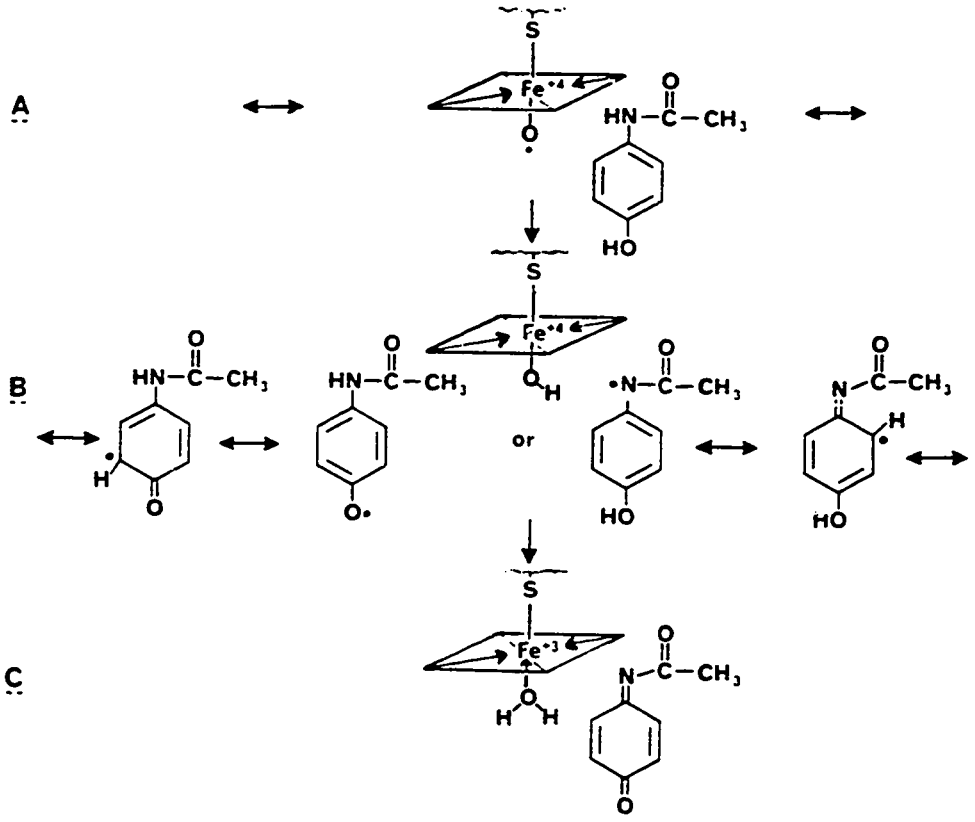
A
B
C
or

(structure C). Alternatively, the quinone imine could be generated as shown in Figure 3.9. This scheme differs from the previous only in the events following radical abstraction. Rather than performing a direct second electron oxidation of the substrate, the radical cage (structure B) could collapse forming a transient ferric-oxyamide complex (structure C). At this point heterolytic cleavage could occur either at the iron-oxygen or oxygen-nitrogen linkage. Scission of the first would yield a hydroxamic acid as observed with phenacetin, acetanilide, and p-chloroacetanilide. However, with acetaminophen the p-hydroxy group is capable of electron pair donation favoring formation of the quinone imine through cleavage of the oxyamide bond in essentially a site-mediated dehydration.

Thus, regardless of whether the homolytic or heterolytic route is invoked, or whether the P-450 reactions are supported by NADPH/O_2 or alkylhydroperoxides, it is most likely that NAPQI formation does not occur through a peroxidase mechanism. Accomodation of the similarities between the peroxidase and P-450-derived arylating metabolites can be made by considering the comproportionation equilibrium below.

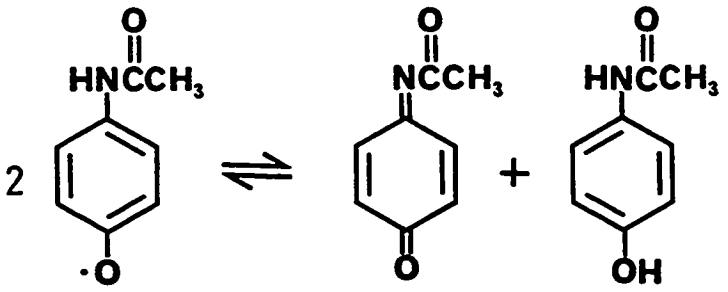

Equation 3.8

Such processes are common with quinonoid molecules[99] and appear to occur with the NAPQI/acetaminophen couple as will be discussed in

FIGURE 3.9: POSTULATED MECHANISM FOR THE CYTOCHROME P-450 OXIDATION OF ACETAMINOPHEN THROUGH A TRANSITORY FERRIC-OXYAMIDE COMPLEX.

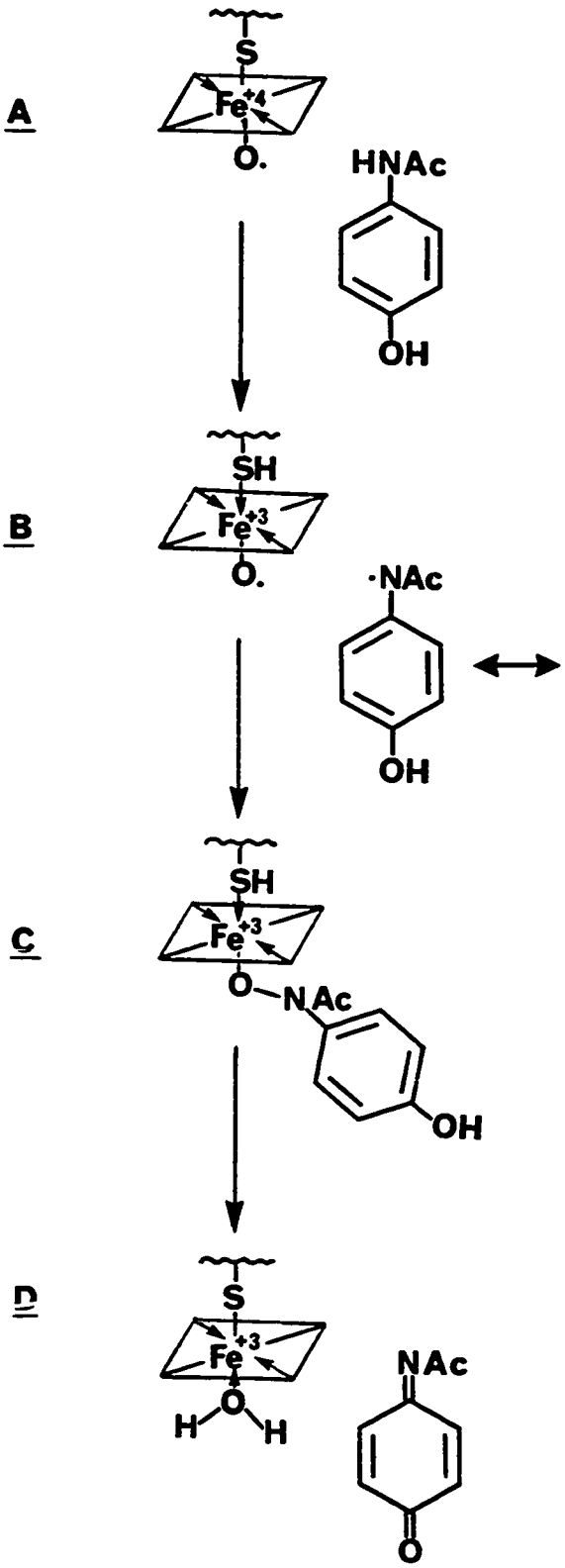
A
S
Fe+4
O.
HNAc
OH
B
SH
Fe+3
O.
·NAc
OH
C
SH
Fe+3
O
NAc
OH
D
S
Fe+3
O
H
H
NAc
O

Chapter IV. Hence, independent of whether the semiquinone imine or the quinone imine is released from the enzyme, acetaminophen, NAPQI, and the radical are expected to be present in equilibrium. This process probably occurs rapidly with very low steady state levels of the semiquinone imine present due to its strong one-electron reduction potential. Accordingly, the binding characteristics of both the peroxidase and P-450-generated reactive species should be similar.

In summary, this chapter has described experiments demonstrating similarities between peroxidase and cytochrome P-450-mediated oxidations of acetaminophen. While common binding properties imply a common arylating metabolite, this cannot be interpreted to mean that the two enzymes catalyze the reaction by the same mechanism. Rather, evidence indicates that there are significant differences between cytochrome P-450 and peroxidase oxidations. The similarities in protein binding characteristics of the reactive metabolites derived from these enzymes are expected in light of the comproportionation equilibrium observed with quinone couples.

D. EXPERIMENTAL

1. MATERIALS

The same instruments and methods listed in Chapter II were used to accomplish the following: mass spectra, NMR spectra, infared spectra, thin layer chromatography, HPLC, counting of radioactive samples, melting points, controlled temperature incubations, and liver microsome

preparation.

Glutathione, horseradish peroxidase (type II), superoxide dismutase (type I), catalase (bovine liver), bovine serum albumin, and xanthine were purchased from Sigma Chemical Company. Acetaminophen was purchased from either Eastman Chemical Company (Rochester, NY), or Aldrich Chemical Company (Milwaukee, WI). Xanthine oxidase was obtained from Dr. Irwin Fridovich, Department of Biochemistry, Duke University. Chromatography solvents were purchased from Matheson, Coleman and Bell (Norwood, OH), or Waters Associates. Acetic-1-^{14}C-anhydride, ^{14}C-p-nitrophenol, and ^{3}H-acetaminophen were obtained from New England Nuclear Corporation (Boston, MA). ^{3}H-Acetaminophen was purified by a combination of TLC and HPLC as in Chapter II.

2. METHODS

Studies of Horseradish Peroxidase-Catalyzed Protein Binding of Acetaminophen and Analogs

Protein binding experiments were carried out in 3.0 ml reaction mixtures containing horseradish peroxidase (0.12 units), H_2O_2 (3.0 µmoles), purified radiolabeled substrate (0.3 µmole; 1000 dpm/nmole acetaminophen and phenacetin, 670 dpm/nmole N-methylacetaminophen), and 6.0 mg of either bovine serum albumin or microsomal protein in potassium phosphate buffer (0.05 M, pH 7.4). Microsomal protein was obtained from the livers of male Swiss Webster mice (20-25 gm) per the procedures described in Chapter II. Additions were consistently made to the reaction mixtures in the following order: buffer (0.5 ml), BSA or

microsomal protein (1.0 ml, 6.0 mg protein/ml buffer), substrate (0.5 ml, 0.6 mM in buffer), H_2O_2 (0.02 ml, 150 mM in water), and finally horseradish peroxidase (1.0 ml, 0.12 units/ml buffer). Other enzymes (0.02 mg/ml superoxide dismutase, 0.2 mg/ml catalase), as well as inhibitors (0.1 mM glutathione, 1.5 mM ascorbic acid) were included with the initial buffer addition. Horseradish peroxidase reactions were run at 20°C in a Dubnoff shaker water bath for 0, 2, 4, 6, or 10 minutes as required for the time course study (see Figures 3.1, 3.2, 3.3), and terminated by the addition of ice cold trichloroacetic acid (2.0 ml). Successive washing of the precipitated protein followed by hydrolysis, Lowry protein assay, and scintillation counting of bound radiolabel were carried out as described in Chapter II. In the incubations containing glutathione, HPLC analyses were performed according to the method of Buckpitt[100] using a μBondapak C-18 column with a mobile phase of 86.5/12.5/1.0 water, methanol, and acetic acid. At a flow rate of 1.0 ml/minute the retention times were acetaminophen 9.2 minutes, and 3-S-glutathionylacetaminophen 12.1 minutes.

Detetection and Spin Trapping of an Acetaminophen Free Radical in Horseradish Peroxidase Incubations of Acetaminophen

Electron spin resonance studies were performed by Dr. G.M. Rosen, Department of Pharmacology, Duke University Medical Center, Durham, NC. The acetaminophen free radical was observed in 0.5 ml incubations with acetaminophen (1.0 mM), horseradish peroxidase (0.02 units), H_2O_2 (1.0 mM), and diethylenetriaminepentaacetic acid (1.0 mM) in potassium phosphate buffer (0.05 M, pH 7.4). The reactions of N-methylacet-

aminophen (1.0 mM) and phenacetin (1.0 mM) were performed under identical conditions.

Spin trapping of the acetaminophen free radical was done using UV photolysis and the water soluble spin trap 5,5-dimethyl-1-pyrroline-N-oxide (DMPO) prepared by the method of Bonnett.[101] Initiation was accomplished by exposing the mixture to UV light (250 nm) for 4.0 minute, after which the light source was removed and the ESR spectrum recorded.

3. SYNTHESIS

N-Methylacetaminophen

N-methylacetaminophen (N-methyl-4'-hydroxyacetanilide) was synthesized by the acetylation of p-[N-methyl]-aminophenol sulfate in a procedure similar to that used by Fernando et al.[102] With heating p-[N-methyl]-aminophenol sulfate (2.0 gm, 6.0 mmole) was dissolved in water (15 ml). Acetic anhydride (1.18 gm, 12 mmole) was added, and a white precipitate immediately formed. The reaction was heated an additional 2.0 minutes then allowed to cool to room temperature overnight. Suction filtration was used to collect the crude product (0.7 gm, 73% yield) which was then recrystallized from 1/1 methanol-chloroform to give white crystals with a melting point of 240-242°C (literature,[103] 243-245°C). Thin layer chromatography (silica, acetone) gave an R_f = 0.56 which was different than acetaminophen at R_f = 0.63. NMR (DMSO-d_6: 60 MHz) δ 1.90 (s, 3H, acetyl H), 3.10 (s, 3H, N-methyl H), 3.60 broad (s, 1H, exchangeable H), 6.75 (d, 2H, $J_{3',2'}$ = 9.0 Hz,

3', 5' aromatic H), 7.10 (d, 2H, $J_{2',3'}$ = 9.0 Hz, 2', 6' aromatic H); chemical ionization mass spectrum (methane): m/e = 166 (M+1).

^{14}C-N-Methylacetaminophen

Radiolabeled N-methylacetaminophen (N-[acetyl-1-^{14}C]-N-methyl-4'-hydroxyacetaminophen) was prepared using the same procedure as that described above. Acetic-1-^{14}C-anhydride (56.3 mCi/mmole, 1.81 mg, 0.018 mmole) was diluted with unlabeled acetic anhydride (98 mg, 0.96 mmole) and added to a solution of p-N-methylaminophenyl sulfate (160 mg, 0.465 mmole) in 2.0 ml water. The labeled N-methylacetaminophen was obtained in 80% yield, and did not require further purification as determined by thin layer chromatography (R_f = 0.56, silica, acetone) and HPLC. With injection of a known quantity of radiolabeled N-methylacetaminophen on the HPLC system previously described, collection of 1.0 minute fractions, and counting by liquid scintillation, 95% of the radioactivity was recovered as N-methylacetaminophen. The final product had a specific activity of 670 dpm/nmole.

CHAPTER IV

SYNTHESIS, CHARACTERIZATION, IN VITRO DETERMINATION, AND TOXICOLOGICAL STUDIES OF N-ACETYL-P-BENZOQUINONE IMINE

A. INTRODUCTION

Chapter IV presents the most extensive investigations contained in this work. While Chapter II provided strong evidence against N-hydroxylation in the metabolic activation of acetaminophen, and Chapter III contributed insight into alternative mechanisms for arylating metabolite formation, this section focuses on the in vitro determination, toxicity, and chemical characterization of the purported toxic acetaminophen metabolite, N-acetyl-p-benzoquinone imine (NAPQI).

Indirect evidence has accumulated which implicates NAPQI as the ultimate arylating species of acetaminophen. Studies by Mulder et al.[104] indicated that an intermediate which possessed characteristics similar to those anticipated for NAPQI was formed in the buffer decomposition of radiolabeled N-hydroxyphenacetin-O-glucuronide. Four products were monitored, including acetaminophen, acetamide, phenacetin, and 2-hydroxyphenacetin-O-glucuronide. With added protein, covalent binding was observed, while the generation of acetaminophen and acetamide were decreased. Glutathione blocked covalent binding as well as acetamide and acetaminophen formation with concomitant production of an acetaminophen-glutathione conjugate. The inclusion of

ascorbic acid also blocked covalent binding and acetamide production, but dramatically enhanced the formation of acetaminophen. It was proposed that N-hydroxyphenacetin-O-glucuronide decomposed in part to NAPQI which underwent protein conjugation, reduction, or hydrolysis. Glutathione reacted with the electrophile blocking these pathways while ascorbic acid reduced NAPQI to acetaminophen at the expense of protein binding and hydrolysis to acetamide. Since the amounts of phenacetin and 2-hydroxyphenacetin-O-glucuronide were unchanged with the additions, it was assumed that these were formed through separate routes not involving NAPQI.

Further indirect evidence has come from a number of laboratories attempting to synthesize the quinone imine. Miner and Kissinger[58] used electrochemical methods to generate NAPQI from acetaminophen in buffer. They found the compound to be moderately stable at physiological pH, decomposing through a half-order kinetic process. But, in the presence of microsomal protein it disappeared rapidly with a half-life of approximately 7 seconds. This was consistent with the observations discussed in Chapter II that the arylating intermediate should be short-lived. Electrochemically produced NAPQI was reacted with a number of thiols including glutathione, and also in accordance with previous observations was the formation of an acetaminophen-glutathione adduct. The authors were unable to detect NAPQI electrochemically as a microsomal product of acetaminophen, but did observe a distribution of unidentified products in these incubations similar to that seen when an electrochemically generated solution of NAPQI was added to microsomes.

Chemical methods for the synthesis of the proposed intermediate had also been attempted by several groups. Calder[105] initially prepared NAPQI by lead tetraacetate oxidation of acetaminophen, but this yielded only a Diels-Alder adduct structurally consistent with transitory quinone imine formation. Dehydration of N-hydroxyacetaminophen also yielded NAPQI, however the compound apparently reacted with remaining N-hydroxyacetaminophen to form several products.[106-108] Blair et al.[59,60] utilized a silver oxide oxidation of acetaminophen to produce stable benzene and chloroform solutions of NAPQI. Again the compound was found to react with glutathione producing 3-S-glutathionylacetaminophen, and thus appeared to possess characteristics common to those observed with the reactive acetaminophen metabolite.

While the use of aqueous and organic solutions of NAPQI had provided much useful information, it was believed that a more direct verification of the role of NAPQI in acetaminophen metabolism would require isolated synthetic standard. Thus, this chapter addresses first the procedures developed for synthesis of pure crystalline NAPQI.[61] Possession of this standard allowed the direct detection of NAPQI in acetaminophen incubations of purified cytochrome P-450 with cumene hydroperoxide.[62] A rapid reduction of NAPQI to acetaminophen by NADPH and NADPH-cytochrome P-450 reductase prevented detection of the metabolite in both microsomal and reconstituted incubations containing these reducing components. However, compelling evidence in the form of metabolite partitioning supported the contention that NAPQI is also a microsomal product of acetaminophen oxidation. Further studies were undertaken to characterize the nature of NAPQI interactions with

proteins, NADH, NADPH, and NADPH-cytochrome P-450 reductase, and to determine the *in vitro* and *in vivo* toxicity of the compound.[68-70]

B. RESULTS

Synthesis of N-Acetyl-p-benzoquinone Imine

The oxidation of acetaminophen to NAPQI was accomplished with silver(I)oxide in chloroform as reported by Blair,[59,60] and as commonly used in the oxidation of hydroquinones to quinones.[109,110] The actual generation of NAPQI using a 1.3-fold molar excess of Ag_2O in chloroform was straight-forward and typically successful with best yields (80%) obtained using purified starting materials and solvent. Substantial effort was required in the development of procedures for the isolation of the reaction product. The work-up was complicated by a considerable propensity of NAPQI to undergo undesirable side reactions. Final yields of NAPQI were enhanced significantly by the addition of approximately 1 mg of the free radical scavenger butylated hydroxy toluene upon reaction completion. A two step purification was employed involving elution through a Florisil (magnesium silicate) column with anhydrous diethyl ether, followed by sublimation under vacuum with heating to yield yellow cubic crystals. While the sublimation procedure produced NAPQI of high purity (>99%) as determined by normal phase HPLC, this was accomplished with the loss of as much as 50% of the product via thermal decomposition. NAPQI obtained by this method possessed spectral and physical characteristics (NMR, EIMS, CIMS, IR, UV, m.p.) consistent with its structure

and previously reported literature values.[59,60] Radiolabeled analogs of NAPQI were prepared by utilizing the corresponding radiolabeled analog of acetaminophen as starting material.

Products and Kinetics of NAPQI Decomposition in Aqueous Media

The decomposition kinetics of NAPQI in buffer were investigated by monitoring the time-dependent disappearance of the quinone imine by reverse phase HPLC. Figure 4.1 presents decomposition rate plots for NAPQI alone and with increasing concentrations of added acetaminophen. The disappearance of 0.4 mM NAPQI in 0.1 M phosphate buffer, pH 7.4, was biphasic with the second phase exhibiting half-order kinetics, indicative of a free radical process (i.e. linear fit $[NAPQI]^{\frac{1}{2}}$ vs. time).[111] An empirically derived rate constant was determined to be 1.1×10^{-4} $M^{\frac{1}{2}}s^{-1}$ with a half-life of approximately 11 minutes. The initial phase was nearly linear when plotted as second-order with an apparent rate constant of 6.25×10^{-1} $M^{-1}s^{-1}$. The inclusion of increasing concentrations of acetaminophen (8 to 80 μM) significantly increased the rate of NAPQI disappearance with the elimination of the initial second-order phase.

The products of 0.05 mM ^{14}C-NAPQI decomposition in buffer are given in the chromatogram of Figure 4.2.A. Separated by gradient elution on reverse phase HPLC, collected, and counted by liquid scintillation spectroscopy, they included acetaminophen (6.5 minutes), benzoquinone (6.8 minutes), and a series of late-eluting peaks designated A through F. The relative proportions of these compounds are given in the figure with the largest being A (32%), followed by F

FIGURE 4.1: DECOMPOSITION KINETICS PLOT FOR 0.4 mM NAPQI IN PH 7.4 BUFFER ALONE (●), AND WITH THE INCLUSION OF 8 (o), 20 (■), 40 (□), AND 80 μM (△) ACETAMINOPHEN.

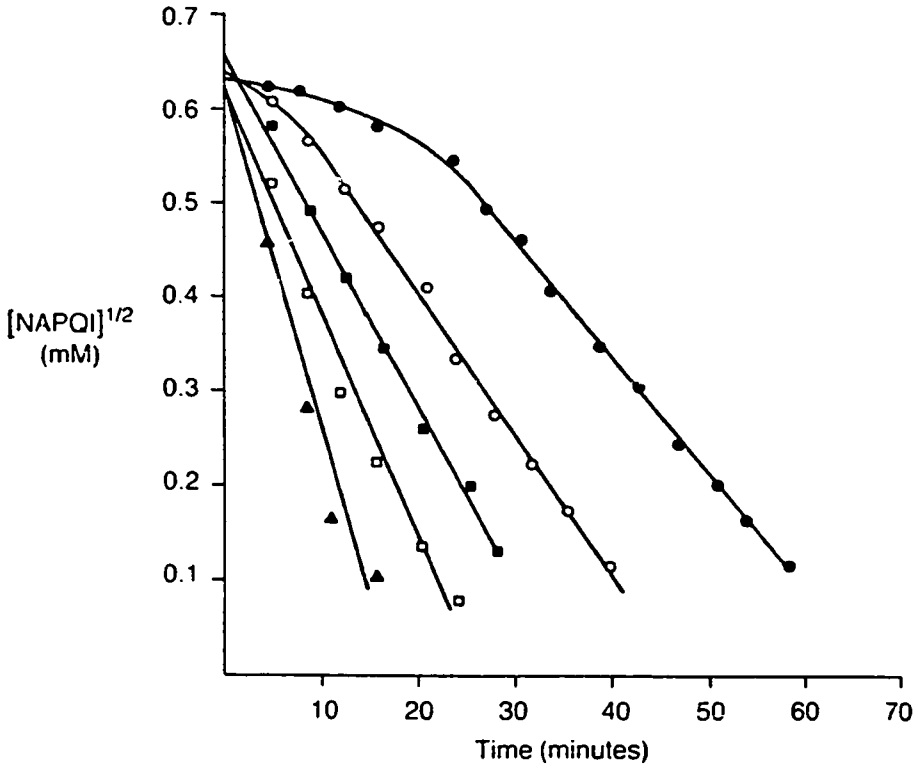
0.7
0.6
0.5
0.4
0.3
0.2
0.1
[NAPQI]1/2
(mM)
10
20
30
40
50
60
70
Time (minutes)

FIGURE 4.2: REVERSE PHASE HPLC CHROMATOGRAMS OF THE DECOMPOSITION PRODUCTS OF [RING-^{14}C]NAPQI IN BUFFER. DETECTED BY COLLECTION OF THE ELUATE AT 1.0 MINUTE INTERVALS FOLLOWED BY LIQUID SCINTILLATION SPECTROSCOPY OF THE FRACTIONS. (A) 0.05 mM NAPQI (0.21 mCI/mMOLE), (B) 1.0 mM NAPQI (0.02 mCI/mMOLE). NUMBERS IN PARENTHESES REPRESENT THE PERCENTAGE OF RECOVERED RADIOLABEL.

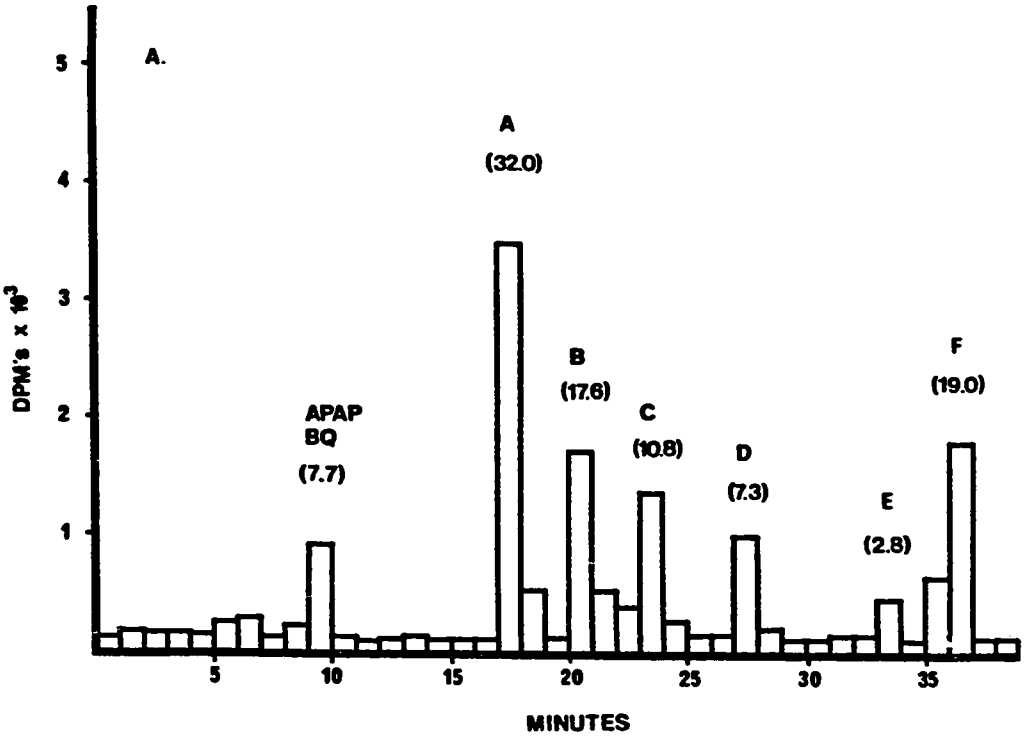
A.
A
(32.0)
B
(17.6)
C
(10.8)
D
(7.3)
E
(2.8)
F
(19.0)
APAP
BQ
(7.7)
DPM's x 10³
MINUTES

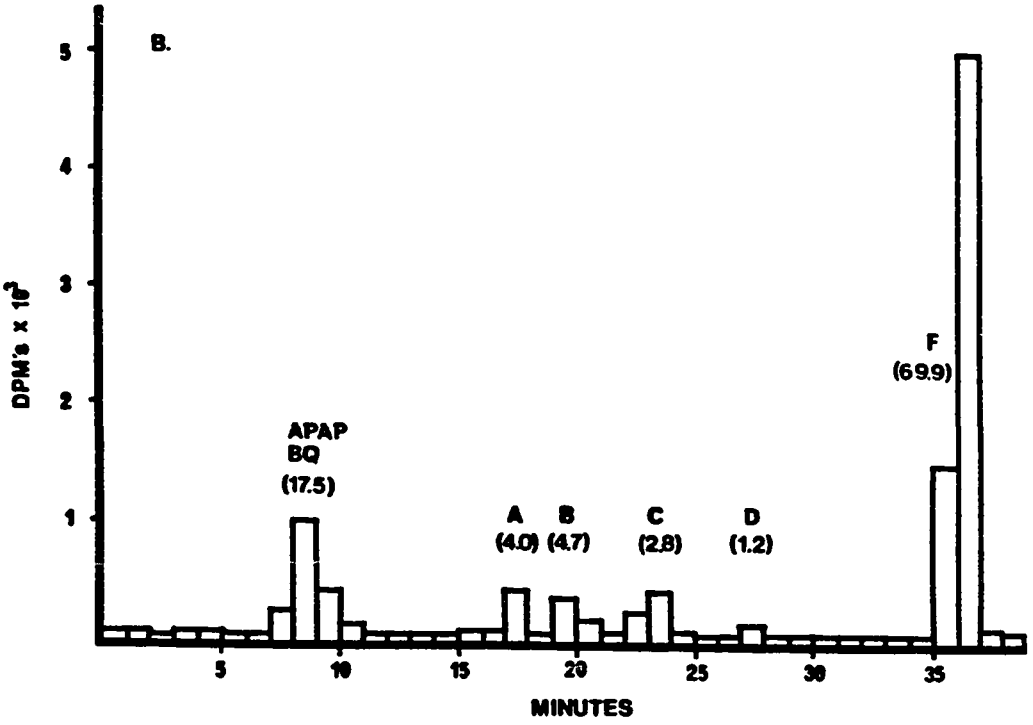
B.
F
(69.9)
APAP
BQ
(17.5)
A
(4.0)
B
(4.7)
C
(2.8)
D
(1.2)
DPM's x 10³
MINUTES

(19%). Acetaminophen and benzoquinone combined accounted for approximately 8% of the radioactivity. Although not resolved in this chromatogram, other reverse phase systems successfully separated these two products showing hydrolytically derived benzoquinone to be a minor (1 to 2%) component (data not shown). Increasing the concentration of ^{14}C-NAPQI in the decomposition reaction from 0.05 mM to 1.0 mM had a significant effect on the partioning of the products. As seen in Figure 4.2.B, component F increased dramatically (70% of injected radiolabel) while acetaminophen showed a more moderate increase (to 18%). Peak E was not detectable in the higher concentration reaction mixture.

The late-eluting compounds A-F were separated from a larger scale decomposition reaction (200 ml, 3.0 mM NAPQI) by semipreparatory reverse phase HPLC. Requiring further purification, the fractions were then subjected to semipreparatory normal phase HPLC. The purified fractions were analyzed by direct insertion probe mass spectroscopy with only A producing an acceptable spectrum. Due to thermal decomposition B through F did not provide structural information regardless of source temperature or ionization mode. Figure 4.3 shows the results of high resolution EIMS analysis of component A. The spectrum is characterized by a parent ion at m/e 300 with fragments at m/e 258 ($M^{+}\cdot$ $-CH_2CO$), and 216 ($M^{+}\cdot$ $-2CH_2CO$). The elemental composition of all ions was confirmed by high resolution mass measurements, and the spectrum corresponds to an acetaminophen dimer. It was assumed that products B through F were also oligomeric products of NAPQI radical reactions.

FIGURE 4.3: CHEMICAL IONIZATION MASS SPECTRUM OF COMPONENT A ISOLATED BY HPLC FROM THE NAPQI DECOMPOSITION REACTION MIXTURE.

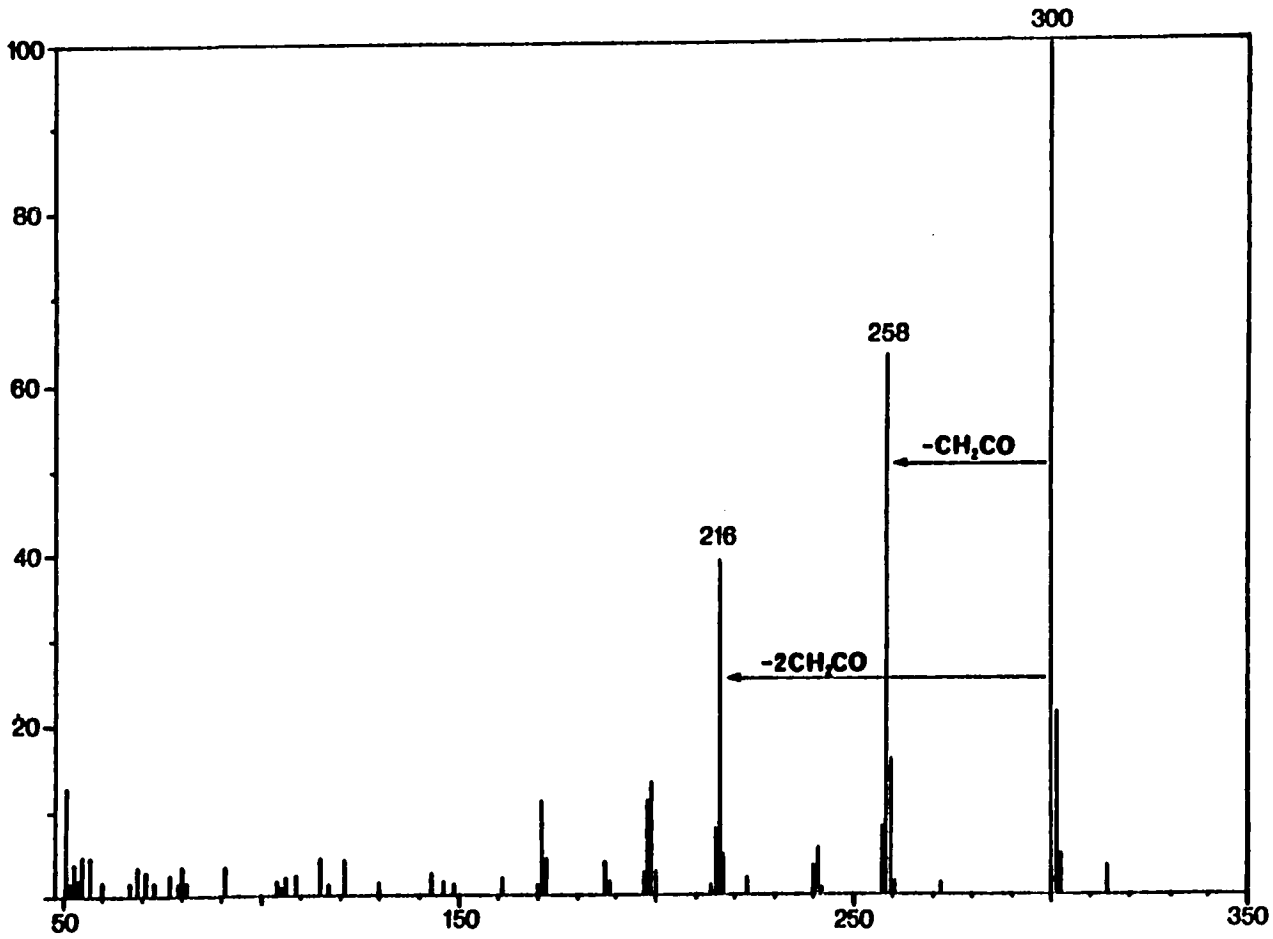
300
100
80
258
60
-CH2CO
216
40
-2CH2CO
20
50
150
250
350

Reduction of NAPQI by NADPH and NADH

Figure 4.4 presents the data from studies of the reduction of NAPQI by NADPH in 0.1 M phosphate buffer, pH 7.4. Followed by reverse phase HPLC, the predominant product of this process with reactants at equimolar concentration (0.5 mM) was acetaminophen with small amounts of benzoquinone (approximately 2%). The disappearance of NADPH was also monitored under the same conditions by UV absorbance at 340 nm. As can be seen from Figure 4.4, the decline in NADPH concentration was rapid and essentially complete in 3 to 4 minutes. In experiments substituting NADH for NADPH the resulting plots were identical to Figure 4.4 (data not shown).

The kinetics of the reduction process were determined to be second-order by monitoring the time dependent disappearance of NADPH (UV, 340 nm) both with equimolar reactants and with an excess of NADPH (pseudo-first-order). Figure 4.5 shows the oxidation of 0.5 mM NADPH by 0.5 mM NAPQI plotted as 1/[NAPQI] versus time (second-order, special case where substrates equimolar: $k_2t = 1/[a-x] - 1/[a]$).[112] The reaction was linear for less than 2 minutes due to significant competing reactions of NAPQI decomposition. The second-order rate constant was determined to be k = 3.81 $mmol^{-1}min^{-1}$. To confirm this, NAPQI reduction kinetics were also examined under pseudo-first-order conditions. Figure 4.6 shows the oxidation of excess NADPH by NAPQI plotted as first-order. With NADPH held constant at 0.5 mM and NAPQI varied from 0.06 to 0.25 mM a series of first-order rate constants were obtained and plotted against the concentration of NAPQI in Figure 4.7. By the method of Bruice[113] the slope of the resulting line gave

FIGURE 4.4: PLOTS OF THE TIME COURSE OF THE REACTION BETWEEN NADPH AND NAPQI AT EQUIMOLAR (0.5 mM) CONCENTRATIONS. (---) OXIDATION OF NADPH MEASURED BY CONTINUOUS UV MONITOR AT 340 NM; (△) ACETAMINOPHEN AND (■) BENZOQUINONE DETERMINED BY THE RADIOCHEMICAL HPLC ASSAY DESCRIBED IN METHODS.

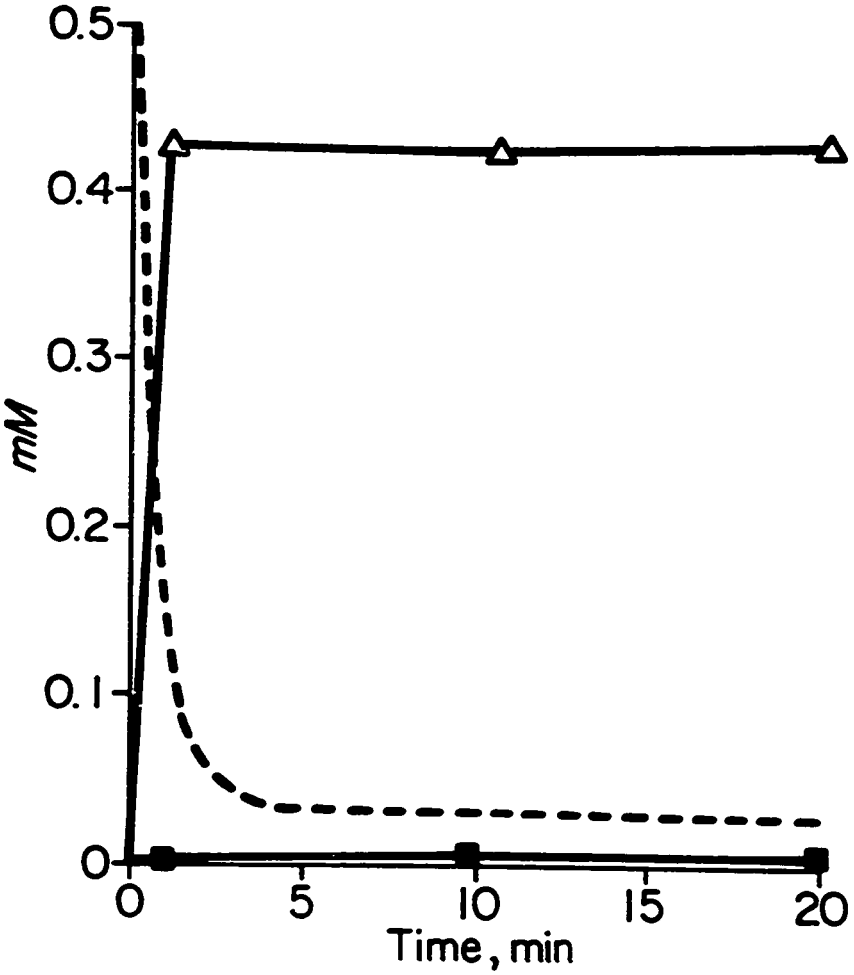
0.5
0.4
0.3
0.2
0.1
0
mM
0
5
10
15
20
Time, min

FIGURE 4.5: SECOND-ORDER PLOT OF THE OXIDATION OF NADPH BY NAPQI AT EQUIMOLAR (0.5 mM) CONCENTRATIONS. THE DISAPPEARANCE OF NADPH WAS MONITORED BY UV ABSORBANCE AT 340 NM. FROM THE SLOPE K_2 = 3.81 $mM^{-1}MIN^{-1}$.

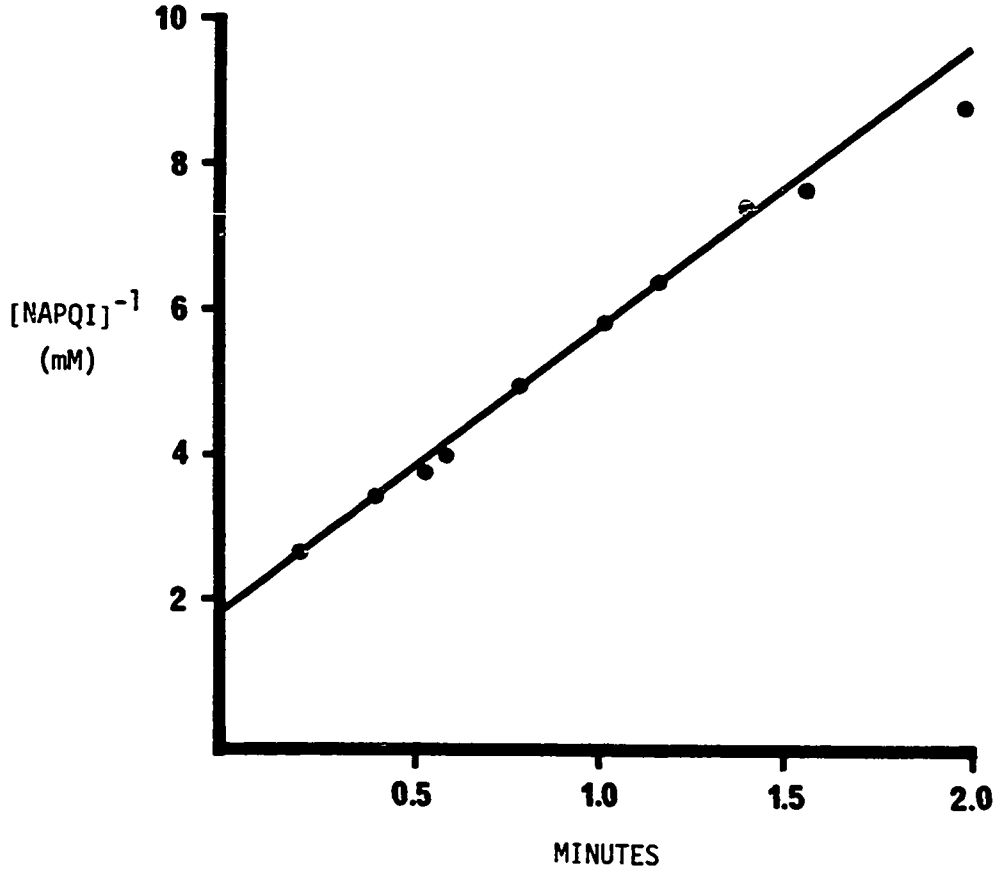
10
8
6
4
2
[NAPQI]$^{-1}$
(mM)
0.5
1.0
1.5
2.0
MINUTES

FIGURE 4.6: FIRST-ORDER PLOTS OF THE OXIDATION OF NADPH BY NAPQI IN REACTIONS CONTAINING AN EXCESS OF NADPH. NADPH WAS HELD AT A CONSTANT CONCENTRATION OF 0.5 mM AND NAPQI WAS VARIED AT 0.0625 mM (●), 0.125 mM (■), AND 0.25 mM (▲). THE REACTION WAS FOLLOWED BY MONITORNG NADPH OXIDATION AT 340 NM.

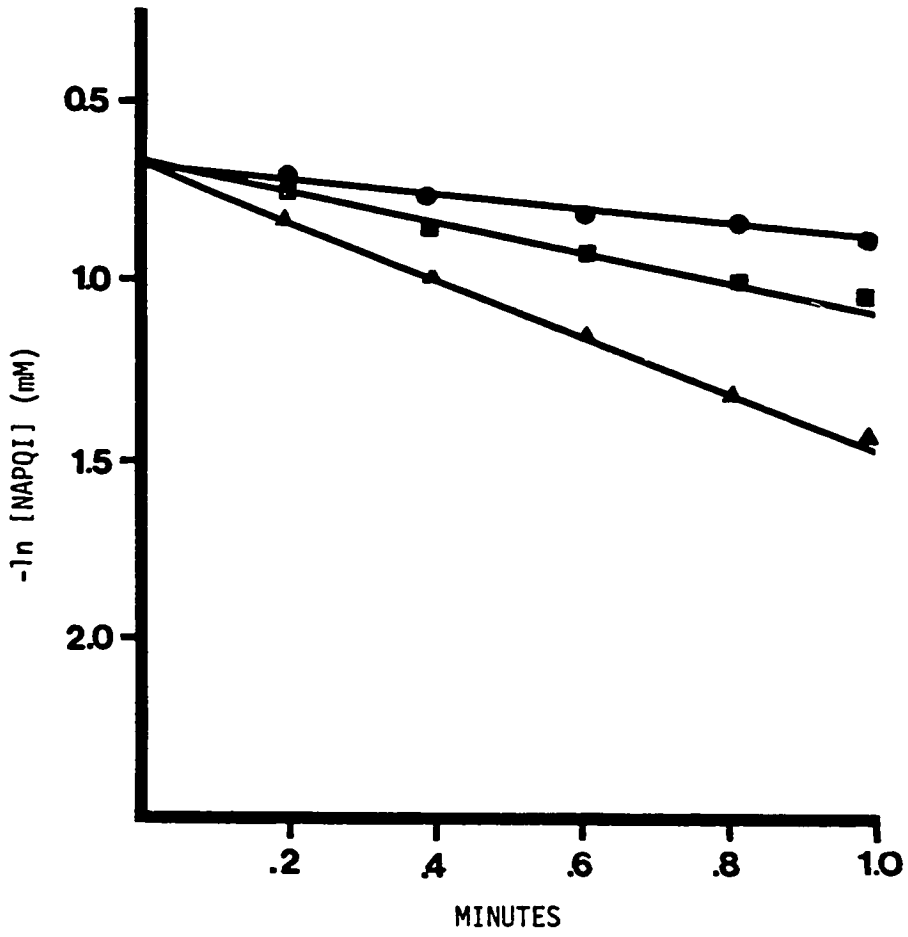
0.5
1.0
1.5
2.0
-ln [NAPQI] (mM)
.2
.4
.6
.8
1.0
MINUTES

FIGURE 4.7: PLOT OF FIRST-ORDER RATE CONSTANTS VERSUS THE CONCENTRATION OF NAPQI. K_2 WAS DETERMINED FROM THE SLOPE TO BE 3.68 $mM^{-1}MIN^{-1}$.

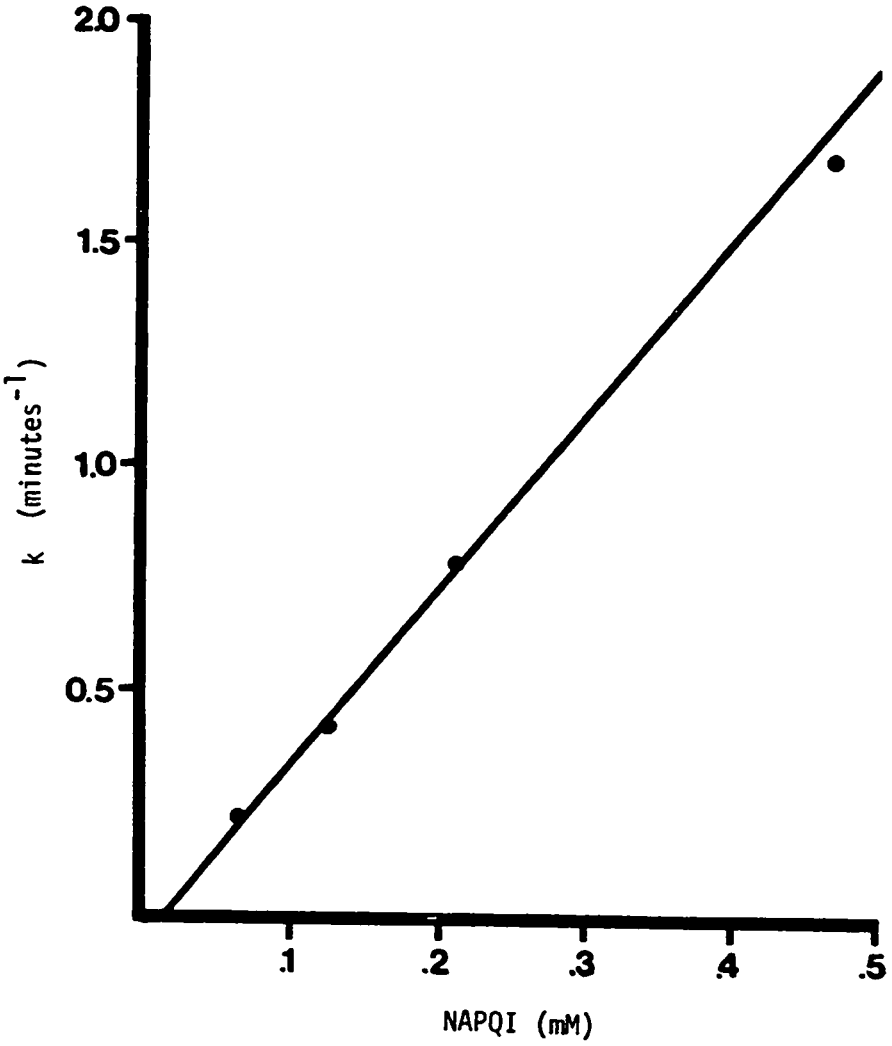
2.0
1.5
1.0
0.5
k (minutes^{-1})
.1
.2
.3
.4
.5
NAPQI (mM)

the second-order rate constant as k_2 = 3.68 $mmol^{-1}min^{-1}$, in agreement with the value obtained under equimolar conditions. As a comparison, the kinetics of benzoquinone reduction by NADPH were also investigated. Data from this study are plotted in Figure 4.8 as 1/[NAPQI] versus time. At equimolar concentrations 0.5 mM NADPH was oxidized by benzoquinone at a rate less than one-tenth that by NAPQI (k_2 = 0.32 $mM^{-1}min^{-1}$).

Reduction of NAPQI by NADPH and NADPH-Cytochrome P-450 Reductase

The enzyme-catalyzed reduction of NAPQI was examined. Figure 4.9 shows a Lineweaver-Burke plot for the metabolism of NAPQI by NADPH and NADPH-cytochrome P-450 reductase. Correction was made for the non-enzymatic reduction of NAPQI by NADPH. Data were obtained by monitoring NADPH oxidation (UV, 340 nm), and the following kinetic constants were calculated: K_m = 4.0 μM; V_{max} = 29.4 μmol/min/mg. The distinct upward turn of the double-reciprocal plot at higher NAPQI concentrations was indicative of substrate inhibition at concentrations above approximately 10 μM. Because of the difficulty in accurately determining the K_m from data at low NAPQI concentrations, an alternative approach was adopted. This was based on measuring the inhibition of NADPH-cytochrome P-450 reductase-mediated reduction of cytochrome c at low concentrations of NAPQI. With cytochrome c, NADPH, and NADPH-cytochrome P-450 reductase present, and varying the concentration of NAPQI, the reduction of cytochrome c was followed by UV absorbance at 550 nm. Figure 4.10 shows an initial inhibition of cytochrome c reduction by NAPQI that diminished with the time dependent metabolism of the quinone imine. Reciprocals of the initial

FIGURE 4.8 SECOND-ORDER PLOT OF THE OXIDATION OF NADPH BY BENZOQUINONE MONITORED BY THE DISAPPEARANCE OF NADPH AT 340 NM. FROM THE SLOPE K_2 WAS CALCULATED AS 0.32 $mM^{-1}MIN^{-1}$.

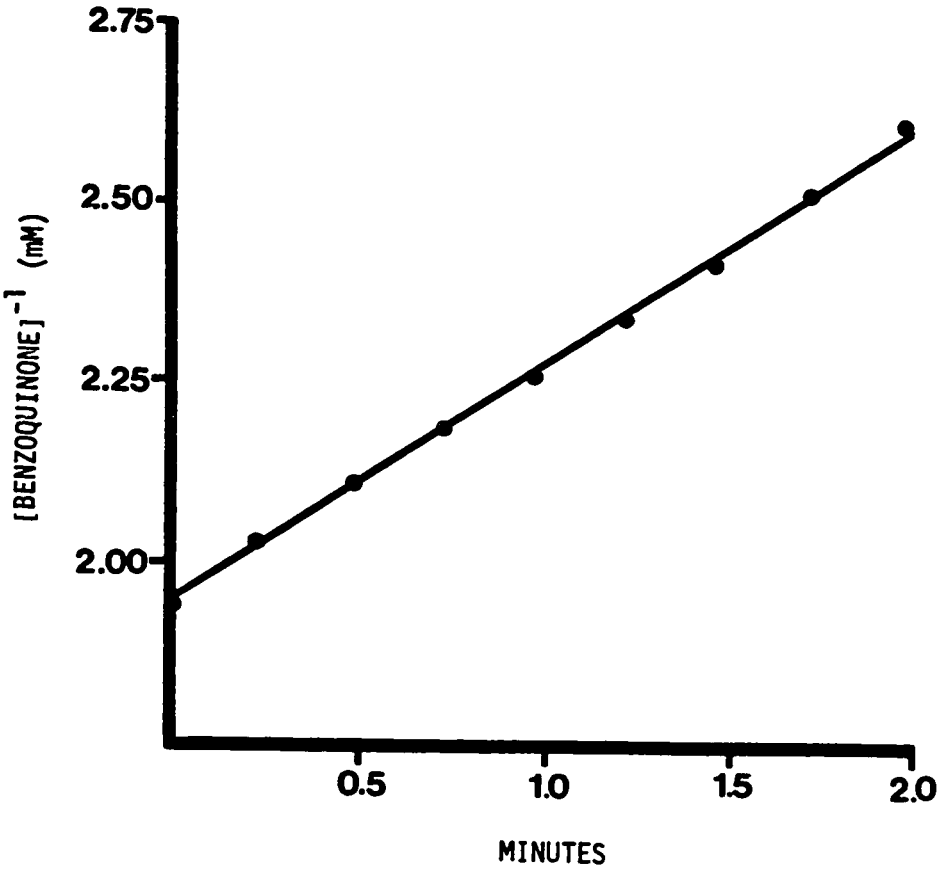
2.75
2.50
2.25
2.00
[BENZOQUINONE]$^{-1}$ (mM)
0.5
1.0
1.5
2.0
MINUTES

FIGURE 4.9: LINEWEAVER-BURKE PLOT FOR THE METABOLISM OF NAPQI BY NADPH-CYTOCHROME P-450 REDUCTASE. NADPH OXIDATION WAS MEASURED AT 340 NM.

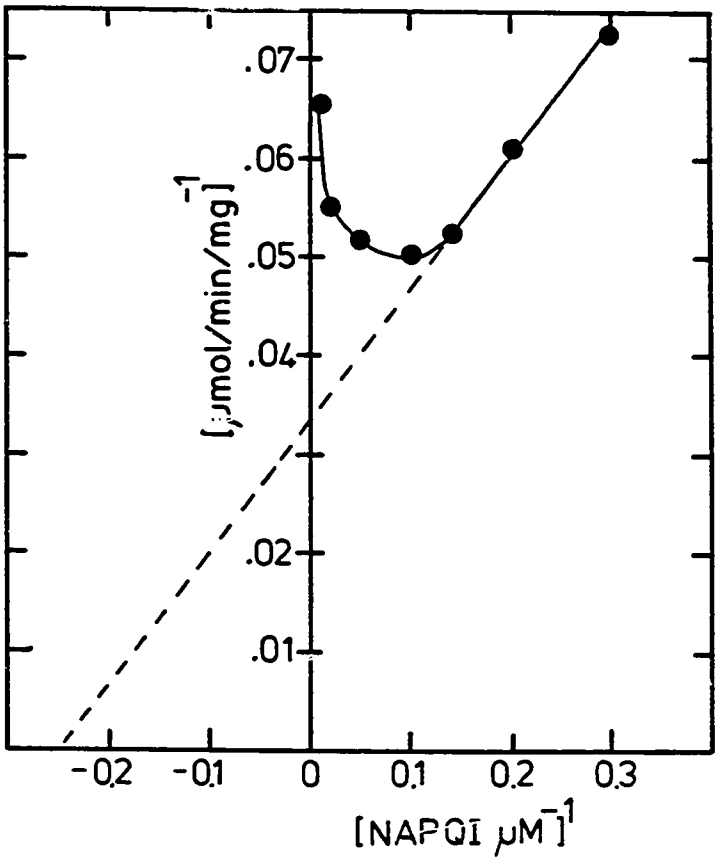
.07
.06
.05
.04
.02
.01
[μmol/min/mg]$^{-1}$
-0.2
-0.1
0
0.1
0.2
0.3
[NAPQI μM^{-1}]$^{-1}$

FIGURE 4.10: TIME-DEPENDENT NAPQI INHIBITION OF CYTOCHROME C REDUCTION BY NADPH-CYTOCHROME P-450 REDUCTASE. THE REACTION WAS INITIATED BY THE ADDITION OF 0.5 mM NADPH AT THE ARROW AND FOLLOWED BY MONITORING CYTOCHROME C REDUCTION AT 550 NM. VALUES NEXT TO THE RECORDINGS ARE NAPQI CONCENTRATIONS IN μM.

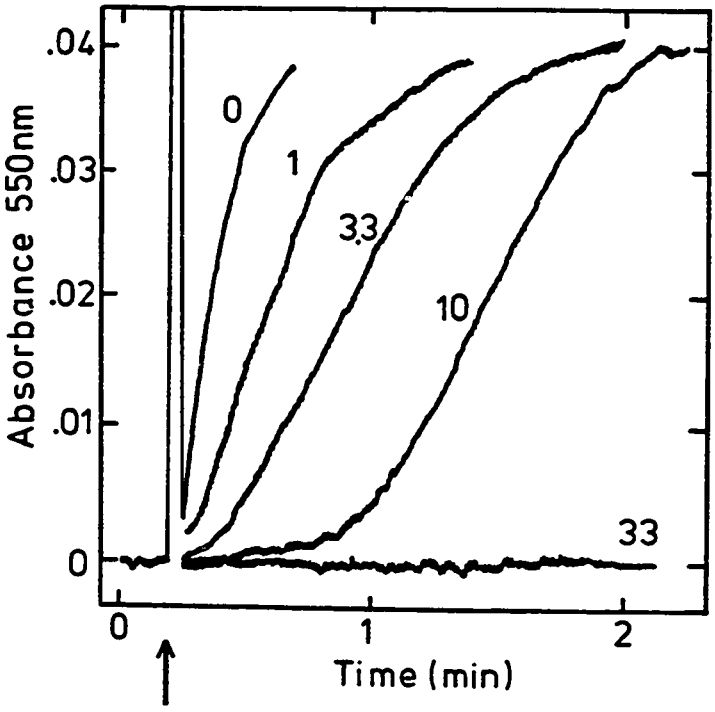
.04
.03
.02
.01
0
Absorbance 550nm
0
1
33
10
33
0
1
2
Time (min)

velocities from these curves were plotted against reciprocal cytochrome c concentrations in Figure 4.11, resulting in a series of slopes corresponding to the inhibitor concentrations. The inhibition of cytochrome c reduction by NAPQI shows some characteristics of noncompetitive inhibition with failure of all points to intersect at the ordinate, but this may be due to a rapid lowering of NAPQI levels through decomposition and enzymatic reduction. With the assumption of competitive inhibition a replot of the obtained slopes versus inhibitor concentration gave a K_I of 1.8 μM.

In spite of the relatively rapid rate of NAPQI metabolism by NADPH-cytochrome P-450 reductase, no superoxide formation could be detected as measured by reduction of acetylated cytochrome c (UV, 550 nm) either in the presence or or in the absence of superoxide dismutase (Table 4.1). Further, superoxide generation by the reductase metabolism of 2,5-dimethylbenzoquinone was blocked by the addition of NAPQI (Table 4.1).

Inhibition of Acetaminophen In Vitro Protein Binding by NADH, NADPH, and NADPH-Cytochrome P-450 Reductase

The reductants of NAPQI studied in the two preceding sections were found to be inhibitors of acetaminophen protein binding in reconstituted P-450 incubations with added BSA. Figure 4.12 shows the results of protein binding experiments in purified cytochrome P-450 incubations of [ring-^{14}C]acetaminophen with either increasing levels of NADPH, or increasing levels of NADH in the presence of an NADPH regenerating system. In the incubations containing the regenerating

FIGURE 4.11: LINWEAVER-BURKE ANALYSIS OF THE NAPQI INHIBITION OF CYTOCHROME C REDUCTION BY NADPH-CYTOCHROME P-450 REDUCTASE. THE REDUCTION OF CYTOCHROME C WAS FOLLOWED AT 550 NM UNDER CONDITIONS INCLUDING: NO NAPQI (●); 0.5 μM NAPQI (□); 1.0 μM NAPQI (○); AND 3.3 μM NAPQI (△).

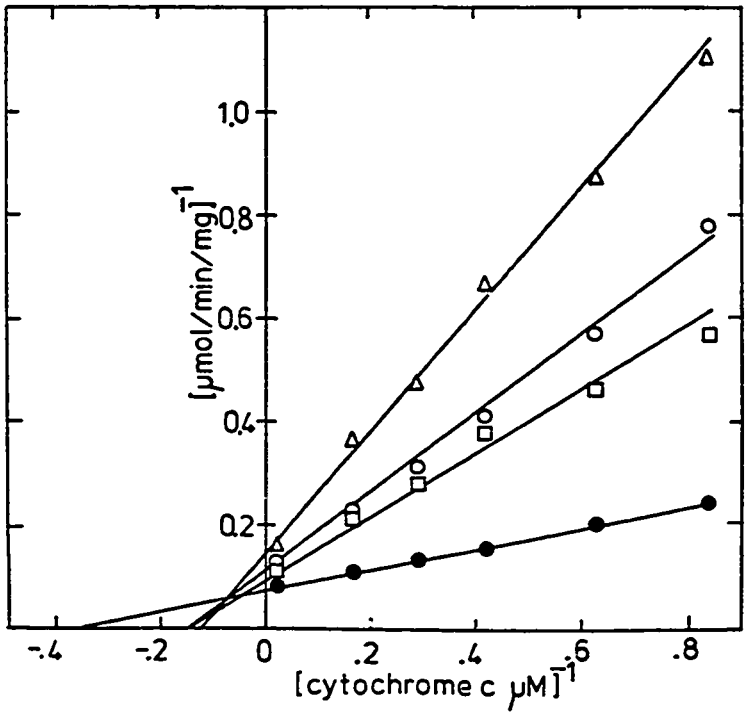
1.0
0.8
0.6
0.4
0.2
[μmol/min/mg]$^{-1}$
-.4
-.2
0
.2
.4
.6
.8
[cytochrome c μM]$^{-1}$

TABLE 4.1

THE EFFECT OF NAPQI ON SUPEROXIDE FORMATION AND ON QUINONE-STIMULATED SUPEROXIDE FORMATION IN INCUBATIONS OF NADPH-CYTOCHROME P-450 REDUCTASE

Conditions	$O_2^{\cdot-}$ Formation nmol/min/mg	10^{-4} M NAPQI nmol/min/mg
Control	31.3 ± 4.8	0.0
10^{-4} M 2,5-Dimethyl-benzoquinone	9465 ± 155	0.0

Incubation conditions are described in text. Superoxide formation was measured as the reduction of acetylated cytochrome c at 550 nm, 37°C. Control incubations contained 0.66 µg/ml SOD. Values represent the mean ± S.D. of three determinations.

FIGURE 4.12: GRAPH ILLUSTRATING THE EFFECTS OF INCREASING CONCENTRATIONS OF NADPH (●) AND NADH (○) ON CYTOCHROME P-450-MEDIATED COVALENT BINDING OF [RING-^{14}C]ACETAMINOPHEN TO BSA. POINTS REPRESENT THE AVERAGE OF THREE SEPARATE INCUBATIONS AND INDIVIDUAL RESULTS DID NOT VARY MORE THAN 13% FROM THE MEAN. PROTEIN BINDING WAS DETERMINED AS DESCRIBED IN METHODS, CHAPTER II.

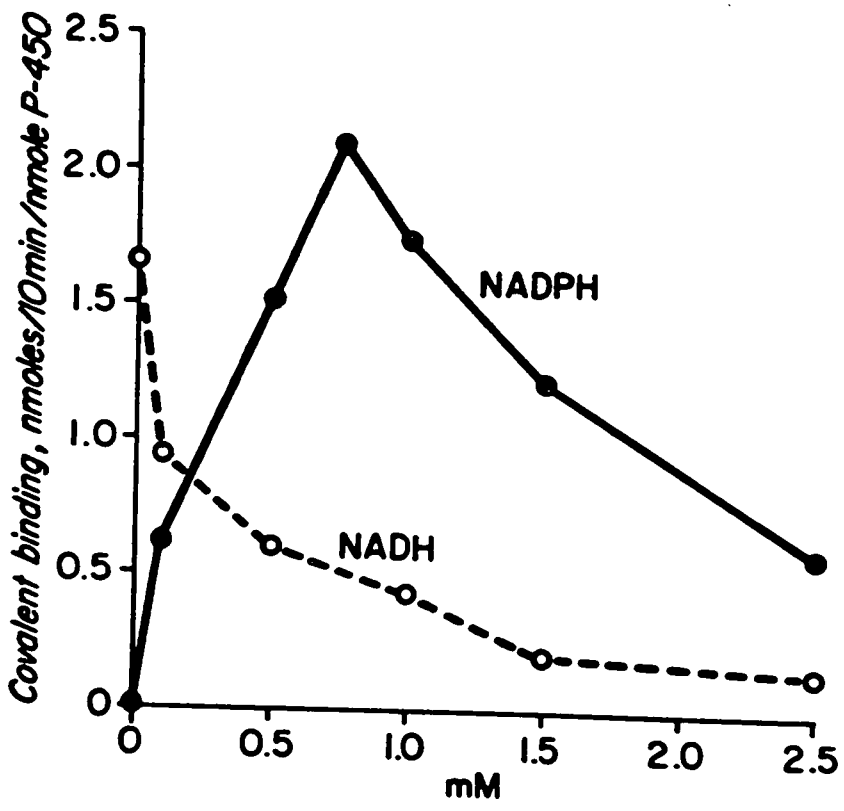
Covalent binding, nmoles/10min/nmole P-450
2.5
2.0
1.5
1.0
0.5
0
NADPH
NADH
0
0.5
1.0
1.5
2.0
2.5
mM

system plus varied concentrations of NADH, covalent binding decreased with increasing NADH, indicating inhibition by the added cofactor. With the addition of NADPH alone, covalent binding increased to a maximum at approximately 0.8 mM NADPH with reaction cofactor dependence, then dropped off as excess NADPH inhibited the binding process.

The effects of NADPH-cytochrome P-450 reductase on acetaminophen metabolite binding to BSA were also investigated. Purified NADPH-cytochrome P-450 reductase was added to reconstituted cytochrome P-450 incubations giving a range of molar reductase to P-450 ratios of 0.2 to 10. Figure 4.13 contains the results of acetaminophen protein binding measurements made in the reductase-fortified incubations supported by an NADPH regenerating system. Similar to that observed with the previous NADPH inhibition experiments, a binding maximum was reached corresponding to the optimal conditions (reductase/P-450 = 1.4) for arylating metabolite formation and binding; it then decreased with additional reductase activity due to the enzyme-catalyzed reduction of NAPQI.

Detection of NAPQI as a Product of Cytochrome P-450 Oxidation of Acetaminophen

NAPQI was detected as an oxidation product of acetaminophen in cumene hydroperoxide-supported incubations of hepatic cytochrome P-450 purified from phenobarbital pretreated rats. Three methods of NAPQI identification were used: (1) reductive electrochemical detection of an enzymatic reaction product with the same reverse phase HPLC retention time as synthetic NAPQI; (2) measurements of radioactivity

FIGURE 4.13: THE EFFECT OF INCREASING THE CONCENTRATION OF PURIFIED NADPH-CYTOCHROME P-450 REDUCTASE ON THE COVALENT BINDING OF [RING-^{14}C]-ACETAMINOPHEN TO BSA IN INCUBATIONS OF CYTOCHROME P-450. POINTS REPRESENT THE AVERAGE OF THREE EXPERIMENTS.

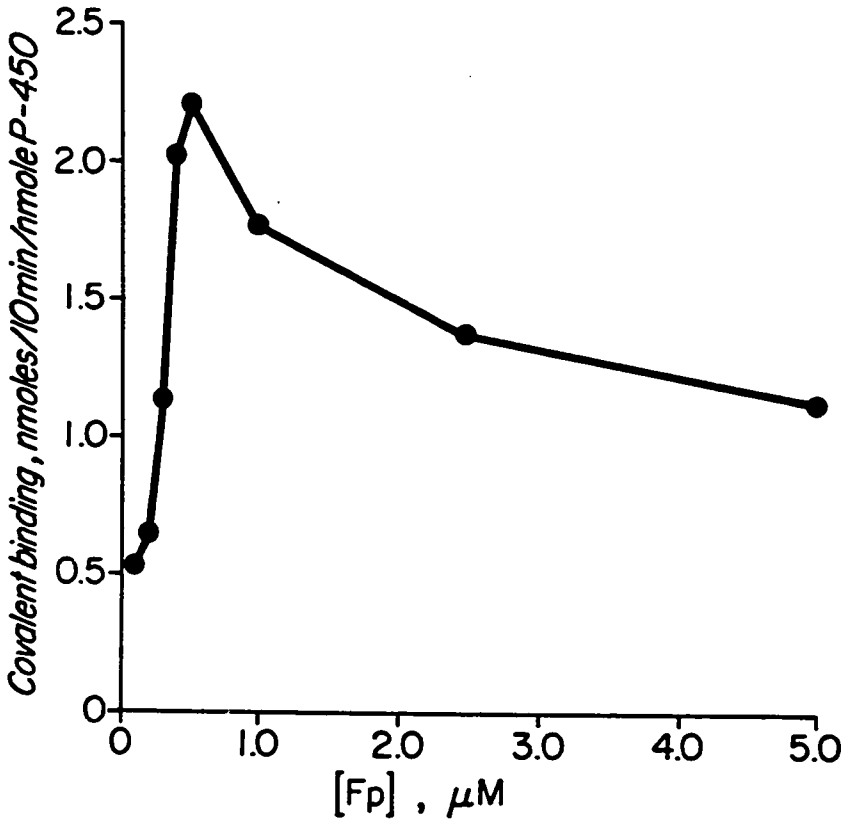
Covalent binding, nmoles/10min/nmole P-450
2.5
2.0
1.5
1.0
0.5
0
0
1.0
2.0
3.0
4.0
5.0
[Fp] , μM

in this product enzymatically derived from ^{14}C-acetaminophen; and (3), collection of the radiolabeled product followed by reduction by L-ascorbic acid to yield ^{14}C-acetaminophen.

Reverse phase HPLC chromatograms monitored by UV detection (254 nm) from incubations containing acetaminophen, purified cytochrome P-450, and cumene hydroperoxide showed only acetaminophen and cumene hydroperoxide (Figure 4.14.A). However, from the same incubations a peak was consistently observed by more sensitive reductive electrochemical detection at the retention time of NAPQI (Figure 4.14.C). From control incubations omitting P-450 or cumene hydroperoxide this peak was not present (Figure 4.14.B). The mean NAPQI concentration (± S.D.) in four complete incubations was (2.6 ± 0.3) x 10^{-7} M. Benzoquinone, a hydrolysis product of NAPQI, was also detected in these incubations at the retention time of acetaminophen (I), but background noise surrounding this peak precluded its quantitation.

Similarly, NAPQI was detected in ^{14}C-acetaminophen incubations with purified cytochrome P-450 and cumene hydroperoxide as a radiolabel-containing peak at the retention time of synthetic NAPQI (Figure 4.14.F). NAPQI was not detected by either UV techniques in complete incubations (Figure 4.14.D), or by scintillation spectroscopy of collections in control incubations (Figure 4.14.E) lacking P-450 or cumene hydroperoxide. The mean concentration of NAPQI (± S.D.) in four complete incubations was (3.4 ± 0.8) x 10^{-7} M as determined from the specific activity of the substrate.

As further evidence that the eluted radiolabel was NAPQI, the ^{14}C-containing peak and 1.0 minute fractions before and after were

FIGURE 4.14: REVERSE PHASE HPLC CHROMATOGRAMS OF NAPQI GENERATED IN ACETAMINOPHEN INCUBATIONS WITH PURIFIED CYTOCHROME P-450 AND SUPPORTED BY CUMENE HYDROPEROXIDE. A, B, AND C WERE PERFORMED WITH CITRATE BUFFER/METHANOL MOBILE PHASE (SEE RESULTS) USING TANDEM DETECTION BY UV AND ELECTROCHEMICAL METHODS. RETENTION TIMES ON THIS SYSTEM WERE ACETAMINOPHEN 6.2 MINUTES (I) AND NAPQI 8.8 MINUTES (II). CHROMATOGRAM A RESULTED FROM UV DETECTION WHILE B AND C ARE FROM ELECTROCHEMICAL DETECTION. A AND C REPRESENT COMPLETE INCUBATIONS INCLUDING ACETAMINOPHEN, P-450, AND CUMENE HYDROPEROXIDE. CHROMATOGRAM B WAS DERIVED FROM AN INCUBATION OMITTING P-450 AND IS REPRESENTATIVE OF THE CONTROLS. THE LEVELS OF NAPQI DETECTED ELECTROCHEMICALLY WERE $(2.6 \pm 0.3) \times 10^{-7}$ M. D, E AND F ARE FROM INCUBATIONS THAT USED [RING-^{14}C]ACETAMINOPHEN (9.78 MCI/MMOL) AS SUBSTRATE, AND SEPARATION WAS ACCOMPLISHED WITH THE PHOSPHATE BUFFER/METHANOL MOBILE PHASE (SEE RESULTS). ON THIS REVERSE PHASE SYSTEM ACETAMINOPHEN WAS RETAINED 7.4 MINUTES (I) AND NAPQI 11.8 MINUTES (II). CHROMATOGRAM D WAS MONITORED BY UV WHILE E AND F ARE REPRESENTED BY BAR PLOTS OF RADIOACTIVITY CONTAINED IN 15-SECOND FRACTIONS OF THE ELUATE. D AND F REPRESENT COMPLETE INCUBATIONS INCLUDING ACETAMINOPHEN, P-450, AND CUMENE HYDROPEROXIDE WHILE C IS THE CHROMATOGRAM OF A REPRESENTATIVE CONTROL OMITTING P-450. THE LEVELS OF NAPQI DETECTED RADIOMETRICALLY WERE $(3.4 \pm 0.8) \times 10^{-7}$ M. THE PEAK RECORDED IN THE UV-DETECTED CHROMATOGRMS BETWEEN ACETAMINOPHEN AND NAPQI WAS DUE TO CUMENE HYDROPEROXIDE.

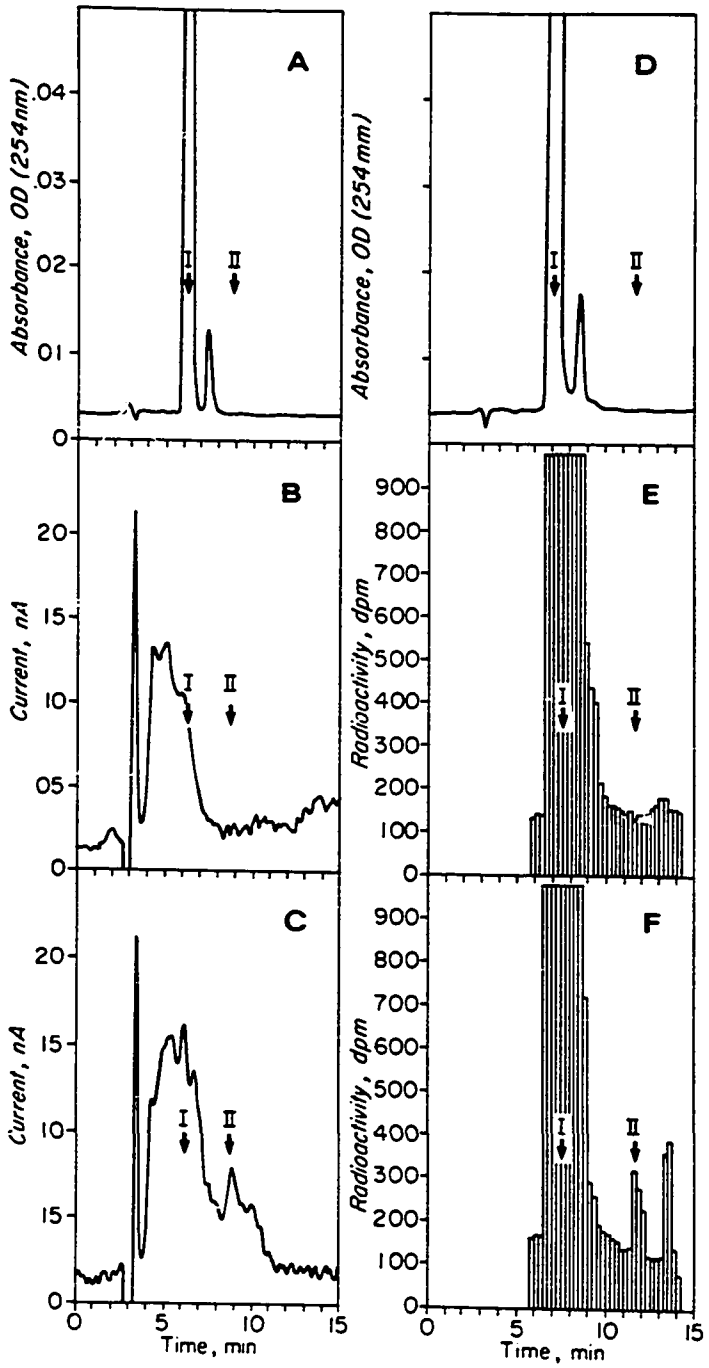
A
B
C
D
E
F
Absorbance, OD (254nm)
Current, nA
Radioactivity, dpm
Time, min
I
II

collected directly into vials containing 5 μl of 1.0 mM ascorbic acid in water. Ascorbate reduced NAPQI to acetaminophen (determined by HPLC to be complete within 15 seconds at equimolar concentration) which was then reanalyzed by reverse phase HPLC. Approximately 88% of the radioactivity collected in the NAPQI peak was accounted for as acetaminophen, whereas the samples derived from the collections 1.0 minute before and after the NAPQI peak eluted no radioactivity with acetaminophen.

The same methods were used in attempts to detect NAPQI formation from acetaminophen in incubations of purified cytochrome P-450 with NADPH and NADPH-cytochrome P-450 reductase, and in mouse liver microsomes with an added NADPH regenerating system. In all cases NAPQI steady state concentrations were below detection limits of 1.1×10^{-7} M, established by generating NAPQI standard curves and calculating as defined by IUPAC using the propagation of errors approach.[114] The inability to detect the quinone imine in these systems was likely due to the rapid reduction of NAPQI back to acetaminophen by NADPH and NADPH-cytochrome P-450 reductase as supported by data previously presented. Therefore, alternative methods were used to determine whether NAPQI was an oxidation product of acetaminophen in these systems.

Metabolite Partitioning Studies of Acetaminophen and NAPQI in Microsomal Incubations

Evidence for the formation of NAPQI from acetaminophen in microsomal incubations with an NADPH regenerating system was obtained by comparing the metabolic fate of acetaminophen and synthetic NAPQI. Because microsomes from mouse liver are significantly more active in the generation of acetaminophen metabolites than those from rat liver, they were used in these studies.[41,115]

In incubations fortified with an NADPH regenerating system [ring-^{14}C]acetaminophen covalently bound to microsomal protein to a slightly lesser extent than [ring-^{14}C]NAPQI at substrate concentrations of 1.0 mM and 0.05 mM, respectively (Table 4.2). Omission of the NADPH regenerating system virually eliminated the binding of acetaminophen, whereas NAPQI binding was increased approximately 4-fold. The addition of either L-ascorbic acid or glutathione decreased the binding of both compounds markedly.

Previously, it had been shown that the aromatic ring of the arylating acetaminophen metabolite was bound to a greater degree than the acetyl group.[116] Both [acetyl-^{14}C]acetaminophen and [acetyl-^{14}C]-NAPQI were bound to microsomal protein to a lesser extent than their ring-^{14}C analogs with approximately the same ratio of label retention (Table 4.2). In the incubations of acetyl-labeled acetaminophen and NAPQI, ^{14}C-acetamide was detected as the released product by HPLC.

The partioning of [ring-^{14}C]NAPQI to its reduction product, acetaminophen, and conjugation products, 3-S-glutathionylacetaminophen and protein bound material, was determined by reverse phase HPLC and

TABLE 4.2

EFFECTS OF NADPH, L-ASCORBIC ACID, GLUTATHIONE AND SITE OF RADIOLABEL ON THE COVALENT BINDING OF REACTIVE METABOLITES OF ACETAMINOPHEN AND NAPQI TO MOUSE LIVER MIRCOSOMAL PROTEIN

Substrate	Covalent Binding nmoles/incubation	% of Control
[Ring-^{14}C]Acetaminophen (1 mM)	12.5 ± 1.0	100.0
- NADPH Regenerating System	0.0 ± 0.0	0.0
+ L-Ascorbic Acid (1 mM)	1.9 ± 0.2	14.8
+ Glutathione (1 mM)	1.5 ± 0.1	12.0
[Acetyl-^{14}C]Acetaminophen (1 mM)	10.1 ± 1.4	80.8
[Ring-^{14}C]NAPQI (50 μM)	18.3 ± 1.2	100.0
- NADPH Regenerating System	70.5 ± 3.2	385.0
+ L-Ascorbic Acid (1 mM)	2.6 ± 0.2	14.2
+ Glutathione (1 mM)	2.7 ± 1.9	14.7
[Acetyl-^{14}C]NAPQI (50 μM)	14.8 ± 1.9	80.9

Values are mean ± S.D. for 4 incubations. Incubation conditions and covalent binding assays are described in METHODS.

protein binding assays for the various incubation conditions contained in Table 4.2. One of the major products under all conditions was acetaminophen (Figure 4.15). Thus, even in incubations lacking NADPH (Figure 4.15.B) substantial reduction of NAPQI to acetaminophen occurred as well as covalent binding to microsomal protein. Reduction was enhanced in incubations containing L-ascorbic acid with a concominent decrease in conjugation products (Figure 4.15.C), whereas glutathione conjugation increased dramatically in the presence of added glutathione at the expense of reduction and binding to proteins (Figure 4.15.D). It was noted that small amounts of glutathione conjugate were detected in all incubations of NAPQI. This contribution was not eliminated by repetitive washes of the microsomal fraction during preparation.

Toxicicity of NAPQI in Isolated Hepatocytes

Rat hepatocytes were isolated by the collagenase perfusion technique, and the cytotoxic effects of NAPQI in suspensions of these cells were measured by trypan blue exclusion[117] and lactate dehydrogenase (LDH) release[118] (see METHODS). The results of studies comparing hepatocyte toxicity of NAPQI, acetaminophen, and N-hydroxyacetaminophen are shown in Figure 4.16. NAPQI concentrations as low as 0.1 mM caused a significant loss of viability measured 5 hours after addition. The decrease in LDH leakage seen in the figure at 1.0 mM was most likely due to NAPQI deactivation of the enzyme. N-Hydroxyacetaminophen was nearly as toxic as NAPQI, but no such effects could be seen with acetaminophen concentrations up to 20 mM.

FIGURE 4.15: BAR GRAPHS SHOWING NANOMOLES OF ACETAMINOPHEN (▨), PROTEIN BOUND ADDUCT (□), AND 3-S-GLUTATHIONYLACETAMINOPHEN (▩) THAT WERE FORMED IN INCUBATIONS OF [RING-^{14}C]ACETAMINOPHEN IN MOUSE LIVER MICROSOMES: (A) WITH AN NADPH REGENERATING SYSYTEM; (B) WITHOUT AN NADPH REGENERATING SYSTEM; (C) WITH THE REGENERATING SYSTEM PLUS 1.0 mM ASCORBIC ACID; AND (D) WITH THE REGENERATING SYSTEM AND 1.0 mM GLUTATHIONE. ASSAYS WERE PERFORMED BY THE HPLC-RADIOMETRIC METHOD AS DESCRIBED IN RESULTS AND METHODS.

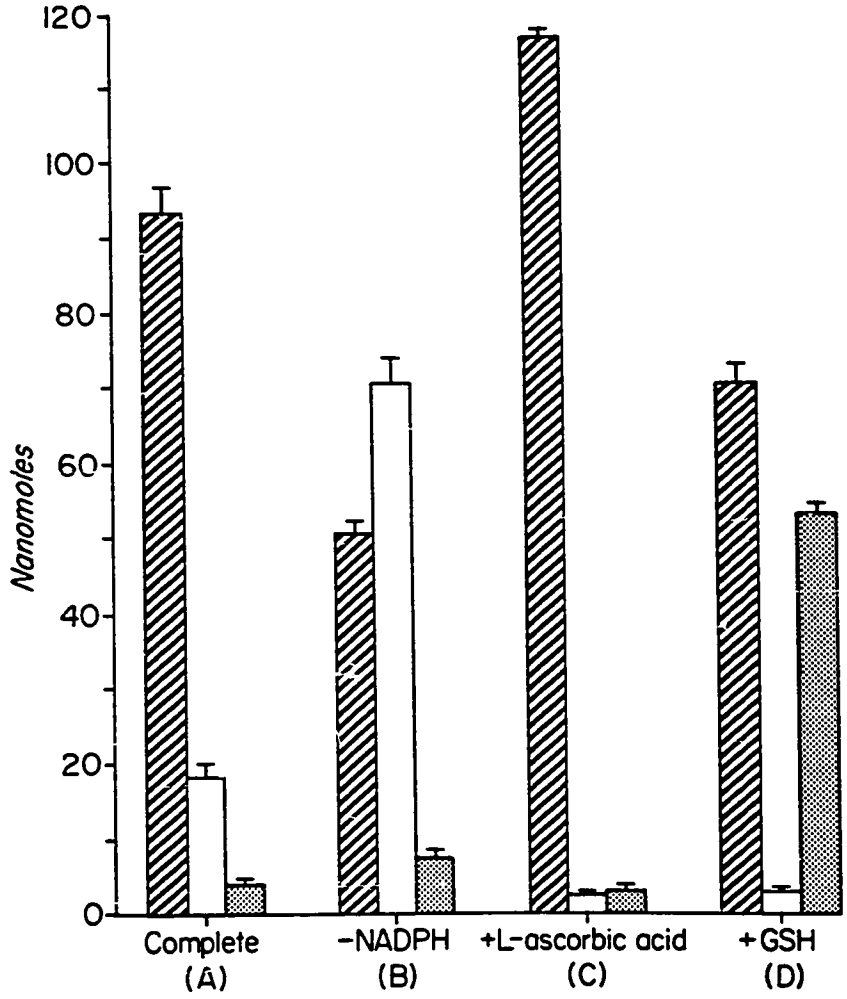
120
100
80
60
40
20
0
Nanomoles
Complete
(A)
-NADPH
(B)
+L-ascorbic acid
(C)
+GSH
(D)

FIGURE 4.16: CONCENTRATION DEPENDENT CYTOTOXICITY OF ACETAMINOPHEN, N-HYDROXYACETAMINOPHEN, AND NAPQI IN ISOLATED RAT HEPATOCYTES. VIABILITY DETERMINED BY TRYPAN BLUE EXCLUSION AND LACTATE DEHYDROGENASE (LDH) LEAKAGE AFTER 5 HOUR INCUBATIONS. VALUES ARE MEANS ± S.D. OF THREE DIFFERENT EXPERIMENTS.

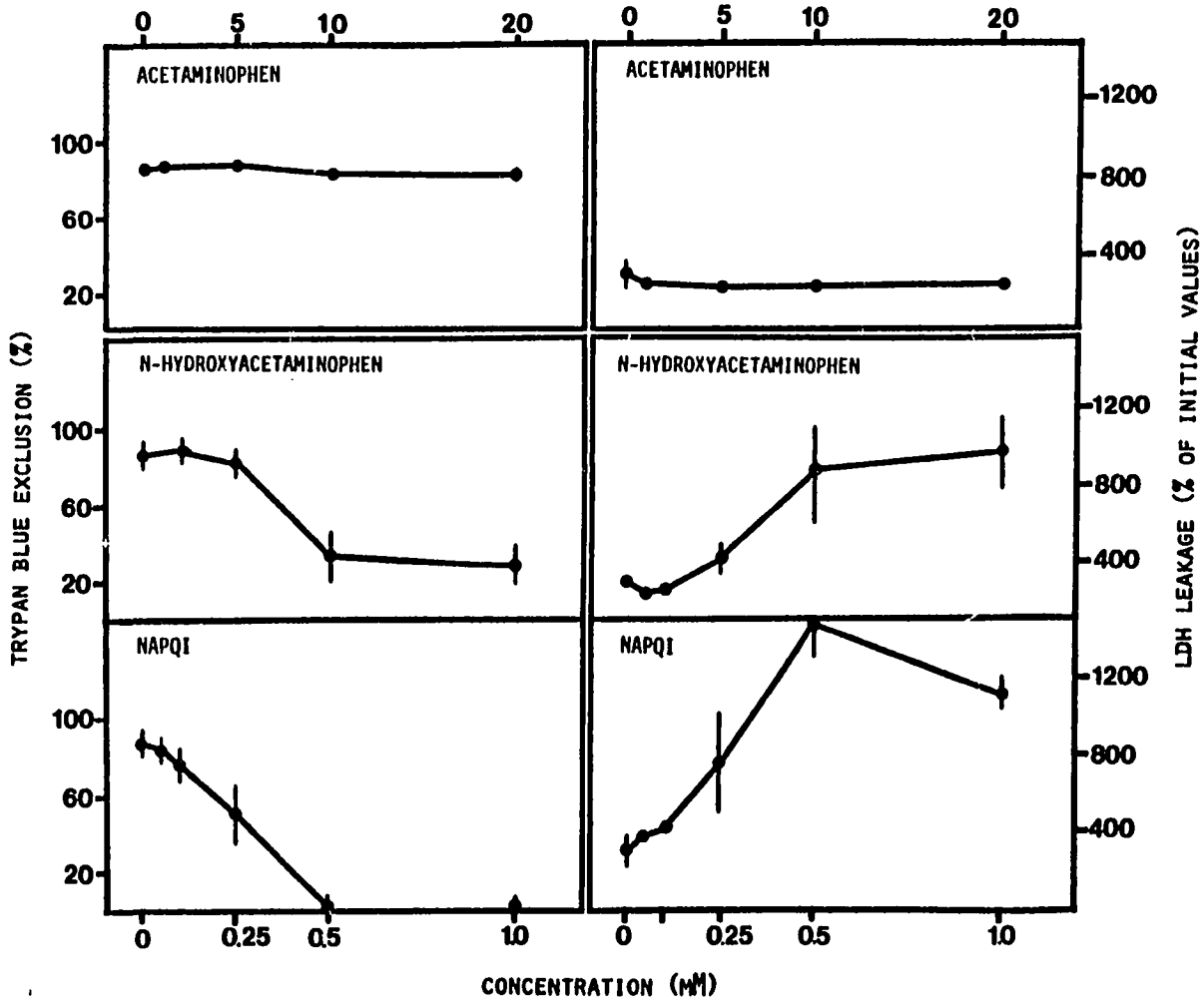
ACETAMINOPHEN
ACETAMINOPHEN
N-HYDROXYACETAMINOPHEN
N-HYDROXYACETAMINOPHEN
NAPQI
NAPQI
0
5
10
20
100
60
20
1200
800
400
0
0.25
0.5
1.0
TRYPAN BLUE EXCLUSION (%)
LDH LEAKAGE (% OF INITIAL VALUES)
CONCENTRATION (mM)

The viability of hepatocytes was monitored at time points over the course of 5 hours with NAPQI concentrations of 0, 0.1, 0.25, 0.5, and 1.0 mM (Figure 4.17). NAPQI at 1.0 mM produced a marked cytotoxity within 10 minutes, and a total loss of viability after 1.0 hour. At concentrations of 0.5 and 0.25 mM, 50% of the cells were killed during the 30-60 minute period and at 5 hours, respectively.

The effect of NAPQI on hepatocyte intracellular glutathione is shown in Figure 4.18, determined by the method of Tietze.[120,121] NAPQI caused a concentration dependent depletion of glutathione with only 10% of the endogenous thiol remaining after a 10 minute exposure to the quinone imine at 0.5 mM.

Several compounds that have been shown to protect against acetaminophen-induced liver necrosis were examined for effects on the hepatocyte toxicity of NAPQI.[119,120] These included N-acetylcysteine, glutathione, L-ascorbic acid, menadione, α-tocopherol, and phenacetin. Table 4.3 shows that all agents protected against NAPQI toxicity with glutathione, N-acetylcysteine, and L-ascorbic acid being most effective. In Table 4.4 a 5 minute exposure to 0.5 mM NAPQI resulted in a significant loss of hepatocyte viability, and this did not increase after 1.0 hour, indicating lethal damage apparently occured early in the incubation. The addition of N-acetylcysteine, glutathione, or ascorbic acid before NAPQI (Table 4.5) resulted in complete protection, whereas the addition of these compounds 5 minutes after NAPQI exposure provided significantly less inhibition of cytotoxicity.

Figure 4.17: TIME COURSE OF CYTOTOXICITY OF NAPQI AT DIFFERENT CONCENTRATIONS IN ISOLATED RAT HEPATOCYTES DETERMINED BY (A) TRYPAN BLUE EXCLUSION AND (B) LACTATE DEHYDROGENASE (LDH) RELEASE. CONTROL WITH NO ADDITIONS (o), 0.1 mM NAPQI (Δ), 0.25 mM NAPQI (●), 0.5 mM NAPQI (▲), AND 1.0 mM NAPQI (=). VALUES ARE MEAN ± S.D. OF THREE EXPERIMENTS.

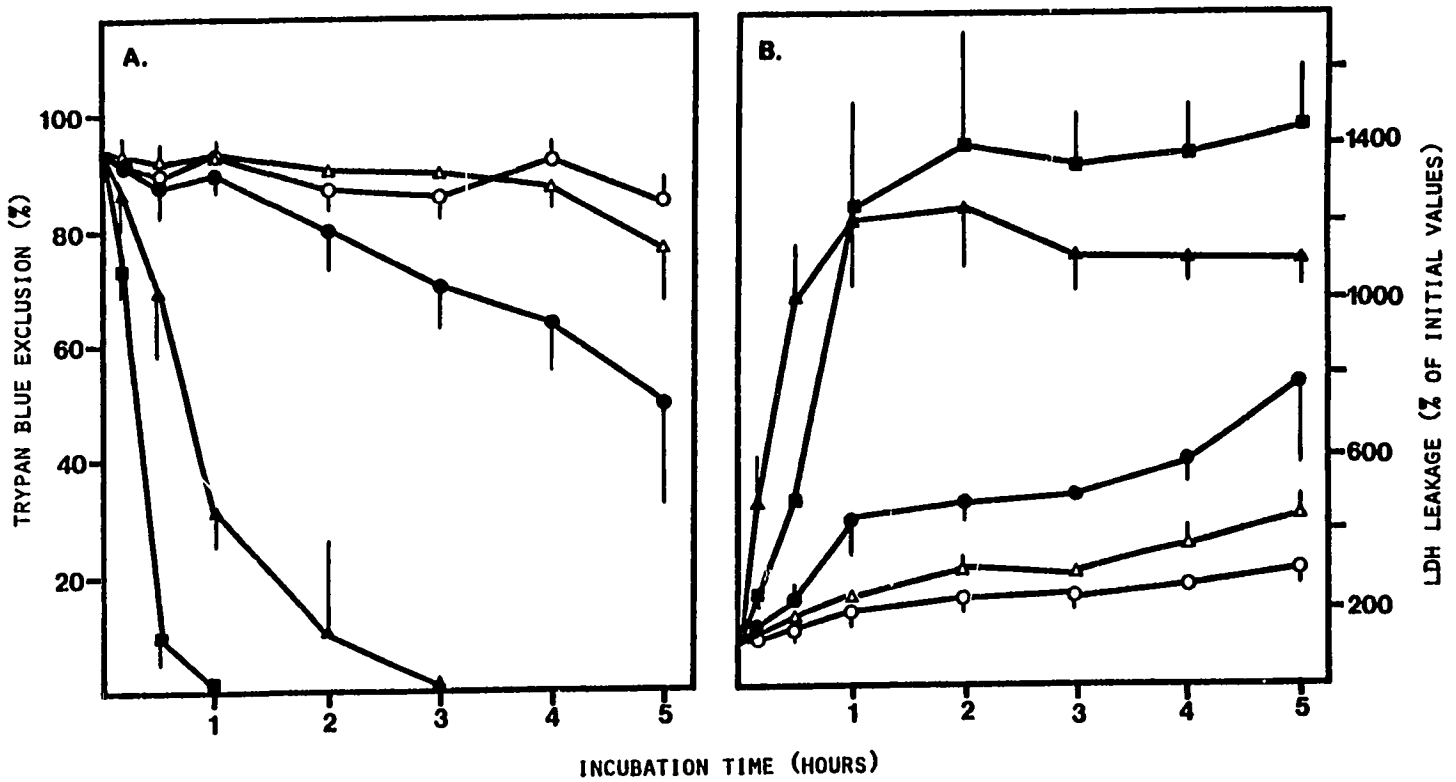
A.
B.
TRYPAN BLUE EXCLUSION (%)
LDH LEAKAGE (% OF INITIAL VALUES)
INCUBATION TIME (HOURS)
100
80
60
40
20
1400
1000
600
200
1
2
3
4
5

FIGURE 4.18: CONCENTRATION DEPENDENCE OF NAPQI-INDUCED GLUTATHIONE DEPLETION IN ISOLATED RAT HEPATOCYTES. SUSPENSIONS OF HEPATOCYTES WERE INCUBATED FOR 10 MINUTES WITH VARIED CONCENTRATIONS OF NAPQI, AFTER WHICH CELLULAR LEVELS OF GLUTATHIONE WERE DETERMINED (SEE METHODS). THE VALUES REPRESENT MEANS ± S.D. OF THREE DIFFERENT EXPERIMENTS.

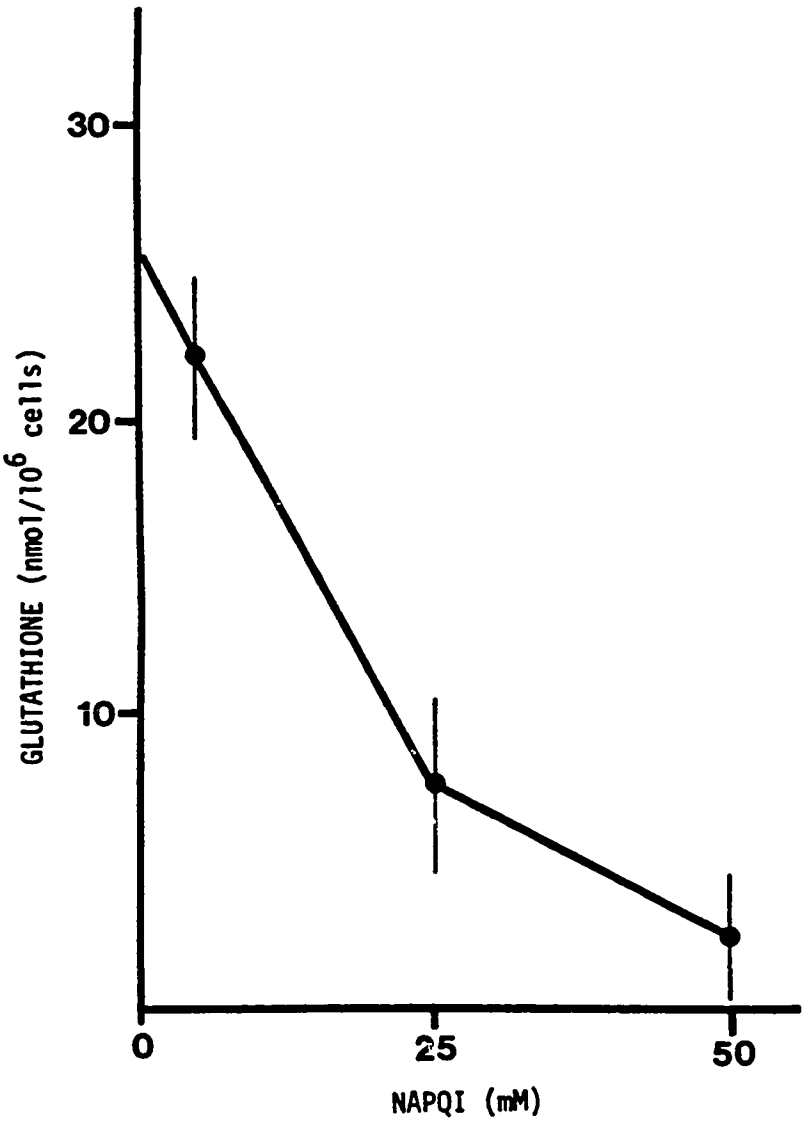
30
20
10
GLUTATHIONE (nmol/10^6 cells)
0
25
50
NAPQI (mM)

TABLE 4.3

THE EFFECTS OF VARIOUS ADDITIONS ON THE CYTOTOXICTY OF NAPQI

Addition	Percent Inhibition of Induced Cytotoxicty	
	Trypan Blue Exclusion	LDH Release
N-Acetylcysteine (1 mM)	97 ± 3	93 ± 6
Glutathione (2 mM)	91 ± 11	92 ± 2
L-Ascorbic Acid (0.5 mM)	99 ± 2	96 ± 5
Menadione (0.1 mM)	48 ± 13	42 ± 19
α-Tocopherol (0.1 mM)	30 ± 21	24 ± 20
Phenacetin (0.5 mM)	45 ± 28	19 ± 25

The hepatocytes were incubated with 0.5 mM NAPQI plus the various additions for 60 minutes. Trypan blue exclusion of the cells exposed to NAPQI was 17.0 ± 9.0% while 91.0 ± 1.0% of those not exposed to NAPQI excluded Trypan blue. NAPQI treatment increased LDH release by 673 ± 284% over unexposed cells. Values represent the mean ± S.D. of four hepatocyte preparations.

TABLE 4.4

THE EFFECT OF NAPQI INCUBATION TIME ON VIABILITY OF ISOLATED HEPATOCYTES

Exposure	Percent of Hepatocytes Excluding Trypan Blue
NAPQI (60 minutes)	36 ± 19
Control	94 ± 2
NAPQI (5 minutes)	21 ± 15
Control	94 ± 4

Hepatocytes were incubated with or without 0.5 mM NAPQI for five minutes. The cells were then centrifuged, resuspended in fresh medium and further incubated for 55 minutes before cytotoxicity was determined. Values represent the mean ± S.D. of four hepatocyte preparations.

TABLE 4.5

THE EFFECTS ON NAPQI HEPATOCYTE TOXICITY OF VARIOUS COMPOUNDS ADDED EITHER WITH OR AFTER NAPQI

Additions	Percent Inhibition of NAPQI-Induced Trypan Blue Exclusion	
	With NAPQI	After NAPQI
N-Acetylcysteine (1 mM)	101 ± 7	37 ± 20
Glutathione (2 mM)	101 ± 4	50 ± 17
L-Ascorbic Acid (0.5 mM)	97 ± 5	30 ± 30
Menadione (0.1 mM)	47 ± 30	49 ± 22

The hepatocytes were incubated with 0.5 mM NAPQI for 5 minutes then centrifuged, resuspended in in fresh medium, and incubated for 55 minutes. Tested compounds were added either with the NAPQI or after resuspension. Values represent the mean ± S.D. of four experiments.

In certain cases (dietary deficiency) acetaminophen has been experimentally shown to induce lipid peroxidation.[123-125] By monitoring the formation of thiobarbituric acid reactive substances at 535 nm, 0.50 mM NAPQI was shown to produce no increase in lipid peroxidation in isolated hepatocytes.. As a comparison, 6.5 mM carbon tetrachloride induced lipid peroxidation to levels of 0.28 $OD_{535}/10^6$ cells.

Oxygen utilization by hepatocyte suspensions was monitored using a Clark oxygen electrode.[68] The tracings in Figure 4.19.A show that NAPQI had no effect on cell oxygen consumption, and completely blocked the increase in oxygen utilization caused by 2,5-dimethylbenzoquinone.[126] The mean values (± S.D.) are given in Table 4.6.

Hepatocyte superoxide release was determined by following the reduction of acetylated cytochrome c (UV, 550 nm).[68,127] As seen in Figure 4.19.B and Table 4.6, NAPQI did not stimulate superoxide release while 2,5-dimethylbenzoquinone caused a significant rise in measured levels. Both NAPQI and superoxide dismutase were effective in blocking the 2,5-dimethylbenzoquionone-stimulated release of superoxide.[126]

In Vivo Toxicity Studies of NAPQI

The in vivo toxicity of NAPQI in male Swiss Webster mice was investigated. NAPQI administered in propylene glycol at 300 mg/kg i.p. rapidly produced cyanosis, readily apparent by a bluish discoloration of the feet, tail, and nose. After expiration of the first mouse (approximately 20 minutes after injection) the other animals were

FIGURE 4.19: NAPQI INHIBITION OF 2,5-DIMETHYLBENZOQUINONE-STIMULATED OXYGEN UTILIZATION AND SUPEROXIDE RELEASE IN ISOLATED RAT HEPATOCYTES. (A) OXYGEN UTILIZATION MEASURED WITH A CLARK OXYGEN ELECTRODE: 1, CONTROL HEPATOCYTES WITH 0.1 mM NAPQI ADDED AT DOTTED LINE; 2, HEPATOCYTES WITH 0.1 mM NAPQI AND 0.1 mM 2,5-DIMETHYLBENZOQUINONE ADDED AT DOTTED LINE; 3, CONTROL HEPATOCYTES (3.0×10^6 CELLS/ML) WITH 2,5-DIMETHYLBENZOQUINONE ADDED AT DOTTED LINE. (B) SUPEROXIDE RELEASE MEASURED MONITORING THE REDUCTION OF ACETYLATED CYTOCHROME C AT 550 NM: 4, CONTROL INCUBATIONS (3.0×10^6 CELLS/ML) WITH 0.1 mM 2,5-DIMETHYLBENZOQUINONE ADDED AT THE DOTTED LINE; 5, HEPATOCYTES WITH 0.066 MG/ML SOD PLUS 0.1 mM 2,5-DIMETHYLBENZOQUINONE; 6, HEPATOCYTES WITH 0.1 mM NAPQI AND 0.1 mM 2,5-DIMETHYLBENZOQUINONE ADDED AT DOTTED LINE.

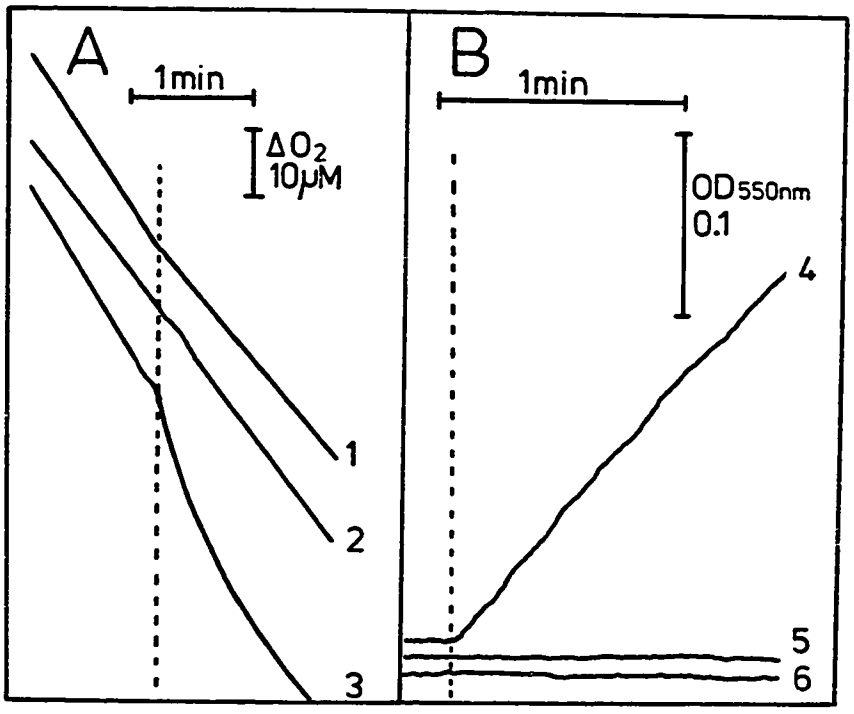
A
1min
ΔO2
10μM
1
2
3
B
1min
OD550nm
0.1
4
5
6

TABLE 4.6

THE EFFECT OF NAPQI ON HEPATOCYTE OXYGEN UTILIZATION AND SUPEROXIDE RELEASE

	Oxygen Utilization		Superoxide Release	
	- NAPQI	+ NAPQI	- NAPQI	+ NAPQI
Control	11.5 ± 0.6	9.2 ± 0.5*	0.3 ± 0.1	0.0 ± 0.0*
2,5-Dimethyl-benzoquinone	20.0 ± 0.4	9.8 ± 0.6*	16.4 ± 0.3	0.0 ± 0.0*

Incubation conditions are described in Figure 4.19. NAPQI and 2,5-dimethylbenzoquinone were at concentrations of 0.1 mM. Units of both oxygen utilization and superoxide release are nmoles/min/10^6 cells. Each value is the mean ± S.D. of three determinations.

*$P < 0.05$ compared to value in absence of NAPQI.

sacrificed and examined for gross evidence of tissue damage. All well-perfused organs (liver, spleen, kidneys, lungs, and heart) possessed the bluish cyanotic discoloration, and the blood appeared to be extensively coagulated and reduced in volume. The liver was hemorrhagic and blotchy, usually an outward sign of necrosis. With doses of 100 mg/kg NAPQI all symptoms were similar except that the first animal expired after 1 hour.

Mice were then dosed in pairs at 12.5, 25, and 50 mg/kg NAPQI and sacrificed after periods of 2 and 18 hours. The animals examined 2 hours after injection of 25 and 50 mg/kg presented a reddish-blue discoloration to the liver, spleen, heart, and kidneys. Again the liver was hemorrhagic, and the blood was reduced in volume and possibly coagulated. Mice given 12.5 mg/kg NAPQI and sacrificed at 2 hours suffered the above symptoms, to a lesser degree. The animals surviving 18 hours showed evidence of recovery, with the above symptoms significantly diminished. An approximate LD_{50} of 20 mg/kg was estimated from these experiments.

More extensive toxicity studies were performed on male BALB/c mice dosed i.p. with 10 and 20 mg/kg NAPQI and killed at 0, 1, 6, and 24 hours after administration. Measurements of blood methemoglobin were performed, and samples of liver, kidney, and lung tissue were obtained for histological scoring. Each sampling at a given dose and time point included three animals. No consistent increase in serum methemoglobin was evident at any time point or dose, and histological examination revealed no evidence of tissue necrosis. While there were no pathologies revealed by the conducted tests, other observations,

including loss of blood volume, possible blood coagulation, and cyanosis, indicated the presence of undetermined lesions induced by NAPQI. It was concluded that NAPQI reacted with blood constituents (probably a large contribution by proteins) and possibly vessel walls, and thus did not reach the liver for induction of a toxicity resembling that of acetaminophen.

More conclusive results were obtained in rats with the infusion of NAPQI in FC-43 emulsion (Oxypherol^{R}). This emulsion, more typically used as an artificial substitute for blood, was employed as a carrier to provide NAPQI protection from reaction with blood constituents. Reverse phase HPLC was used to determine that NAPQI had a half-life of approximately 5.0 minutes in this solvent. While not as stable as in buffer ($t_{\frac{1}{2}}$ = 11 minutes), this represented a marked improvement over the instability of NAPQI in the presence of blood proteins as anticipated from the determination by Kissinger[58] of a 7 second half-life with added microsomal protein. Direct portal infusion was made of NAPQI in FC-43 at a concentration giving <u>in vivo</u> levels of 20 mg/kg. After administration the rats, both NAPQI-infused and FC-43-infused control, were maintained for 5 hours. The animals were then sacrificed, and samples of liver and kidney tissue, blood, and urine were taken. The results of histological scoring of these tissue samples are shown in Table 4.7. Periportal necrosis graded from 1 to 2+ (see METHODS) and marked by pyknosis of the nuclear material was evident in liver samples from the NAPQI-infused rat. No necrosis was detected in kidney tissues from the NAPQI-treated rats, or in any samples from control animals. Serum samples were tested for SGPT

TABLE 4.7

TISSUE NECROSIS AND SERUM GPT LEVELS
AFTER PORTAL INFUSION OF NAPQI IN RATS

Tissue Sample		NAPQI-Infused	Control
Liver:	Lobe 1	2+	0
	Lobe 2	0	0
	Lobe 3	1 - 2+	0
	Lobe 4	1 - 2+	0
Kidney:	1	0	0
	2	0	0
Serum GPT Levels		30	207

NAPQI infused portally in Oxypherol at 20 mg/kg. SGPT values in units of mU/ml plasma. Scoring of tissue damage based on the scale of: 0, necrosis absent; 1+, necrosis of less than 6% of hepatocytes; 2+, necrosis in 6 to 25%; 3+, 26 to 50% of the hepatocytes necrotic; 4+, greater than 50% incidence of necrosis. Experimental values given represent determinations from one rat.

levels, and interestingly, enzyme concentrations were high in the control, but normal in the NAPQI- infused animal (Table 4.7). This may have been caused by physical damage to the control animal during infusion with a deactivation of the serum enzyme in the NAPQI rat.

Comparative Studies of NAPQI, N-Acetyl-2,6-dimethyl-p-benzoquionone Imine, and N-Acetyl-3,5-dimethyl-p-benzoquinone Imine Reactions with Glutathione

NAPQI and its analogs, N-acetyl-2,6-dimethyl-p-benzoquinone imine (2,6-dimethylNAPQI) and N-acetyl-3,5-dimethyl-p-benzoquinone imine (3,5-dimethylNAPQI), were reacted with glutathione in buffer. Conjugation products and reduced quinone imines (acetaminophen and 3,5-dimethylacetaminophen) were identified by TLC, NMR, UV, and HPLC techniques. Formation of oxidized glutathione (GSSG) was measured through the glutathione reductase-catalyzed oxidation of NADPH monitored by UV absorption at 340 nm.[69,127]

The reaction of 0.5 mM 2,6-dimethylNAPQI with 1.0 mM glutathione proceeded slowly as determined by a shift in the λ_{max} of the quinone imine (255 nm to 296 nm). Upon reaction completion the addition of NADPH and glutathione reductase resulted in no NADPH oxidation, indicating that GSSG was not formed. 3-S-Glutathionyl-2,6-dimethylacetaminophen formed in this reaction was eluted as a resolved peak from reverse phase HPLC. Reduction of the collected compound with activated Raney nickel in refluxing ethanol produced 2,6-dimethylacetaminophen as determined by chromatographic comparison to synthetic standard. In addition, the electron impact mass spectrum of the

cleavage product was identical to authentic 2,6-dimethylacetaminophen with major ions recorded at m/e 179 ($M^{+}\cdot$), 137 (M -$COCH_2$), and 122. High resolution ^{1}H-NMR analysis of the glutathione conjugate produced the spectrum in Figure 4.20. This spectrum was similar to that reported for 3-S-glutathionylacetaminophen with the expected changes in the aromatic and aliphatic regions.[45] The singlet at 6.63 ppm integrated for one proton and was assigned to C-5 of the aromatic ring. Resonance absorption occured at 2.08 ppm for the aryl methyl protons. In comparing this spectrum with that obtained from the acetaminophen-glutathione conjugate, more deshielding was obsevred for the α-cysteine and α-glycine resonances. This may have been caused by differences in the conditions since the spectrum in Figure 4.20 was recorded at pH 3.0 while that of the acetaminophen conjugate was done at pH 7.4. However, decoupling experiments with irradiation of the α-cysteinyl proton resonance at 4.75 ppm caused the β-cysteinyl quartet at 2.95 ppm and the β'-cysteinyl quartet at 3.24 ppm to collapse to doublets (J_{gem} = 14.5 Hz). Similarly, irradiation of the β-glutamyl resonance at 2.12 ppm caused the α-glutamyl triplet at 3.79 ppm and the γ-glutamyl quartet at 2.51 to collapse to singlets, further confirming the resonance assignments. Hence, it appeared that glutathione reacted with 2,6-dimethylNAPQI as a nucleophile and not as a reductant (Figure 4.21.A).

3,5-DimethylNAPQI (0.5 mM) reacted rapidly with 1.0 mM glutathione producing GSSG determined as described above. The only other product detected in the reaction mixture was 3,5-dimethyl-

FIGURE 4.20: HIGH RESOLUTION ^{1}H-NMR OF 3-S-GLUTATHIONYL-26,-DIMETHYL-ACETAMINOPHEN ISOLATED BY REVERSE PHASE HPLC FROM THE REACTION OF GLUTATHIONE WITH 2,6-DIMETHYL-P-BENZOQUINONE IMINE.

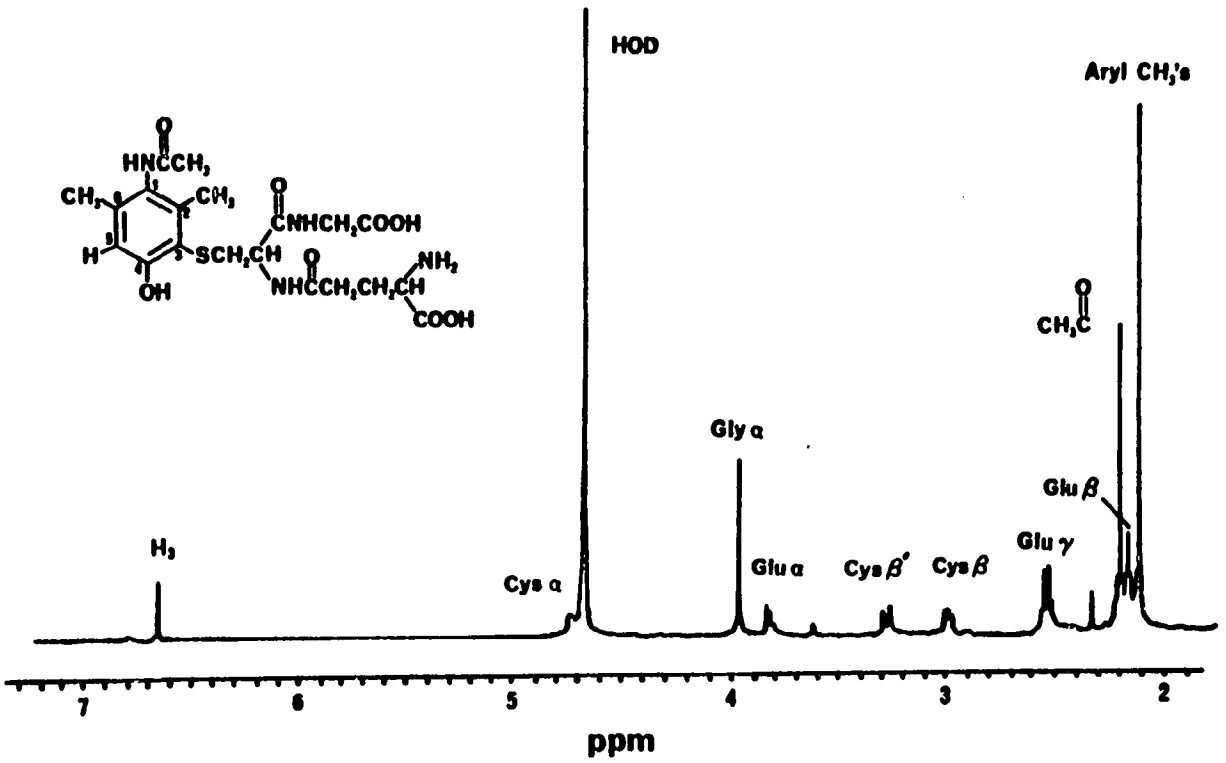
HOD
Aryl CH3's
Gly α
Glu β
Glu γ
Glu α
Cys β'
Cys β
Cys α
H3
7
6
5
4
3
2
ppm

FIGURE 4.21: REDUCTIVE AND CONJUGATIVE REACTIONS OF (A) 2,6-DIMETHYL-NAPQI, (B) 3,5-DIMETHYLNAPQI, AND (C) NAPQI WITH GLUTATHIONE.

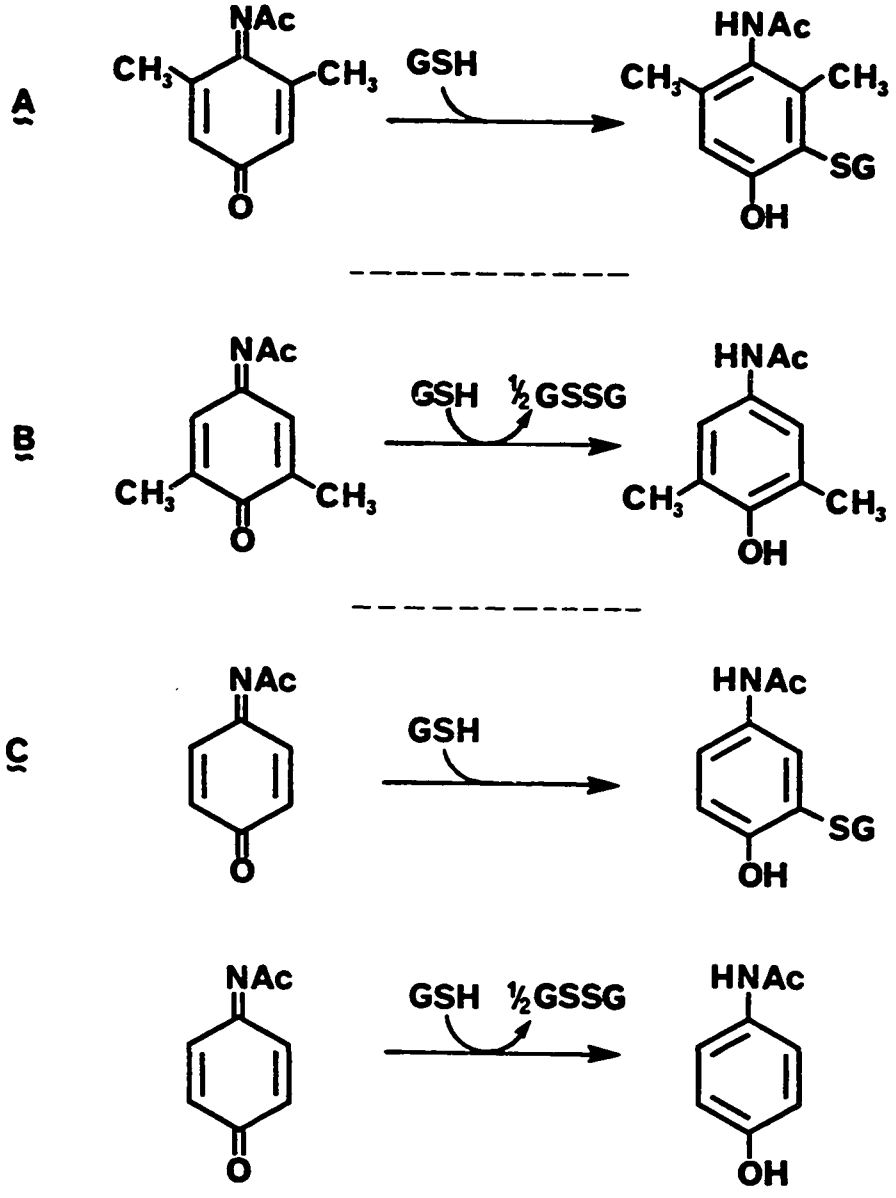
A
NAc
CH3
CH3
O
GSH
HNAc
CH3
CH3
SG
OH
B
NAc
CH3
CH3
O
GSH
½GSSG
HNAc
CH3
CH3
OH
C
NAc
O
GSH
HNAc
SG
OH
NAc
O
GSH
½GSSG
HNAc
OH

acetaminophen. Therefore, in the case of 3,5-dimethylNAPQI glutathione reacted as a reductant and not as a nucleophile (Figure 4.21.B).

Reaction of 0.5 mM NAPQI with 1.0 mM glutathione gave both 3-S-glutathionylacetaminophen and acetaminophen as products. Analysis was performed of the reaction mixture by reverse phase HPLC showing that the conjugate comprised 50% of the product with 36% acetaminophen and 14% unidentified components. Thus, in the interaction with NAPQI, glutathione reacts both as a nucleophile and as a reductant (Figure 4.21.C).

Studies on the Acetaminophen Semiquinone Imine Radical

In DMSO under anaerobic conditions NAPQI was reduced by $NaBH_4$ to produce the ESR spectrum in Figure 4.22. Splitting resulted in a five-line spectrum with relative intensities of 1:3:4:3:1 and a g-value of 2.0033. This was interpreted as a signal from the semiquinone imine of acetaminophen with the unpaired electron delocalized on the π-system of the ring. Splitting was attributed to spin interactions with two nonequivalent ring protons (H_A and H_B) and a nitrogen nucleus. Residence time on the nitrogen exceeded that on the quinone oxygen such that $A_N \cong A_H^{\beta} = 1.7$ G and $A_H^{\beta} = 0.34$ G. No ESR signals were measurable with reduction of NAPQI in aqueous media by $NaBH_4$, or by NADPH with NADPH-cytochrome P-450 reductase, or in rat liver microsomes in the presence of NADPH (Figure 4.22.B,C,D). Hence, an alternative approach was taken to indirectly monitor the presence of the acetaminophen radical from reductase metabolism of NAPQI by spin-exchange (Figure 4.23) with the cyclic hydroxylamine OXANOH

FIGURE 4.22: ESR SPECTRA OF THE ACETAMINOPHEN RADICAL UNDER THE CONDITIONS OF: (A) REDUCTION OF 5.0 mM NAPQI BY 3.75 mM SODIUM BOROHYDRIDE IN DMSO; (B) REDUCTION OF 5.0 mM NAPQI BY 3.75 mM SODIUM BOROHYDRIDE IN 0.15 M POTASSIUM CHLORIDE, 10 mM POTASSIUM PHOSPHATE BUFFER, PH 7.0; (C) REDUCTION OF 5 mM NAPQI BY 1.4 U/ML NADPH-CYTOCHROME P-450 REDUCTASE AND 1.0 mM NADPH IN PHOSPHATE BUFFER; (D) 5.0 mM NAPQI IN PHOSPHATE BUFFER WITH 1.0 MG/ML RAT LIVER MICROSOMES AND 1.0 mM NADPH.

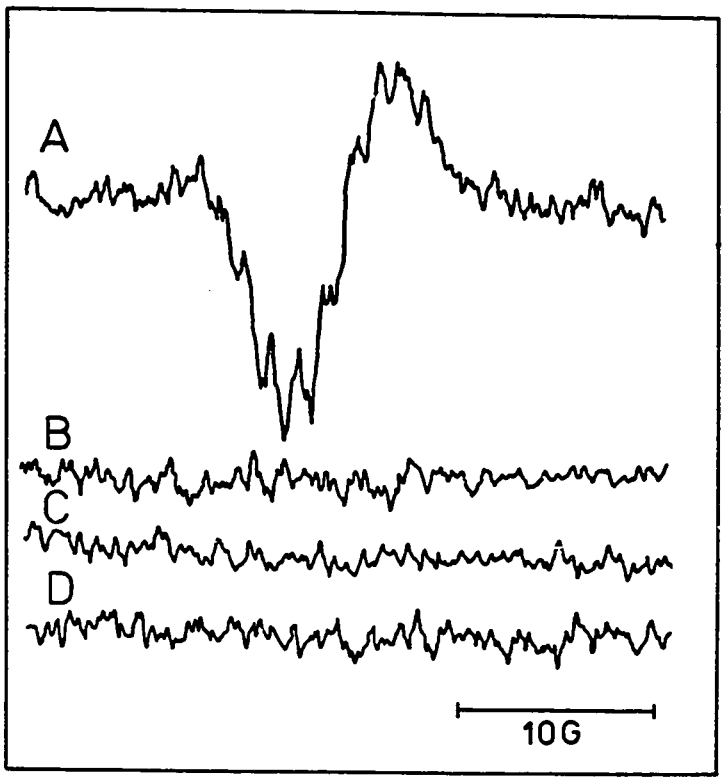
A
B
C
D
10 G

FIGURE 4.23: MECHANISM OF THE SPIN-EXCHANGE BETWEEN THE ACETAMINOPHEN RADICAL AND OXANOH FORMING THE NITROXIDE RADICAL OXANO.

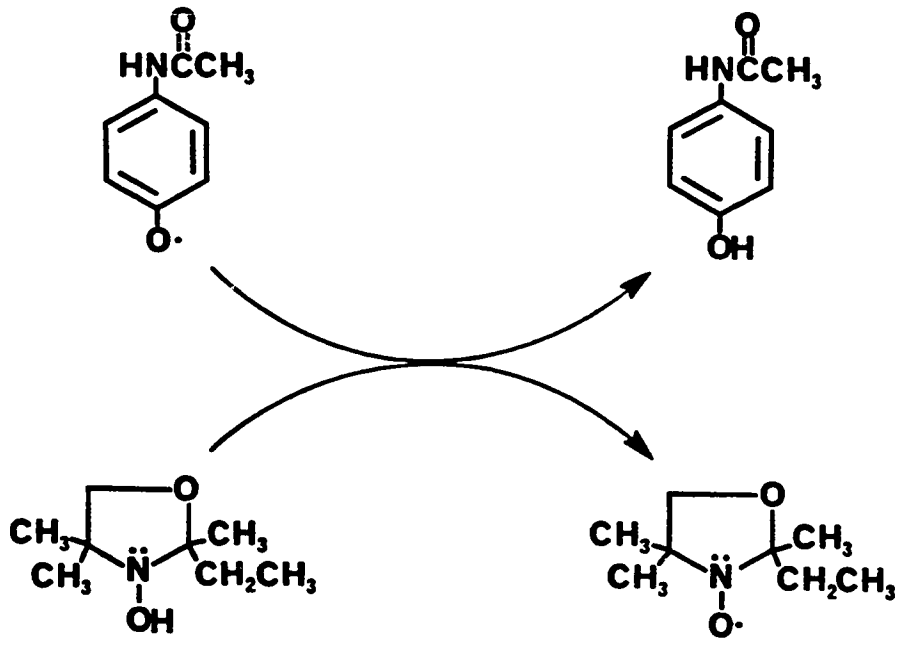

OXANOH

OXANO

(2-ethyl-1-hydroxy-2,5,5-trimethyl-3-oxazolidine) forming the corresponding nitroxide radical OXANO (2-ethyl-2,5,5-trimethyl-3-oxazolidinoxyl).[128,129] Anaerobic incubation of OXANOH with NAPQI, NADPH, NADPH-cytochrome P-450 reductase, and SOD lead to the rapid formation of OXANO as measured by ESR. Control experiments omitting either NAPQI or NADPH resulted in OXANO formation at levels less than 10% those in the complete incubations, indicating a probable reaction between OXANOH and the semiquinone imine.

Similar spin-exchange techniques were used to confirm the presence of the acetaminophen radical in aqueous solutions of acetaminophen and NAPQI. Formed through a comproportionation reaction between NAPQI and acetaminophen (Equation 3.8), as typically seen with quinonoid couples,[99] the acetaminophen radical underwent reaction with OXANOH producing the nitroxy radical OXANO and was detected by ESR. Complete reactions contained the cyclic hydroxylamine, NAPQI, acetaminophen, and SOD. Controls without acetaminophen resulted in OXANO formation 90% lower than the complete reactions.

The presence of superoxide generated from comproportionation-derived semiquione imine was determined using the spin trap DMPO (5,5-dimethyl-1-pyrroline-N-oxide). DMPO-OOH (5,5-dimethyl-2-hydroperoxyl-1-pyrrolinoxyl) was detected by ESR in solutions of NAPQI, acetaminophen, and DMPO (Figure 4.24), and structurally verified by comparison to the spectrum obtained from the reaction of tetramethylammonium superoxide with DMPO.[150]

Pulse radiolysis studies were conducted by Dr. Garth Powis on solutions of NAPQI in buffer with either isopropanol or sodium formate

FIGURE 4.24: ESR SPECTRUM OF THE DMPO SPIN ADDUCT OF SUPEROXIDE GENERATED DURING THE COMPROPORTIONATION REACTION OF ACETAMINOPHEN AND NAPQI. STUCTURE OF THE ADDUCT WAS VERIFIED BY COMPARISON TO THE SPECTRUM PRODUCED FROM THE REACTION OF DMPO WITH TETRAMETHYLAMMONIUM SUPEROXIDE.

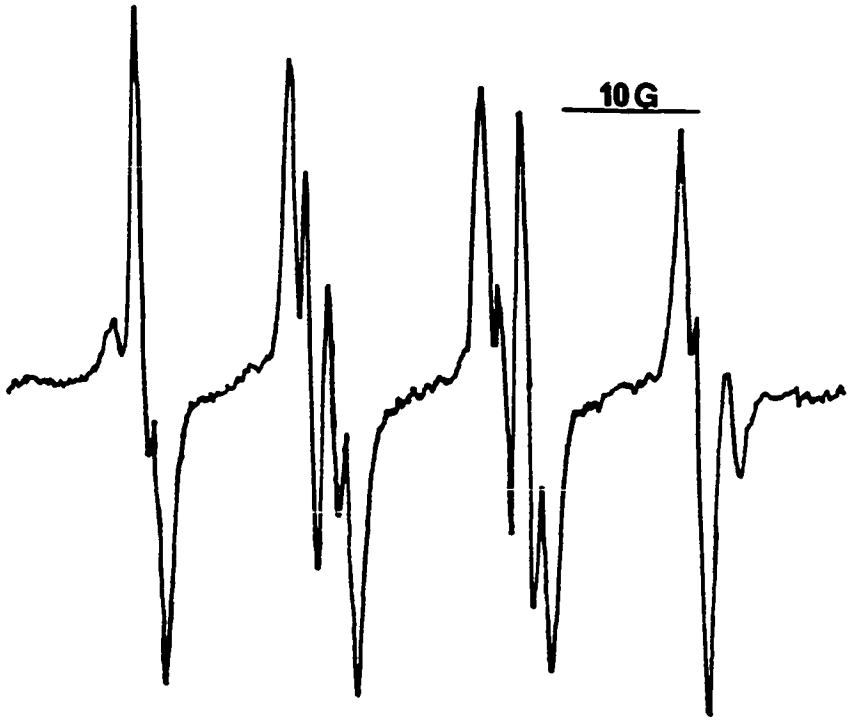
10 G

present as hydroxyl radical scavengers.[131,132] The semiquinone imine was generated by irradiation of a deaerated 0.1 mM solution of NAPQI in triply distilled water with a known dose of electrons from a 5 MeV Van der Graff accelerator. Time-resolved absorption measurements were made at 10 nm intervals from 280 to 500 nm resulting a difference spectrum (Figure 4.25) typical of that seen with simple semiquinones.[134] The absorption at 440 nm was used to monitor radiolysis-generated semiquinone imine revealing a second-order decay process also similar to other semiquinones[134] with $k = 1.2 \times 10^9$ $M^{-1}s^{-1}$ in the presence of isopropanol and $k = 2.9 \times 10^9$ $M^{-1}s^{-1}$ with sodium formate. From this the short-lived radical was calculated to have a half-life of 350 μseconds.

The one-electron reduction potential of NAPQI at pH 7.0 (E_7^1) was calculated by the rate of approach to equilibrium method (see METHODS).[135] This involved measuring the pseudo-first-order appearance of the durosemiquinone radical at 360 nm in pulsed solutions of duroquinone and NAPQI at varied concentrations ratios. A plot of the observed pseudo-first-order rate constant for equilibration at each NAPQI concentration ($K_{obs}/[A]$) versus the duroquinone-NAPQI concentration ratio ([Q]/[A]) is shown in Figure 4.26. Values for the intercept and slope were used to obtain the equilibrium constant which was directly related to the difference in the one-electron reduction potentials of the known duroquinone/durosemiquinone couple (-244 mV)[136] and the unknown NAPQI/semiquinone imine couple. This method gave a value of E_7^1 = -251 mV for NAPQI.

FIGURE 4.25: DIFFERENCE SPECTRUM OBTAINED 20 μSECONDS AFTER PULSE RADIOLYSIS OF AN 0.1 mM SOLUTION OF NAPQI IN 5.0 mM POTASSIUM PHOSPHATE BUFFER, PH 7.0. ISOPROPANOL WAS PRESENT AT 0.1 M AS A HYDROXYL RADICAL SCAVENGER AND RADIOLYSIS WAS CONDUCTED AT ROOM TEMPERATURE UNDER NITROGEN.

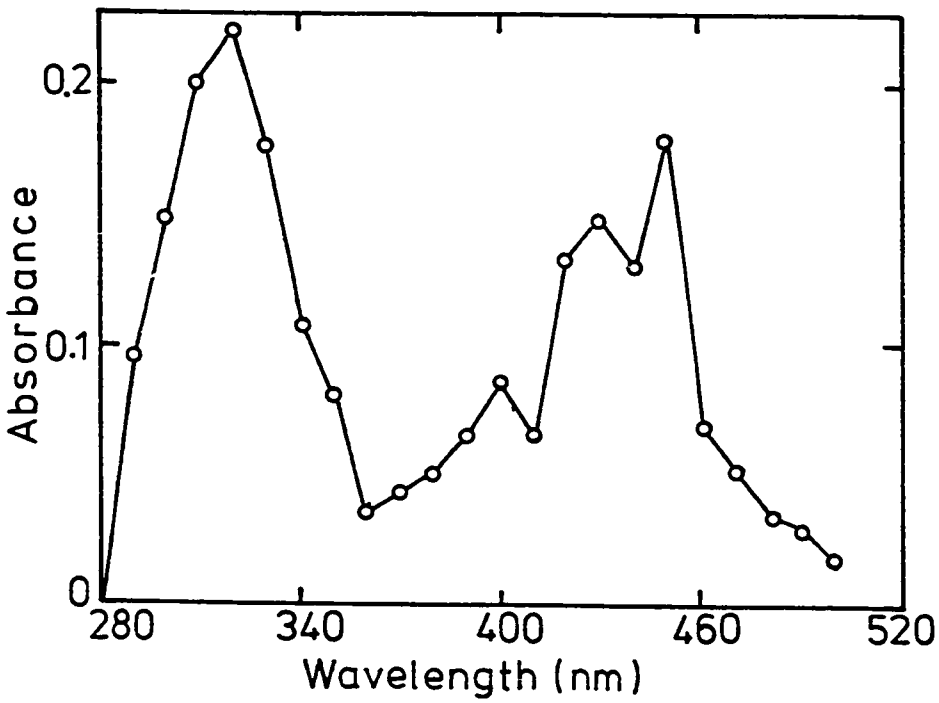
0.2
0.1
0
Absorbance
280
340
400
460
520
Wavelength (nm)

FIGURE 4.26: PLOT OF THE OBSERVED FIRST-ORDER RATE CONSTANT/[NAPQI] (K_{OBS}/A) AGAINST [DUROQUINONE]/[NAPQI] (Q/A) MEASURED AS THE DECAY OF DUROSEMIQUINONE AT 360 NM. VALUES OF K_F (INTERCEPT) AND K_R (SLOPE) OBTAINED FROM THIS PLOT ARE 0.18×10^9 $M^{-1}S^{-1}$ AND 0.12×10^9 $M^{-1}S^{-1}$, RESPECTIVELY.

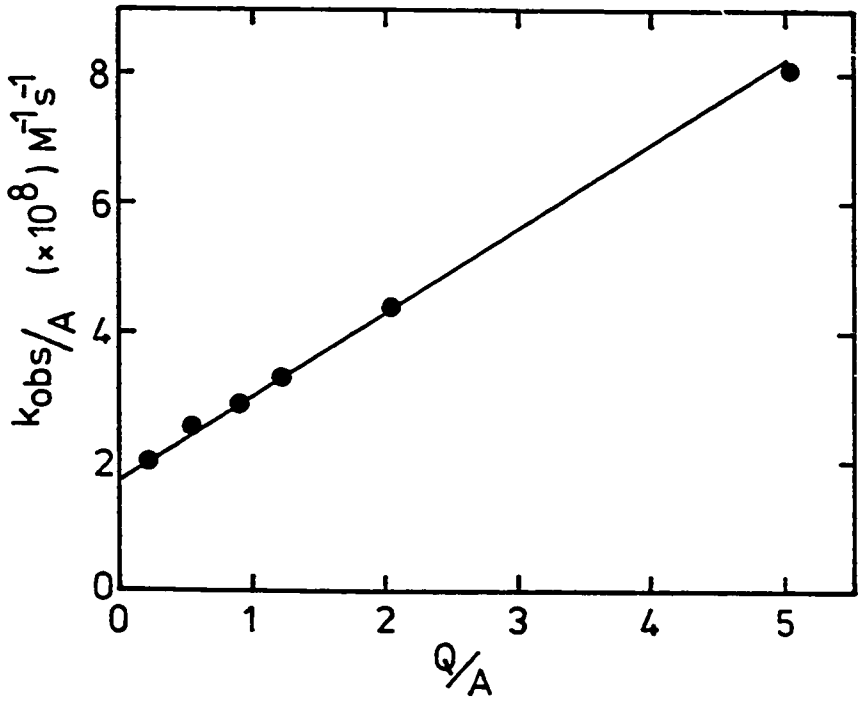
k_{obs}/A ($\times 10^8$) $M^{-1}s^{-1}$
8
6
4
2
0
0
1
2
3
4
5
Q/A

Similar methods were employed to study the interaction between the acetaminophen radical and oxygen. Using 0.1 mM NAPQI solutions equilibrated with varying ratios of nitrogen to oxygen (up to 80% O_2), the pseudo-first-order approach to equilibrium of pulse-generated quinone imine was monitored by absorbance of the acetaminophen radical at 440 nm. The data plotted in Figure 4.27 were used to calculate E_7^1 = -225 mV as previously described. The one-electron reduction potential for NAPQI determined using the oxygen/superoxide reference couple (-330 mV) must be considered less reliable because of the curvature in the Figure 4.27 plot at low oxygen concentrations. However, constants obtained in the kinetic analysis of this experiment (see DISCUSSION and METHODS) indicated that the interaction between the semiquinone imine and molecular oxygen was slow, one to two orders of magnitude less than those of other quinonoid radicals.[131,133]

C. DISCUSSION

The synthesis of NAPQI, its detection as a cytochrome P-450 product of acetaminophen oxidation, and the characterization of its interactions with biochemically relevant molecules and enzymes are discussed in this chapter. These studies resulted in a clearer understanding of acetaminophen metabolic activation, and have provided insight into the interaction of NAPQI with cellular components important in its metabolism and toxicity.

Experiments were initially undertaken to determine the chemical behavior of NAPQI in aqueous media. Based on observations made during

FIGURE 4.27: PLOT OF THE OBSERVED FIRST-ORDER RATE CONSTANT/[OXYGEN] (K_{OBS}/O_2) AGAINST [NAPQI]/[OXYGEN] (A/O_2) MEASURED AS THE APPEARANCE OF THE ACETAMINOPHEN RADICAL AT 440 NM. THE REACTION MIXTURE CONTAINED 0.1 mM NAPQI IN PHOSPHATE BUFFER, PH 7.0, WITH EITHER 0.1 M ISOPROPANOL (●) OR 0.1 M SODIUM FORMATE (○) EQUILIBRATED WITH CALIBRATED MIXTURES OF O_2 IN N_2 OR AIR. THE O_2 CONCENTRATION IN SOLUTION UNDER 1 ATM OXYGEN WAS ASSUMED TO BE 1.25 mM AND LINEARLY DEPENDENT ON PARTIAL O_2 PRESSURE. VALUES OF K_F (INTERCEPT) AND K_R (SLOPE) FROM THIS PLOT ARE 13.6×10^6 $M^{-1}S^{-1}$ AND 2.0×10^6 $M^{-1}S^{-1}$, RESPECTIVELY.

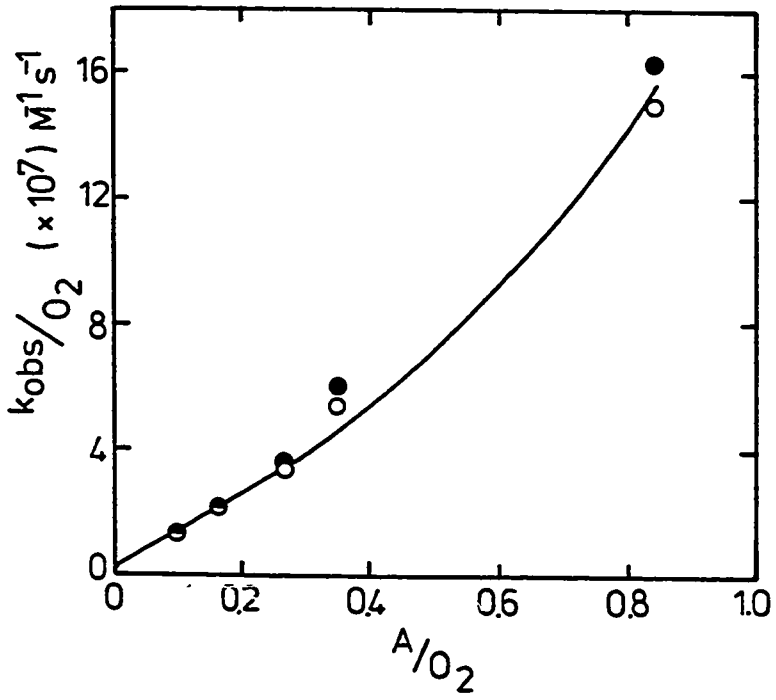
k_{obs}/O_2 ($\times 10^7$) $M^{-1}s^{-1}$
16
12
8
4
0
0
0.2
0.4
0.6
0.8
1.0
A/O_2

the development of synthetic procedures, several reactions were likely under physiological conditions, including reduction to acetaminophen, hydrolysis to benzoquinone, and free radical processes leading to polymeric products. All three were found to occur in buffer at pH 7.4.

Evidence for free radical reactions was provided by half-order kinetics in the second phase of the biphasic decomposition plot (Figure 4.1). Such kinetics are predicted in radical chain reactions involving first-order initiation, second-order propagation, and second-order termination steps,[111] and had previously been observed in the disappearance of electrochemically generated NAPQI.[58] The time dependent decrease in NAPQI concentration was plotted as $[NAPQI]^{\frac{1}{2}}$ versus time from Equation 4.1. below:

$$C^{\frac{1}{2}} = C^{\frac{1}{2}} - (k/2)t \qquad \text{Equation 4.1}$$

The initial phase of the NAPQI decomposition curve was nearly linear when plotted as second-order. Addition of increasing concentrations of acetaminophen shortened and eventually eliminated the second-order phase with a concurrent increase in the half-order rate of NAPQI disappearance. This was also consistent with a radical process since increasing the hydroquinonoid component of quinone couples is known to elicite a first-order increase in the rate of semiquinone radical formation through comproportionation equilibria (as with Equation 3.8).[111]

Analysis of aqueous decomposition reaction mixtures provided insight into the relative rates of competing NAPQI reactions in

buffer. The products acetaminophen and benzoquinone (Figure 4.2.A,B) were indicative of reduction and hydrolysis reactions, respectively. Depending on the whether the decomposition reactions were conducted at 0.05 mM or 1.0 mM NAPQI, the yield of acetaminophen varied from 8 to 18%. Unresolved benzoquinone, based on results from other reverse phase HPLC separations, comprised a small percentage of the acetaminophen peak. However, at lower NAPQI concentrations, as expected in the _in vivo_ generation of NAPQI from acetaminophen, the relative contribution of the hydrolytic reaction may be more significant.

The late-eluting components A through F illustrated the prominence of free radical reactions in NAPQI aqueous decomposition. At the NAPQI concentrations employed, A-F comprised 80 to 90% of the total reaction yield, and were probably all polymeric compounds. This was supported by the very significant difference in retention time between acetaminophen and components A-F in the reverse phase gradient elution system. A more pronounced difference was seen under isocratic conditions, compound F requiring a 7 to 8-fold greater elution volume than acetaminophen. Structural analysis of _A_ further supported the contention of polymeric products. High resolution EIMS (Figure 4.3) indicated _A_ to be an acetaminophen dimer.

Thus, in buffer solution at physiological pH NAPQI degrades through several competing routes. Most prominent, based on kinetic and product analysis, was the free radical process with reduction and hydrolysis contributing measurably. Extrapolation of this information to the considerably lower levels of NAPQI derived enzymatically _in vitro_ or _in vivo_ would not be valid. Certainly a contribution by all

three processes would be expected. But, the partitioning would most likely be different than observed in these studies, especially in the presence of cellular constituents that have been shown to interact rapidly with NAPQI through reductive and conjugative reactions. None the less, in addition to revealing NAPQI reactions that probably have some *in vitro* and *in vivo* contribution, this information proved useful in the development of further studies contained in this chapter.

In addition to the reactions of NAPQI in aqueous solution, its interactions with the important cellular constituents NADH, NADPH, and NADPH-cytochrome P-450 reductase were examined. NADPH and NADH were found to reduce NAPQI rapidly to acetaminophen in a nonenzymatic process (Figure 4.4). Small amounts of benzoquinone from the hydrolysis of the quinone imine were also detected. The kinetics of the reduction of NAPQI by NADPH were second-order with a rate constant of $k = 3.81\ mmol^{-1}min^{-1}$ (Figure 4.5). Comparitive experiments with benzoquinone resulted in an approximately 10-fold lower rate of second-order reduction by NADPH (Figure 4.8).

With the addition of purified NADPH-cytochrome P-450 reductase the rate of NAPQI reduction by NADPH was approximately doubled over the nonenzymatic reaction. The apparent kinetic parameters of K_m = 4.0 μM and V_{max}= 29.4 μmol/min/mg were obtained from a double reciprocal plot of the initial rate data (Figure 4.9), however this displayed evidence of substrate inhibition at NAPQI concentrations above 10 μM. Since this permitted parameter determination from the lower NAPQI concentration values only, an alternative approach was used to verify the assignment of the K_m. The K_I of NAPQI inhibition of the NADPH-

cytochrome P-450 reductase-mediated reduction of cytochrome c at low NAPQI concentrations was determined as a value for comparison to the K_m. The inhibition of cytochrome c reduction was time dependent with NAPQI itself being metabolized by the reductase. As a result substrate inhibition diminished over time, and cytochrome c reduction approached, but never reached, the rate observed in the absence of NAPQI (Figure 4.10). From kinetic analysis the inhibition by NAPQI appeared to be competitive with a K_I of 1.8 μM. Since this was in agreement with the previously obtained value, the K_m was taken to be 1.8 to 4.0 μM.

Thus, NADH, NADPH, and NADPH-cytochrome P-450 reductase, biochemical factors relevant to both in vivo and in vitro oxidations of acetaminophen, were found to rapidly reduce NAPQI to acetaminophen. It was evident that if NAPQI was a cytochrome P-450 product of acetaminophen these components should inhibit the in vitro protein binding of radiolabel through reduction of the reactive metabolite back to acetaminophen. Hence, studies were performed to determine whether such an inhibition occured. The addition of increasing concentrations of NADPH, or of NADH with an added cofactor regenerating system to reconstituted cytochrome P-450 incubations of ^{14}C-acetaminophen demonstrated the reductive deactivation of the arylating metabolite. With varied levels of NADPH (Figure 4.12) measured covalent binding to BSA increased to an optimum, reflecting the cofactor dependence of metabolite generation, then decreased as high NADPH concentrations reduced NAPQI back to acetaminophen. Similarly, the addition of increasing concentrations of NADH to purified P-450 incubations of

acetaminophen supported by an NADPH regenerating system demonstrated inhibition of NAPQI binding to BSA through reduction by the cofactor (Figure 4.12). However, in this case enzymatic generation of the reactive metabolite was not dependent on the inhibiting cofactor, and thus binding decreased continuously as NADH was increased. The enzyme-catalyzed process was also shown to be effective in reduction of the acetaminophen-derived reactive metabolite. Experiments in which the molar ratio of purified NADPH-cytochrome P-450 reductase to P-450 was serially increased resulted in a covalent binding pattern similar to that seen in the NADPH inhibition experiments. Hence, binding reached a maximum with P-450 dependence on reductase and NADPH, then diminished through NAPQI reduction with excess reductase activity. The correlation between reduction of NAPQI by NADH, NADPH, and NADPH-cytochrome P-450 reductase, and the inhibition by these agents of acetaminophen protein binding in incubations of purified cytochrome P-450 provided strong indirect evidence in support of NAPQI intermediacy.

More direct evidence for the role of NAPQI in acetaminophen metabolism was established in incubations of acetaminophen with purified cytochrome P-450 supported by cumene hydroperoxide where NAPQI was determined as an oxidation product using several HPLC analytical techniques. Similar attempts were made to detect the presence of NAPQI in acetaminophen incubations with purified P-450, NADPH, and purified NADPH-cytochrome P-450 reductase, and in mouse liver microsomes with an added NADPH regenerating system. In these experiments NAPQI levels were below the detection limits (1.1×10^{-7}

M). The reduction of P-450-generated NAPQI, through both the enzymatic and nonenzymatic reactions previously discussed, was considered responsible for the diminished reactive metabolite levels. In the cumene hydroperoxide-supported incubations, that lacked the propensity for rapid NAPQI reduction by omission of NADPH, the quinone imine was detected by both electrochemical and radiochemical HPLC methods. The electrochemical detection system was similar to that employed by Miner and Kissinger.[58] A carbon paste-electrode was set at -0.240 V, and current fluctuations (in the nanoampere range) caused by passage of materials in the HPLC eluate that were reducible at this potential were measured with an amperometer (Figure 4.14.B,C). The mean concentration of NAPQI detected in complete incubations was (2.6 ± 0.03) x 10^{-7} M (± S.D., n = 4). This was an enzymatic process as shown by the absence of NAPQI in incubations lacking cumene hydroperoxide, P-450, or acetaminophen.

Using radiochemical methods ^{14}C-NAPQI was also detected as an oxidation product in cumene hydroperoxide-supported incubations of ^{14}C-acetaminophem with purified cytochrome P-450 (Figure 4.14.E,F). Measured using liquid scintillation spectroscopy of the HPLC eluate, NAPQI was determined to be present at (3.4 ± 0.8) x 10^{-7} M (± S.D., n = 4). Again this was shown to be an enzyme dependent product by the absence of a ^{14}C-containing peak at the retention time of NAPQI from incubations omitting cumene hydroperoxide or P-450.

As a confirmation that the radiolabel peak contained NAPQI, collections were made into solutions of ascorbic acid which reduced NAPQI rapidly to acetaminophen. Reinjection of the mixture on HPLC

resulted in the elution of an acetaminophen peak containing the radiolabel originally eluted as NAPQI.

Thus, NAPQI was determined directly to be a product of cytochrome P-450 oxidation of acetaminophen. Multiple detection methods were used in these studies, providing the following observations consistent with NAPQI formation: (1) the peak detected had the same HPLC retention time as synthetic NAPQI standard; (2) the reductive potential successfully employed in the electrochemical system was in agreement with literature values[58]; (3) the product detected was formed through an enzymatic process; (4) radiolabel from acetaminophen was present in the enzyme dependent NAPQI peak; and (5), the radiolabeled product was reduced by ascorbic acid to acetaminophen.

Since NAPQI detection in microsomal incubations of acetaminophen supported by NAPDH was not feasible because of the previously discussed reduction processes, experiments were designed which provided indirect evidence that acetaminophen is oxidized to NAPQI in such systems. This evidence was in the form of metabolite partitioning, demonstrating close correlations between the fate of synthetic NAPQI added to microsomes and the reactive metabolite generated from acetaminophen. Protein binding by both [ring-^{14}C]NAPQI and [ring-^{14}C]acetaminophen was present in mouse liver microsomes containing an NADPH regenerating system (Table 4.2). When the cofactor regenerating system was omitted virtually no covalent binding of acetaminophen was seen, whereas that of NAPQI was increased nearly 4-fold. This reflected the NADPH dependence of reactive metabolite generation from acetaminophen, and the removal of the reductive

inhibition of NAPQI binding. Both acetaminophen and NAPQI binding were inhibited by ascorbic acid and glutathione. Significantly, the same fractional decreases in binding were seen for both NAPQI and acetaminophen with these inhibitors (Table 4.2; reported as percentage of noninhibited controls; glutathione lowered NAPQI binding to 14.7% and acetaminophen binding to 12.0% while ascorbate lowered NAPQI binding to 14.2% and acetaminophen binding to 14.8%). This reflects very similar reactivities of NAPQI and the acetaminophen metabolite toward both glutathione and ascorbate that is difficult to explain except by the intermediacy of NAPQI in acetaminophen metabolism.

Differential label studies had previously demonstrated a greater binding of the acetaminophen ring than of the acetyl group in microsomal incubations.[116,119] This was also demonstrated with NAPQI with studies comparing the microsomal protein binding of ring and acetyl-labeled analogs of acetaminophen and NAPQI (Table 4.2). Results indicated that for both acetaminophen and NAPQI, acetyl-binding was approximately 19% less than that of the ring. The recovery of ^{14}C-acetamide in the incubations of both acetyl-labeled substrates indicated that the bound material probably included a benzoquinone-protein adduct.

The relative amounts of acetaminophen, 3-S-glutathionylacetaminophen, and covalently bound material produced by the addition of [ring-^{14}C]NAPQI to microsomal incubations were determined under the following conditions: omission of NADPH regenerating system; complete incubations; and, complete incubations plus glutathione or ascorbic acid (Table 4.2). As was seen in Figure 4.15, a major product under

all conditions was acetaminophen. Even in incubations omitting NADPH where NAPQI protein binding was greatest, reduction was a significant contribution to the metabolite partitioning. As expected, the inclusion of ascorbic acid elicited a pronounced increase in the reduction product acetaminophen at the expense of protein binding. Glutathione addition resulted in the formation of both the conjugation product, 3-S-glutathionylacetaminophen, and the reduction product acetaminophen. As was presented in RESULTS, and as will be discussed later in this section, glutathione reacts with NAPQI both as a reductant and as a nucleophile, thus explaining the formation of these two products. NAPQI was also subject to both reactions in the complete microsomal incubations containing an NADPH regenerating system. The partition ratio between reduction and conjugation (including covalent binding plus endogenous glutathione conjugation) was 4.4. In other words, nearly 80% of the NAPQI added to the complete microsomes underwent reduction to acetaminophen. A similar portion of the NAPQI generated from acetaminophen in microsomes or in vivo would be expected to undergo such a conversion, indicating that the oxidative metabolism of acetaminophen may be much more extensive than formerly believed. Such an effect was not previously observable with acetaminophen as substrate since NADPH is required for generation of the reactive metabolite, and since high substrate levels would preclude the determination of product recycling.

In verifying the role of metabolites such as NAPQI in the toxicity of metabolically activated compounds, it is generally considered important to demonstrate that the proposed intermediate is

capable of producing toxic effects similar to and more potent than those elicited from the metabolism of the parent compound. Hence, in the earlier work with N-hydroxyacetaminophen, administration of the compound revealed than liver necrosis was not as great as anticipated, thereby raising questions about the intermediacy of the hydroxamic acid.[53,54]

Toxicity studies of NAPQI were conducted in isolated hepatocytes. NAPQI proved to be slightly more toxic than N-hydroxyacetaminophen and much more toxic than acetaminophen over a course of 5 hours (Figure 4.16). The half-maximal effect of NAPQI occured at 0.25 mM, a concentration at which there was no significant toxicity from either acetaminophen or N-hydroxyacetaminophen. NAPQI was also found to be a potent depletor of intracellular glutathione; concentrations of 0.5 mM caused a loss of 90 % of the thiol after 10 minutes (Figure 4.16). Time course studies showed that NAPQI-mediated loss of hepatocyte viability occured relatively early in the incubation period (Figure 4.17, marked toxicity within 10 minutes at 1.0 mM NAPQI). This rapid course of cell death implied that NAPQI required no further metabolism. This was in accordance with the inhibitor studies (Tables 4.3, and 4.4) which showed that administration of ascorbic acid, glutathione, or N-acetylcysteine before NAPQI afforded complete protection. However, in marked contrast, addition after a 5.0 minute preincubation with NAPQI did not protect against cytotoxicity.

Acetaminophen has been demonstrated to induce low levels of lipid peroxidation in malnourished animals.[123,125] By monitoring the formation of substances that react with thiobarbituric acid,[123] NAPQI

was found not to induce such effects in suspensions of isolated hepatocytes. In contrast, carbon tetrachloride, which is known to cause significant lipid peroxidation, produced measurable levels (0.28 $OD_{535}/10^6$ cells) of thiobarbituric acid reacting-substances.[137] These results were in agreement with the inability of NAPQI to cause an increase in hepatocyte oxygen utilization (Figure 4.19.A and Table 4.5) and superoxide release (Figure 4.19.B), and the inhibition of these parameters stimulated by 2,5-dimethylbenzoquinone.

Preliminary *in vivo* toxicity studies of NAPQI were conducted in mice by i.p. injection. While a toxicity was observed at doses as low as 12.5 mg/kg (approximate LD_{50}= 20 mg/kg), this had the appearance of intravascular toxicity rather than the tissue necrosis which is predominantly observed in acetaminophen overdose. Administration of NAPQI resulted in a blue discoloration, most likely due to a disruption of hemoglobin oxygen binding. The blood was viscous and significantly lowered in volume. While these last two observations could be explained in part by coagulation, an increase in vessel wall permeability may have also played a role, resulting in blood seepage into the extravascular spaces. Histological examination of liver, kidney, and lung tissues revealed no evidence of necrosis, and testing of blood samples for methemoglobin gave highly variable values not clearly indicating formation of the ferric hemeprotein. From these results it was concluded that NAPQI was reacting with blood constituents, and that it was too short-lived under such conditions conditions of administration to reach the target organs.

The results of rat portal vein infusion of NAPQI in FC-43 emulsion were more conclusive. With this procedure NAPQI was protected from rapid degradation by minimizing exposure to blood proteins during its short transport to the liver ($t_{\frac{1}{2}}$ in FC-43 = 5 minutes determined by HPLC; $t_{\frac{1}{2}}$ in presence of microsomal proteins = 7 seconds).[58] This was visually evident during the infusion with the blood almost completely displaced from the portal vein and the occurance of significant blanching in the liver lobes. NAPQI-induced periportal necrosis was histologically observed, graded at 1 to 2+ in three of four lobes (see METHODS) and marked by pyknosis of the nuclear material (Table 4.7). These symptoms were produced at a dose of 20 mg/kg, considerably lower than that required to induce necrosis in unpretreated rats with acetaminophen (1000 mg/kg).[35] Typically the localization of liver damage in animals given high doses of acetaminophen is centrilobular, corresponding to the region with the highest levels of cytochrome P-450.[16] While this was different than the localization of necrosis caused by NAPQI infusion, such was anticipated since the periportal area was the first exposed to NAPQI via entry through the portal circulation. Contrary to expectations, levels of serum GPT were higher in the FC-43 infused-rat than in the NAPQI-dosed animal. This could be explained by physical damage during infusion causing a release of the enzyme with deactivation of SGPT occuring in the presence of NAPQI. This type of phenomenon was observed in the hepatocyte toxicity experiments, the levels of released LDH showing an apparent decrease at higher NAPQI concentrations.

The claim of similar toxicities in acetaminophen overdose and NAPQI infusion partially rested on the assumption that infused NAPQI entered the hepatocytes. An external toxic interaction of NAPQI with the cell membrane certainly could elicit cell death. But, the situation would clearly be different than that observed with the formation of NAPQI within the cell matrix. While hepatocyte uptake of NAPQI could not be verified conclusively in these experiments, the appearance of pyknosis indicated some absorption since this is generally observed only with toxins acting intracellularly.[138] In addition, the previously discussed hepatocyte studies demonstrated depletion of endogenous glutathione by added NAPQI. With such experiments NAPQI conjugation could only occur within the cell.

Thus, NAPQI possessed toxicity characteristics similar to the reactive metabolite of acetaminophen. With the exception of the explainable periportal localization of liver damage observed with NAPQI infusion in rats, the cellular features of necrosis were identical histologically to that seen with acetaminophen overdose. Hepatocyte studies revealed a rapid cytotoxic interaction of NAPQI with cells, and a pronounced depletion of endogenous glutathione. Furthermore, inhibitors of acetaminophen-induced necrosis were also effective in blocking the hepatocyte cytotoxicity of NAPQI.

Additional experiments were carried out to compare reactions of NAPQI, 2,6-dimethylNAPQI, and 3,5-dimethylNAPQI with glutathione. They revealed that the thiol can react with the acetaminophen metabolite both as a nucleophile and as a reductant. While both reactions were observed with NAPQI, the 2,6-dimethyl analog participated only in

conjugation, and 3,5-dimethylNAPQI was predominantly reduced by glutathione yielding 3,5-dimethylacetaminophen and GSSG. It is interesting that in mice and rats 3,5-dimethylacetaminophen displays a hepatotoxicty very similar to that of acetaminophen while little tissue damage is observed with administration of 2,6-dimethylacetaminophen.[102] While considerable work remains in this area, it is consistent with the results presented in this thesis and implied by the toxicity studies with the dimethylacetaminophen analogs, that the reactive metabolite of acetaminophen appears to be capable of undergoing both conjugation and reduction. The question can then be put forth as to which reactivity of NAPQI is responsible for acetaminophen toxicity. The chemical and metabolic behavior of acetaminophen, NAPQI, and their dimethyl analogs may implicate a toxicity mediated by the depletion of glutathione, NADPH, and NADH through reductive and conjugative reactions, with binding to proteins having less significance. In support of this, N-acetylcysteine administered to rats 4 to 6 hours after overdose rescued the livers from serious necrosis, but no significant inhibition of protein binding was observed.[139] Thus, protein binding and necrosis may represent two independnet processes. Further, ethanol administration has been shown to inhibit acetaminophen toxicity if given with the overdose,[140] presumably by increasing cellular resistence to oxidative stress through NADH production during the alcohol dehydrogenase metabolism of ethanol to acetaldehyde. It has been proposed by Orrenius[141-143] that the actual events leading to cell death involve the depletion of endogenous thiol stores. Thiols, most notably

glutathione, play a major role in the maintenance of extramitochondrial calcium levels. The depletion of endogenous thiol levels is followed by changes in membrane morphology, eventual influx of extracellular calcium, and death. Processes leading to significant glutathione depletion would therefore be expected to contribute to the loss of viability. Thus, the electrophilic properties of NAPQI may play a role in cell death through glutathione conjugation, but possibly not through protein conjugation directly. On the other hand, the oxidative capabilities of the quinone imine could contribute to necrosis through direct glutathione depletion by formation of GSSG, or more significantly through the consumption of cellular reducing equivalents important in the maintenance of reduced thiol stores. Especially important in this light is that a major fraction of NAPQI formed undergoes reduction back to acetaminophen. With the establishment of this futile cycle acetaminophen could significantly compromise the ability of the cell to maintain levels of reduced thiols, thereby elicting the events described above leading to cell death. Such proposals are clearly speculation at this time. Studies are planned in this laboratory to elucidate more of the mechanistic details of acetaminophen-induced necrosis through the use of the dimethyl analogs of acetaminophen and NAPQI.

The ESR studies of the semiquinone imine were performed in an attempt to further understand its contribution to NAPQI decomposition reactions and toxicity, and its role in the metabolism of acetaminophen by peroxidase. No ESR signals were detected from NAPQI in aqueous media either with reduction by $NaBH_4$ or by NADPH-cytochrome

P-450 reductase, or in rat liver microsomes with NADPH (Figure 4.23). However, a signal was generated upon $NaBH_4$ reduction of NAPQI in DMSO, and from the hyperfine splitting was interpreted as a signal from the semiquinone imine. Why an acetaminophen radical was not observable in aqueous solution is not understood. However, the rate of radical formation or the maintenance of steady state levels may be dependent on protonation, this either enhancing the rate of further reactions or influencing selection between two nonequivalent radical states differing in stability. These distinct acetaminophen radicals are defined by two sets of resonance structures involving unpaired electron residence time on either oxygen or nitrogen (Figure 4.28).

An alternative method was used to detect the acetaminophen radical formed during the NADPH and NADPH-cytochrome P-450 reductase-catalyzed reduction of NAPQI in buffer. Spin-exchange of the semiquinone imine with the cyclic hydroxylamine OXANOH produced the nitroxide radical OXANO, and provided evidence that the acetaminophen radical was present in aqueous media during the reductase-catalyzed reaction. Since rate data were not obtained in these experiments, a distinction between radical production from the enzymatic process and production through comproportionation could not be made.

Some quinonoid molecules such as adriamycin[4,5,6] are known to generate superoxide anion through reductase-catalyzed seminquinone formation and subsequent reduction of molecular oxygen by the radical. This has toxicological significance since activated oxygen species (hydroxyl radical, singlet oxygen) that are formed in this process are thought to promote lipid peroxidation.[33,144] Therefore, it was of

FIGURE 4.28: RESONANCE STRUCTURES OF TWO DISTINCT ACETAMINOPHEN FREE RADICALS.

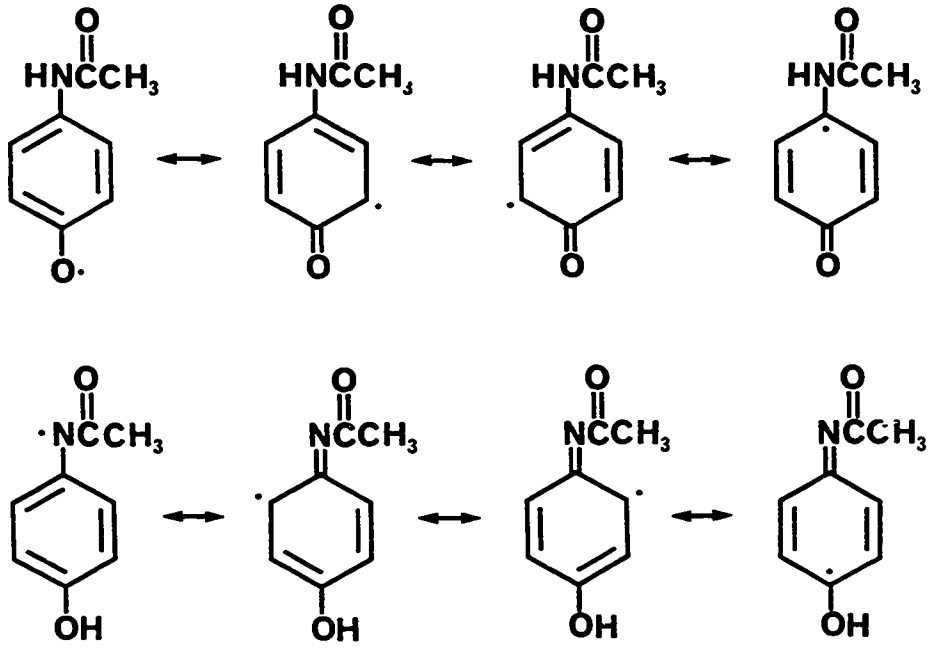
HNCCH3
O
O·
·NCCH3
NCCH3
OH

interest to monitor possible superoxide generation by N-acetyl-p-benzosemiquinone imine. Interestingly, no superoxide was detected in incubations of NAPQI with NADPH and NADPH-cytochrome P-450 reductase using an acetylated cytochrome c assay (Table 4.1). Furthermore, NAPQI significantly decreased the levels of superoxide anion that were formed in the reduction of 2,5-dimethylbenzoquinone by NADPH-cytochrome P-450 reductase. While the cytochrome c assay used in these studies may not have been sensitive enough to detect very low levels of superoxide, it did show that the reduction of NAPQI resulted in significantly lower levels of superoxide anion than those following the reduction of 2,5-dimethylbenzoquinone. These data were consistent with studies demonstrating a lack of NAPQI-induced oxygen consumption (Figure 4.2, Table 4.5) and lipid peroxidation in isolated hepatocytes. Moreover, NAPQI also inhibited the stimulation of oxygen consumption and lipid peroxidation by 2,5-dimethylbenzoquinone in isolated hepatocytes. The mechanism of this inhibition is not known, but it may involve reduction of NAPQI by superoxide anion, or reduction of superoxide or the dimethylbenzoquinone radical by the semiquinone imine of NAPQI.

It had been established that quinonoid couples, such as benzoquinone/hydroquinone, react through a comproportionation process yielding the semiquinone radical.[99] Such a reaction (see Equation 3.8) with the NAPQI/acetaminophen couple was postulated earlier in this chapter as an explanation for the enhancement of NAPQI decomposition with added acetaminophen (Figure 4.1), and in Chapter III to account for the similar binding properties of the acetaminophen metabolites

derived from P-450 and horseradish peroxidase oxidations. Evidence for such a comproportionation between acetaminophen and NAPQI was provided by spin-exchange experiments OXANOH. Furthermore, reaction of acetaminophen with NAPQI in the presence of the spin trap DMPO resulted in an ESR spectrum corresponding to DMPO-OOH (Figure 4.24). Thus, it appears that superoxide is a product of the reaction between molecular oxygen and the semiquinone imine formed through comproportionation of NAPQI and acetaminophen.

These results are not totally consistent with the results from studies demonstrating that NAPQI did not lead to superoxide formation (Figure 4.19.B), oxygen consumption (Figure 4.19.A, Table 4.6), or lipid peroxidation in isolated hepatocytes. While it can be argued that the DMPO spin trap was more sensitive than any of the above procedures in the detection of superoxide, this does not explain NAPQI inhibition of the generation of superoxide anion and consumption of oxygen mediated by 2,5-dimethylbenzoquinon. Rather, these experiments indicated that NAPQI or the semiquinone imine interact with superoxide or the dimethylbenzoquinone radical in an inhibitory manner, and should not therefore be able to generate superoxide from dioxygen.

The reduction of NAPQI by pulse radiolysis produced a short-lived species with an absorption spectrum similar to that seen with other semiquinones (Figure 4.25).[133] The free radical decayed rapidly through a second-order process with $k = 2.0 \times 10^9\ M^{-1}s^{-1}$. This constant was similar to values reported for simple semiquinones, and at a concentration of 1.0 μM the half-life was calculated to be 350 μseconds.[134] Determined by the approach-to-equilibrium method (see

METHODS), the one-electron reduction potential of NAPQI was determined as E_7^1= -251 mV compared to the standard duroquinone/durosemiquinone couple. Similar procedures using the oxygen/superoxide couple as a standard resulted in nonlinear plots, and were therefore not considered as accurate in determining the one-electron reduction potential of NAPQI. These studies did, however, reveal that in spite of the relatively strong reduction potential of the NAPQI/semiquinone imine couple, the reaction between the acetaminophen radical and oxygen was slow ($k = 2.0 \times 10^6\ M^{-1}s^{-1}$). This was in contrast to other simple semiquinones which can react with oxygen almost two orders of magnitude more rapidly, and with the more complex adriamycin radical capable of faster reaction with oxygen by approximately one order of magnitude.[131,133]

In summary, NAPQI has been prepared in stable crystalline form and has been shown to be an oxidation product of acetaminophen in reactions catalyzed by purified rat liver cytochrome P-450 and cumene hydroperoxide. Partitioning experiments of radiolabeled NAPQI have provided compelling evidence that this quinone imine is the major metabolite formed by hepatic microsomal oxidation of acetaminophen. Chemical and biochemical studies with NAPQI have shown it to be both a good oxidant and electrophile. Based on preliminary studies with methylated analogs of NAPQI, the oxidant properties appear to be most important in eliciting cytotoxicity. However, a large amount of work remains to be done to substantiate this hypothesis, especially in light of conflicting evidence for and against the propensity of NAPQI

or its semiquinone radical to react with molecular oxygen and superoxide anion.

D. EXPERIMENTAL

1. MATERIALS

The instruments described in Chapters II and III were used to carry out HPLC separations, liquid scintillation, NMR, and IR spectroscopy, melting points, pH measurements, liver microsome preparation, and protein binding assays.

Some of the HPLC applications described in this chapter also ulitized a Waters Associates 660 solvent programmer, and an LC-4 amperometric detector with a carbon-paste electrode (Bioanalytical Systems, West Lafayette, IN). Radioladeled components were collected from HPLC eluates using an LKB 2112 Redirac fraction collecter.

Mass spectral analyses were performed on a VG 7070H Micromass spectrometer, and the high field proton-NMR spectrum of the glutathione adduct of 2,6-dimethylacetaminophen was recorded on a Bruker WM-500 superconducting NMR spectrometer. Electron spin resonance studies were performed on a Bruker ER-420 using a quartz capillary sample cuvette, i.d. 0.2 cm. Kinetics were determined spectrophotometrically on a Shimadzu UV 250.

Hepatocyte oxygen utilization was measured with a Yellow Springs Instruments Model 53 Clark oxygen electrode (New York, NY).

Collagenase, menadione, α-tocopherol, and cytochrome c were purchased from Sigma Chemical Company, while silver(I)oxide, Florisil, p-aminophenol, and L-ascorbic acid were obtained from Aldrich Chemical Company. Cumene hydroperoxide and [1-^{14}C]acetic anhydride were purchased from ICN (Plainview, NJ, and Irvine, CA, respectively), and [ring U-^{14}C]acetaminophen was obtained from Pathfinder Laboratories Incorporated. Oxypherol was from Green Cross Corporation (Osaka, Japan) and other chemicals were purchased from the following sources: ultrapure chloroform from Burdick and Jackson; Raney nickel from K and K Laboratories; and butylated hydroxy toluene from Nutritional Biochemicals Corporation (Cleveland, OH).

2. METHODS

Preparation of Buffers and Miscellaneous Solutions

Buffers:

a) The perfusion buffer used in the isolation of hepatocytes was made up as a concentrated stock solution containing per liter: NaCl (70.7 gm, 0.121 M); KCl (4.47 gm, 6.0 mM); $MgSO_4$ (1.48 gm, 0.6 mM); KH_2PO_4 (1.01 gm, 0.74 mM); $NaHCO_3$ (10.08 gm, 12.0 mM); and, glucose (9.00 gm, 5.0 mM). The stock solution was diluted with distilled water 10:1 to a final volume of 750 ml followed by saturation with carbogen (95% O_2, 5% CO_2). The pH was adjusted to 7.4 with 0.1 N HCl, and the solution was maintained at 37°C.

b) The wash buffer for hepatocyte isolation consisted of 25 ml of a stock solution diluted to 250 ml. The stock buffer was made by

adding to 1.00 liter: NaCl (76.5 gm, 0.131 M); KCl (3.88 gm, 0.2 mM); $MgSO_4 \cdot 7H_2O$ (2.22 gm, 0.9 mM); $CaCl_2 \cdot 2H_2O$ (0.176 gm, 0.12 mM); and, Na_2HPO_4 (4.26 gm, 3.0 mM). After dilution the buffer was saturated with carbogen and the pH adjusted to 7.10. Once perfusion was established with this solution, collagenase (75 mg) was added in a solution of $CaCl_2$ (1.0 ml, 100 mM).

c) Incubation buffer was prepared by the dilution of 10.0 ml stock wash buffer to 100 ml with distilled water. Tris and (121 mg) bovine serum albumin (1.0 gm) were then added and the solution was saturated with carbogen. Final pH adjustment was made to 7.35 with 0.1 N HCl.

d) Buffered formalin for the storage of tissue samples contained in 1.0 liter: $NaH_2PO_4 \cdot H_2O$ (4.0 gm), $Na_2PO_4 \cdot 7H_2O$ (12.3 gm), and 37% aqueous formaldehyde (100 ml). Final pH was approximately 7.07.

Miscellaneous Solutions:

a) Citrate mobile phase form HPLC was made by mixing 800 ml 0.1 M citrate buffer (pH 7.2) and 200 ml methanol. The citrate buffer was prepared fresh each day from stock solution of 0.1 M citric acid and 0.1 M trisodium citrate. The pH was adjusted before combination with the methanol using 10% HCl. Filtration and degassing were accomplished as in METHODS Chapter II.

b) The phosphate buffer used in the reverse phase gradient elution system was prepared by mixing KH_2PO_4 (10.2 gm, 0.075 M) and acetic acid (10.0 ml) with distilled water to a volume of 1.0 liter. The solvent was filtered and degassed before use.

c) Cofactor regenerating system was prepared by combining NADP (8.0 mg) and glucose-6-phosphate (80 mg) in 0.1 M phosphate buffer (5.0 ml), pH 7.4, then adding 1.0 M $MgCl_2$ (0.2 ml) and glucose-6-phosphate dehydrogenase (20 units).

Synthesis of N-Acetyl-p-benzoquinone Imine

NAPQI was prepared by the oxidation of acetaminophen with silver(I)oxide in chloroform.[59-60] Best yields necessitated the use of pure starting materials. Hence, commercially available ultrapure Ag_2O (Aldrich Gold Label, >99.99%) was utilized, and acetaminophen and chloroform were purified before use. Acetaminophen was first dissolved in distilled and deionized water, and the solution was acidified to pH 5 with 10% HCl. The acetaminophen was extracted with HPLC-grade ethylacetate, leaving a significant p-aminophenol impurity in the aqueous phase. This was followed by removal of the organic solvent, recrystallization from hot water, and drying overnight at 110°C. Chloroform was purchased as HPLC-grade without the ethanol stabilizer. To remove any potential phosgene, the solvent was shaken with a small volume of concentrated H_2SO_4 then washed four times with pure water. After drying over anhydrous sodium carbonate the chloroform was distilled and stored in tightly sealed amber bottles.

The synthesis of NAPQI was typically performed on a scale of 1.0 gm acetaminophen (6.62 mmoles), 2.0 gm Ag_2O (8.62 mmoles), and 1.0 gm anhydrous sodium sulfate in 100 ml chloroform. After stirring for 60 minutes at room temperature, butylated hydroxy toluene (approximately 1.0 mg) and a small amount of activated charcoal were added. The crude

NAPQI solution was filtered through Celite and the resulting yellow solution was rotory evaporated to approximately 2.0 ml. This was eluted through a 3.6 x 14 cm column of dried Florisil (magnesium silicate) with anhydrous diethyl ether and collected as a distinct yellow band. The collection volume was reduced to 2 ml by rotory evaporation and transfered to a sublimation apparatus where solvent removal was completed with a stream of dry nitrogen. Yields at this point were as high as 80%. The NAPQI was sublimed (45-50°C at 0.07 mm Hg) to give yellow cubic crystals (0.4 gm, 40% yield): m.p. 74-75°C; IR (KBr pellet) ν_{max} 3050 (m), 2990 (w), 1700 (s, CH_3CO), 1651 (s, CO), 1620 (s), 1579 (s, CH), 1430 (m), 1362 (m), 1210 (s), 1103 (m), 885 (s) cm^{-1}; ^{1}H-NMR (C_6D_6) δ 1.79 (s, 3H, acetyl H), 6.00 (d, 2H, J_{BA} = 9.0 Hz), 6.38 d, 2H, (J_{AB} = 9.0 Hz); UV λ_{max} (n-hexane) 236 nm (ϵ = 3.3 x 10^4 $M^{-1}cm^{-1}$), 376 (1.6 x 10^2). Elemental analysis $C_8H_7NO_2$ (C,H,N).

Purity was greater than 99% (>1% acetaminophen) as determined by peak comparison using normal phase HPLC on a Partisil PXS 5/25 column with ethyl acetate as mobile phase and UV detection. At a flow rate of 1.0 ml/minute, the retention times were 4.5 minutes for NAPQI and 9.0 minutes for acetaminophen. A sample of this material was submitted to high resolution mass spectral analysis. The EI spectrum Figure (4.29.A) was characterized by a parent ion at m/e 149 with the fragments m/e 134 ($M^+\cdot$ -CH_3), 107 ($M^+\cdot$ -CH_2CO), 106 ($M^+\cdot$ -CH_3CO), and 43 (CH_3CO^+); the elemental composition of all ions was determined by high resolution mass analysis. Interestingly, at lower source temperatures a significant M + 2 peak appeared in the spectrum (Figure

FIGURE 4.29: DIRECT INSERTION PROBE MASS SPECTRA OF SYNTHETIC NAPQI. (A) EI MASS SPECTRUM OF NAPQI WITH ION SOURCE TEMPERATURE OF 200°C; (B) EI MASS SPECTRUM OF NAPQI WITH SOURCE TEMPERATURE AT 160°C SHOWING A SIGNIFICANT $[M + 2]^{+\cdot}$; (C) EI MASS SPECTRUM OF NAPQI WITH ION SOURCE AT 160°C AND 1 μL OF D_2O INJECTED INTO THE SOURCE DEMONSTRATING THE SHIFT FROM $[M + 2]^{+\cdot}$ TO $[M + 4]^{+\cdot}$; (D) CI MASS SPECTRUM (METHANE) OF NAPQI.

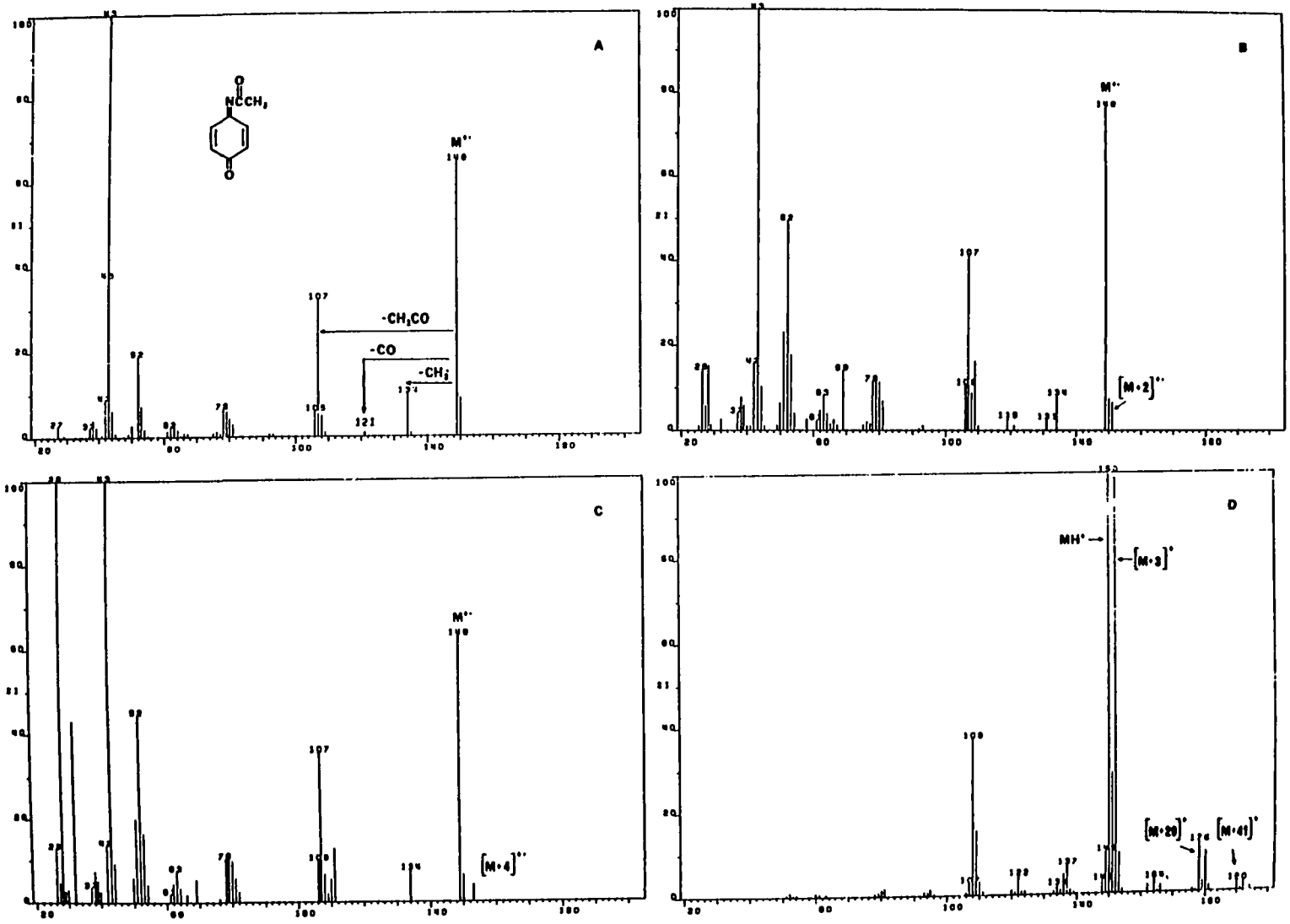
A
B
C
D
M+·
-CH3CO
-CO
-CH3
[M+2]+·
[M+4]+·
MH+
[M+3]+
[M+29]+
[M+41]+

4.29.B). This is common with quinonoid molecules and appears to have been due to protonation by traces of residual water in the ion source followed by rapid reduction.[145] The injection of 1 µl D_2O into the source shifted the M + 2 peak to M + 4, which was consistent with the proposed mechanism (Figure 4.29.C). In comparison, acetaminophen under the same conditions gave a different abundance pattern for the M + X ions, negating the possibility that the M + 2 peak arose from an acetaminophen impurity. High resolution CI (methane) gave a quasi-molecular ion m/e 150 and the addition products M + 29 = 178 and M + 41 = 190 (Figure 4.29.D). The prominant M + 3 peak in this spectrum was attributed to the quasimolecular ion of acetaminophen produced by the reduction previously described.

Synthesis of [Ring-^{14}C]NAPQI and [Acetyl-^{14}C]NAPQI

[Ring-^{14}C]Acetaminophen (100 mg, 0.66 mmoles, 0.20 mCi/mmole) or [acetyl-^{14}C]acetaminophen (100 mg, 0.66 mmoles, 0.21 mCi/mmole) were reacted with 200 mg silver oxide in 10 ml dry chloroform. The reactions and purifications were carried out as above. Radiochemical purity of the NAPQI analogs was verified by collection and counting of eluate fractions from the normal phase HPLC system used for the the purity check of nonlabeled NAPQI.

[Ring-^{14}C]acetaminophen was purchased from a commercial supplier (9.79 mCi/mmole) and required purification using a reverse phase HPLC system of 86.5/12.5/1 water, methanol, and acetic acid on a µBondapak C-18 column. The acetyl-labeled starting material was synthesized by the acetylation of p-aminophenol with ^{14}C-acetyl chloride. The amine

(242 mg, 2.22 mmoles) was dissolved in 16 ml diethyl ether. A bicarbonate slurry (2.0 ml of 8.0 gm sodium bicarbonate/25 ml water) was added followed by the slow addition of the acetyl chloride in ether (200 mg/25 ml, 7.85 mCi/mmole). The reaction was followed to completion by TLC, and a 2-fold volume of 0.2 N NH_4OH was added then neuatralized to pH 7.0 with solid monobasic sodium phosphate. The reaction mixture was extracted three times with ethyl acetate, dried over sodium sulfate then filtered through Celite. The product was partially purified by passage through a silica column with ethyl acetate, then recrystallized from hot water to give 62 mg of product (overall yield 18%). Radiochemical purity was determined on the methanol/water/acetic acid system to be 98.4% for the acetyl-labeled compound and 99% for the ring-labeled compound.

Products and Kinetics of NAPQI Decomposition in Aqueous Media

The half-order rate plots of NAPQI decomposition (Figure 4.1) were generated by reacting 0.4 mM NAPQI in 0.1 M sodium phosphate buffer, pH 7.4, prepared as described in METHODS, Chapter II. NAPQI was added in 0.01 ml acetone (18 NAPQI mg/ml) to 3.0 ml buffer and the time course of NAPQI disappearance was followed at approximately 4 minute intervals by reverse phase HPLC. A C-18 μBondapak column was used with a solvent system of 80% 0.1 M citrate buffer, pH 7.2, and 20% methanol. At a flow rate of 2.0 ml/minute the retention times of acetaminophen and NAPQI were 2.5 and 3.3 minutes, respectively. NAPQI concentration values were calculated from peak height based on a NAPQI standard curve. Acetaminophen was added to the buffer before the

addition of NAPQI to obtain concetrations of 8.0, 20.0, 40.0, and 80.0 μM.

The products of [ring-^{14}C]NAPQI decomposition (Figure 4.2) were determined by gradient elution reverse phase HPLC. NAPQI was added to phosphate buffer (4.0 ml, 0.1 M, pH 7.4) in 10 μl ultrapure DMSO to obtain final concetrations of 0.05 mM (0.21 mCi/mmole) or 1.0 mM (0.01 mCi/mmole). Decomposition was allowed to proceed for 30 minutes, and the solutions were saturated with ammonium sulfate. The products were then extracted into two volumes of acetone and the organic phase was dried over anhydrous magnesium sulfate and evaporated. HPLC was used to verify that all reaction products were carried through the extraction. After reconstitution in 75 μl methanol, the volumes were injected on an HPLC fitted with a 5μ Ultrasphere ODS column (4.6 mm x 25 cm). Separation was accomplished with nonlinear gradient elution (program 10, Waters Associates Model 660 M solvent programmer) of 0.075 M KH_2PO_4 and 1% acetic acid with 5% methanol increasing over 12 minutes to 30%. Retention times were: acetaminophen, 6.5 minutes; benzoquinone, 6.8 minutes; component A, 14.5 minutes; B, 17.5 minutes; C, 21.0 minutes; D, 24.5 minutes; and E, 30.5 minutes. Compound F eluted upon column flush with 95% methanol. Collections were made at 1.0 minute intervals over the course of the entire chromatogram and concentrations of the eluted reaction products were determined by liquid scintillation counting in 10 ml Aquasol 2. The recoveries of radiolabel were 100% and 98% for the 1.0 mM and 0.05 mM reactions, respectively, determined by comparison to counted aliquots of the reaction extracts.

The late-eluting peaks A through F were separated by semipreparatory reverse phase HPLC (μBondapak column, 7.8 mm x 30 cm) using the same gradient elution system as above but at 3.5 ml/minute. Retention times on this system were: acetaminophen and benzoquinone, 14.0 minutes; component A, 17.8 minutes; B, 20.0 minutes; C, 23.2 minutes; D, 28.4 minutes; E, 33.0 minutes; and F eluted with a 95% methanol wash. The fractions required further purification and were injected on a semipreparatory normal phase column (μPorasil 7.8 mm x 30 cm) using varying ratios of hexane/isopropanol or methanol/isopropanol for each component. Interestingly, the elution order of the decomposition products was the same on both the normal phase and the reverse phase systems.

The purified fractions were analyzed by direct insertion probe EI mass spectroscopy. Component A produced the spectrum in Figure 4.3 characterized by a parent ion at m/e 300 with fragments at m/e 258 ($M^{+}\cdot$ $-CH_2CO$), and 216 ($M^{+}\cdot$ $-2CH_2CO$). The elemental composition of all ions was confirmed by high resolution mass measurments. The other late-eluting compounds, B through F, decomposed in the mass spectrometer source and did not produce useful spectra in either the EI or CI mode.

Reduction of NAPQI by NADH and NADPH

Radiolabeled NAPQI (ring-^{14}C, 0.21 mCi/mmole) and NADH, or NAPQI and NADH were combined in 1.0 ml 0.1 M phosphate buffer, pH 7.4, at equmolar concentrations of 0.5 mM. The formation of acetaminophen and benzoquinone were monitored at approximately 10 minute intervals using

the same HPLC-radiochemical assay described for the experiments determining the products of NAPQI decomposition.

The oxidation of unlabeled NADPH by NAPQI was followed in identical reaction mixtures by monitoring the decrease in absorbance at 340 nm continuously for 20 minutes. Time-dependent concentration values were calculated from an NADPH standard curve and plotted in Figure 4.4 at 0.2 minute intervals for the first 2 minutes of reaction and every 1 minute thereafter. The same methods were employed to determine the reduction of NAPQI by NADPH under pseudo-first-order conditions (Figure 4.8).

Reduction of NAPQI by NADPH and NADPH-Cytochrome P-450 Reductase

NADPH-cytochrome P-450 reductase was purified from the livers of phenobarbital-pretreated (80 mg/kg i.p. for 3 days) Sprague-Dawley rats by Dr. Garth Powis (Department of Developmental Oncology, Mayo Clinic, Rochester, MN) according to the method of Yasukochi and Masters.[146] The specific activity of the reductase was 67.9 U/ml (1 unit defined as the quantity of enzyme catalyzing the reduction of cytochrome c at an initial rate of 1 nmole/minute at 26°C under the conditions of Philips and Langdon).[147]

Incubation mixtures contained NADPH-cytochrome P-450 reductase (0.4 to 8.0 §g/ml) $MgCl_2$ (5.0 mM), and EDTA (0.1 mM) in of Tris/KCl buffer (3.0 ml, 0.1 M, pH 7.4). Immediately after the addition of NAPQI (final concetrations of 0.5 µM to 100 µM in 10 µl DMSO) the reactions were initialized by the addition of NADPH (0.05 mM). The rate of NADPH oxidation was measured by UV absorbance at 340 nm

(Figure 4.9). Correction was made for the nonenzymatic oxidation of NADPH by NAPQI in controls where reductase was omitted.

Studies of the inhibition of NADPH-cytochrome P-450 reductase-mediated cytochrome c reduction were performed under the reaction conditions described above with the additional inclusion of 1.2 to 6.0 §M cytochrome c. The rate of cytochrome c reduction was followed by UV absorbance at 550 nm (Figure 4.10).

Superoxide formation was determined by the reduction of acetylated cytochrome c at 550 nm.[68] Incubations were as described above for the reductase-NAPQI experiments except that 60 µM acetylated cytochrome c was added as well as either 0.1 mM 2,5-dimethylbenzoquinone or 66 µg/ml superoxide dismutase (Table 4.1).

Inhibition of In Vitro Protein Binding of Acetaminophen by NADH, NADPH, and NADPH-Cytochrome P-450 Reductase

Incubations used to investigate inhibition of acetaminophen protein binding by NADH, NADPH, and NADPH-cytochrome P-450 reductase contained: purified hepatic cytochrome P-450 from phenobarbital-pretreated rats (0.5 nmoles), phosphatidyl choline (20 µg), [ring-^{14}C]acetaminophen (5.0 µmoles, 0.98 mCi/mmole), and bovine serum albumin (10 mg) in potassium phosphate buffer (1.0 ml, 0.1 M, pH 7.4). NADH or NADPH were added in buffer to final concentrations of 0, 0.1, 0.5, 1.0, 1.5, and 2.5 mM (Figure 4.12) to incubations used in the study the inhibitory effects of these cofactors. The inhibition of acetaminophen covalent binding by NADPH-cytochrome P-450 reductase was determined in reactions to which the reductase was added to obtain

final concentrations of 0.1, 0.2, 0.3, 0.4, 0.5, 1.0, 2.5, and 5.0 μM. These additions resulted in reductase-to-P-450 ratios ranging from 0.2 to 10 (Figure 4.13). The reductase and NADH-inhibited incubations were supported by an NADPH-regenerating system that included glucose-6-phosphate (5.0 mM), NADP (1.0 mM), $MgCl_2$ (3.0 mM), glucose-6-phosphate dehydrogenase (0.2 U/ml). The purification of cytochrome P-450 and NADPH-cytochrome P-450 reductase was carried out by Dr. Anthony Y.H. Lu and Dr. Gerald T. Miwa, Merck Sharp and Dohme Research Laboratories, Rahway, NJ, according to published procedures.[148,149] Incubations were carried out at 37°C for 10 minutes in the studies with reductase and NADH, and for 5.0 minutes in the experiments with NADPH. Reactions were terminated by protein precipitation with ice cold trichloroacetic acid (0.4 mM). Protein binding was determined as previously described in Chapter II, METHODS.

Detection of NAPQI as a Product of Cytochrome P-450 Oxidation of Acetaminophen

The direct detection of NAPQI as an oxidation product of acetaminophen (Figure 4.14) was carried out in cumene hydroperoxide-supported incubations of purified hepatic cytochrome P-450 from phenobarbital pretreated rats. The incubations consisted of 0.5 μM P-450, 2.0 mM cumene hydroperoxide, and 0.5 mM acetaminophen in 0.2 ml sodium phosphate buffer, pH 7.4. In the experiments detecting NAPQI as a radioladeled product, purified [ring-^{14}C]acetaminophen (9.78 mCi/mmole) was used as the substrate. Reactions were run for 6.0 minutes at 37°C, afterwhich time a 25 μl sample of the incubation was

injected directly onto a C-18 μBondapak column. With the citrate buffer-methanol mobile phase previously described and a flow rate 1.0 ml/minute, NAPQI eluted at 8.8 minutes, acetaminophen at 6.2 minutes, and benzoquinone at 6.2 minutes.

In the electrochemical detection of NAPQI, HPLC flow was directed through a UV detector utilizing a 254 nm filter in series with an amperometric detector connected to a carbon-paste electrode at -240 mV. Under these reductive conditions NAPQI and benzoquinone were readily detectable, but acetaminophen could only be monitored by UV. The concentrations of NAPQI formed from the P-450 oxidation of acetaminophen, as well as the determination of detection limits (1.1×10^{-7} M NAPQI), were established by generating standard curves with synthetic NAPQI and calculating limits of detection [$c_{L(k=3)}$] as defined by IUPAC using the propagation of errors approach.[114]

In the radiochemical detection of NAPQI, cumene hydroperoxide-supported P-450 incubations of [ring-^{14}C]acetaminophen were carried out as above. Aliquots of 25 μl were injected directly onto the HPLC with a C-18 μBondapak column and a mobile phase of 80% 0.1 M phosphate buffer, pH 7.4, and 20% methanol. With this system NAPQI was retained 11.8 minutes and acetaminophen 7.4 minutes. Collections of the eluate were made at 15 second intervals, and radioactivity was monitored by liquid scintillation counting of the fractions in 10 ml Aquasol 2. The detection limit with this method was calculated to be 6.7×10^{-8} M using [ring-^{14}C]NAPQI standards in the propagation of errors approach.

Verification that the radiolabel peak contained NAPQI was made by collection of the NAPQI, as well as 1.0 minute fractions before and

after the peak, into vials containing 5 µl L-ascorbic acid. Reduction of the NAPQI was rapid and complete as verified by HPLC analysis. A carrier pool of unlabeled acetaminophen (50 µg) was added to the NAPQI collection solutions which were then saturated with sodium sulfate and extracted twice with 2.0 ml ethyl acetate. The organic phase was dried over sodium sulfate, evaporated under a stream of nitrogen, and reconstituted in 250 µl methanol. A volume of 50 µl was injected on reverse phase HPLC using the mobile phase utilized in the NAPQI radiochemical assay. With collection and liquid scintillation counting of the fractions eluting at the retention time of acetaminophen, 88% of the radiolabel that eluted as NAPQI was recovered as acetaminophen, whereas the fractions collected before and after the NAPQI contained no radiolabel above background.

Metabolite Partitioning Studies of Acetaminophen and NAPQI in Microsomal Incubations

Microsomes were prepared from the livers of male Swiss-Webster mice (20 to 25 gm) as described (Chapter II, METHODS). Complete incubations included: microsomes (2 mg/ml protein), an NADPH (0.5 ml) regenerating system, and either acetaminophen (1.0 mM, [acetyl-^{14}C], 0.41 mCi/mmole, or [ring-^{14}C], 0.48 mCi/mmole) or NAPQI (0.05 mM, [acetyl-^{14}C], 0.21 mCi/mmole, or [ring-^{14}C], 0.20 mCi/mmole) in phosphate buffer (3.0 ml, 0.1 M, pH 7.4). L-Ascorbic acid (1.0 mM) and glutathione (1.0 mM) were added in buffer to the appropriate incubations as inhibitors (Table 4.2). The reactions were run for 20 minutes at 37°C in a shaker-water bath, and terminated by the addition of 1.5

ml ice cold acetone. Centrifugation was used to isolate the precipitated proteins, and covalent binding was determined as discussed in Chapter II (METHODS). Metabolites were assayed by injecting 75 µl aliquots of the supernatant fraction onto a 5µ Ultrasphere ODS column which was eluted with the nonlinear gradient system that was used in the determination of NAPQI decomposition products. Retention times of standards as determined by UV absorption were: benzoquinone, 9.1 minutes; acetaminophen, 12.4 minutes; and 3-S-glutathionylacetaminophen, 15.5 minutes. Between injections the column was flushed with 95% methanol. Fractions were collected at 1.0 minute intervals throughout the chromatogram, and metabolite levels were determined by liquid scintillation counting.

The assay for ^{14}C-acetamide in the reactions containing acetyl-labeled acetaminophen or NAPQI was performed as described by Nelson et al.[116] This involved the addition of 50 µg nonlabeled acetamide to the 3.0 ml incubation supernatants followed by two extractions with 5 ml diethyl ether and twice more with 5 ml ethyl acetate. The supernatants were then saturated with ammonium sulfate and extracted three times with 5 ml acetaone. The acetone was rotary evaporated, and the removal of residual water was enhanced by the azeotrope with ethanol. Samples were reconstituted in 0.25 ml methanol and injected on normal phase HPLC using a Partisil PXS 5/25 column with a mobile phase of 97.5/2.0/0.5 ethylacetate, methanol, and acetic acid at 1.0 ml/minute. The acetamide peak (16 to 25 minutes) was collected and counted by liquid scintillation spectroscopy.

Toxicity of NAPQI in Isolated Hepatocytes

Adult male Sprague-Dawley rats (180 to 280 gm) were anesthetized with ether, and surgically opened to expose the portal vein. Two ligatures were loosely tied around the portal vein approximately 1 cm apart just above the juncture of the mesenteric vein. The lower ligature was tied off and used to aid in the insertion of a 22g cannula. Once inserted into the vessel, the cannula was fixed firmly with the second ligature.

During this procedure perfusion buffer was maintained at a flow rate of approximately 3 ml/minute/gm liver weight through the cannula using a peristaltic pump. Once the cannula was inserted the hepatic artery and superior vena cava were cut, and the liver gently removed and placed in a perfusion box. This apparatus allowed collection and recycling of buffers used later in the procedure, as well as the maintenance of the temperature at 37°C. After approximately 10 minutes of perfusion the flow was switched to the wash buffer, and after another 30 seconds 75 mg of collagenase in 100 ml in 0.1 M $MgCl_2$ was added and recycled for 12 to 15 minutes. Cell suspension was accomplished by carefully tearing the membranous sack enclosing the organ and gently shaking the cells into wash buffer. After filtering though cheese cloth the cells were repeatedly centrifuged (50 g, 30 seconds) and washed until a viability of 90 to 96% was achieved as judged by trypan blue exclusion.

The hepatocytes were diluted to a concentration of 1.5×10^6 cells/ml in incubation buffer containing 1% BSA to minimize aggregation. Chemical additions were made directly to the medium, or in the

case of NAPQI in 10 µl DMSO. Reactions were terminated by placing on ice, and cell viability was determined by trypan blue[117] exclusion and by measurement of lactate dehydrogenase release.[118]

The trypan blue exclusion test was done by adding 0.1 ml of the cell suspension with 0.9 ml trypan blue (0.4% in wash buffer). Cells excluding trypan blue under microscopic examination were considered viable and were quantitated as the percentage of total hepatocytes.[117]

Intracellular glutathione levels were measured by the method of Tietze.[120,121] Hepatocyte suspensions were centrifuged and the cells lysed in cold 10 mM phosphate/5mM EDTA buffer, pH 7.5. Aliquots of 25 µl were mixed with a standard glutathione assay solution to a final volume of 1.0 ml. The assay solution contained 0.6 µmole DTNB (Ellman reagent, 5,5'-dithiobis-2-nitrobenzoic acid), 0.2 µmole TPNH (triphosphopyridine), and 10 µg glutathione reductase. Concentrations of glutatione were determined by the change in absorbance at 412 nm calculated from a glutathione standard curve.

Lipid peroxidation was assessed by measuring the presence of thiobarbituric acid (TBA) reacting substances.[123] Aliquots (25 µl) of the cell suspensions were added to 0.5 ml 10% trichloroacetic acid. TBA was added (1.0 ml of 0.07%), followed by heating at 100°C for 15 minutes. After a 15 minute centrifugation at 4300g the supernatants were monitored by UV at 532 nm. Lipid peroxidation was expressed as absorbance units/10^6 cells.

In Vivo Toxicity Studies of NAPQI

Preliminary toxicity studies were conducted in male Swiss-Webster mice by i.p. injection of NAPQI in propylene glycol (0.2 ml). After decapitation of the mice, tissue samples were immediately removed and stored in buffered formalin. Histological examinations were conducted by Dr. Randy McMurtry, Denver Presbyterian Hospital, Denver, CO. Cellular damage was determined by the method of Mitchell et al.[62] and quantified according to the scale of: 0, necrosis absent; 1+, necrosis of less than 6% of the hepatocytes; 2+, necrosis in 6% to 25% of the hepatocytes; 3+, 26% to 50% of the hepatocytes necrotic; and 4+, greater than 50% incidence of necrosis in the hepatocytes.

The direct portal infusion studies were done in male Sprague-Dawley rats (340 gm) anesthetized with urethane at 0.5 gm/kg. NAPQI was added to FC-43 emulsion in tetrahydrofuran (1.0 mg/25 µl) and infused into the portal vein with a 26g needle giving a concentration of 20 mg/kg (20 mg NAPQI/10 ml FC-43/kg). The injections were made slowly (3.4 ml in 3 to 4 minutes) to avoid rupture of the vessel, afterwhich the needle was carefully removed and moist gauze held over the portal vein for 7 to 10 minutes. The animals were surgically closed and maintained in metabolic cages for 5 hours under a heat lamp. Upon sacrifice blood samples were withdrawn from the heart with heparinized needles and urine was obtained directly from the bladder. Liver and kidney specimens were removed and stored in buffered formalin. Serum GPT values were determined by Pathologists Central Laboratory, Seattle, WA.

Comparative Studies of NAPQI, 2,6-DimethylNAPQI, and 3,5-DimethylNAPQI Reactions with Glutathione

N-Acetyl-3,5-dimethyl-p-benzoquinone imine and N-acetyl-2,6-dimethyl-p-benzoquinone imine were prepared by the lead tetraacetate oxidation of 3,5-dimethylacetaminophen and 2,6-dimethylacetaminophen as described by Fernando.[102] 3,5-Dimethylacetaminophen was prepared by the reaction of 2,6-dimethylphenol with sodium nitrite yielding 2,6-dimethyl-4-nitrosophenol. Catalytic reduction (H_2/Pt) in a mixture of acetic acid and acetic anhydride gave 3',5'-dimethyl-4'-hydroxyacetanilide which was purified by recrystallization from water. The synthesis of 2,6-dimethylacetaminophen involved diazotization of sulfanilic acid and reaction with 3,5-dimethylphenol to yield 4-amino-3,5-dimethylphenol. Acetylation was performed using acetic anhydride followed by recrystallization from chloroform/petroleum ether giving 2',6'-dimethyl-4'-hydroxyacetanilide.

The reactions of NAPQI, 2,6-dimethylNAPQI, and 3,5-dimethylNAPQI with glutathione contained quinone imine (0.5 mM) and glutathione (1.0 mM) in potassium phosphate buffer (3.0 ml, pH 7.4). With the reaction of 2,6-dimethylNAPQI with glutathione, reaction progress was monitored by the shift in UV absorbance from 255 nm (λ_{max} of 2,6-di-methylNAPQI) to 296 (λ_{max} of product). The formation of 3-S-glutathionyl-2,6-dimethylacetaminophen was confirmed by analysis of the product eluting (18.6 minutes) from the nonlinear HPLC gradient system previously described for the NAPQI decomposition studies. Cleavage of the conjugate with Raney nickel in refluxing ethanol yielded 2,6-dimethylacetaminophen as determined by HPLC comparison to synthetic standard

and by mass spectroscopy. The EI mass spectrum was characterized by major ions at m/e 179 ($M^{+\cdot}$), 137 (M - CH_2CO), and 122. A high resolution ^{1}H-NMR spectrum was obtained for the glutathione conjugate reconstituted in D_2O after lyophilization. This was performed on a 500 MHz spectrometer with the following parameters: pulse width 0.15 μseconds; sweep width 6600 Hz; and, 16K data point accumulation. ^{1}H-NMR (D_2O) δ 2.08 (s, 1H, aromatic H), 2.12 (h, 2H, Glu-β H), 2.19 (s, 3H, acetyl H), 2.51 (q, 2H, Glu-γ H), 2.95 (q, 1H, Cys-β H), 3.24 (q, 1H, Cys-β' H), 3.79 (t, 2H, Glu-α H), 4.75 (t, 1H, Cys-α H), 6.63 (s, 1H, aromatic H). Interpretation of the spectrum was aided by comparison to the spectrum of 3-S-glutathionylacetaminophen. Glutathione oxidation to GSSG was found not to occur in the reaction. This was determined by monitoring NADPH oxidation at 340 nm after the addition to the reaction mixture of 0.13 mM NADPH and 0.1 U/ml glutathione reductase in 50 mM pH 7.4 sodium phosphate buffer containing 1.0 mM DETAPAC.

In the reactions of NAPQI and 3,5-dimethylNAPQI with glutathione, the products acetaminophen and 3,5-dimethylacetaminophen were identified by reverse phase HPLC of the reaction mixtures using the nonlinear gradient elution system. Oxidized glutathione was determined again by the glutathione reductase-catalyzed oxidation of NADPH by GSSG.

Studies of the Acetaminophen Semiquinone Imine Radical

Electron spin resonance studies were performed by Dr. Garth Powis, Department of Developmental Oncology, Mayo Clinic, Rochester,

MN. The instrument settings were: field set 3410 G; microwave frequency 9.375 GHz; modulation/receiver frequency 100 kHz; microwave attenuation 20 dB; and detector current 200 μA. The spectrometer was calibrated using 1.0 mM sodium hydrosulfite, or the DMPO spin trap of hydroxyl radical generated by Fenton reagent.[150] Biochemical incubations were conducted under anaerobic conditions at room temperature with a system containing NAPQI (5.0 mM), NADPH-cytochrome P-450 reductase (1.4 U/ml), and NADPH (1.0 mM) in 0.15 M KCl, 10 mM phospate buffer (pH 7.0). NAPQI (5.0 mM) was also reduced by $NaBH_4$ (3.73 mM) in both DMSO and the phosphate buffer described above.

Electron spin resonance studies in which the acetaminophen radical was detected by spin-exchange with OXANOH during the reductase metabolism of NAPQI, and in solutions of NAPQI and acetaminophen, were performed by Dr. Gerald M. Rosen, Department of Pharmacology, Duke University, Durham, NC. OXANOH was prepared by bubbling hydrogen through a 10.0 mM water solution of OXANO[151] in the presence of platinum oxide for 15 minutes.[129] The spin-exchange studies of the acetaminophen radical formed during the reduction of NAPQI by NADPH-cytochrome P-450 reductase were conducted in incubations containing NAPQI (1.0 mM), reductase (1.5 U/ml), NADPH (1.0 mM), OXANOH (1.0 mM), and SOD (5.0 μg/ml) in phosphate buffer (0.1 M, pH 7.4) containing DETAPAC (1.0 mM). Controls were performed omitting NAPQI or NADPH.

The comproportionation-derived acetaminophen radical was detected in reactions of acetaminophen (1.0 mM) with NAPQI (1.0 mM) in phosphate buffer (0.1 mM, pH 7.4) containing OXANOH (1.0 mM) and SOD (5.0 μg/ml). The control experiments lacked acetaminophen.

DMPO (5,5-dimethyl-1-pyrroline-1-oxide) was prepared according to the method of Bonnett[101] and used as a spin-trap in studies superoxide anion formation during the anaerobic reaction of acetaminophen and NAPQI. The reactions contained NAPQI (1.0 mM), acetaminophen (1.0 mM), and DMPO (10.0 mM) in phosphate buffer (0.5 ml, 0.1 M, pH 7.4). Structural verification of the superoxide adduct of DMPO was made by comparison to the spectrum obtained from the reaction of DMPO with tetramethyl ammonium superoxide.[130]

The pulse radiolysis studies were conducted by Dr. Garth Powis, Mayo Clinic, Rochester, MN, and utilized a 5 MeV Van der Graaff accelerator directing pulsed beams of electrons through a quartz cell. The sample cell contained solutions of NAPQI in potassium phosphate buffer (5.0 mM, pH 7.0, prepared using triply distilled water), and either isopropanol (0.1 M) or sodium formate (0.1 M) as hydroxyl radical scavengers. Electron pulses were calibrated by dosimetry irradiation of KSCN (10 mM) to produce the $(SCH)_2^{-\cdot}$ radical with G = 2.9 and $\varepsilon_{480} = 7.1 \times 10^3\ M^{-1}cm^{-1}$.

The UV spectrum of the acetaminophen radical was established by the irradiation of a deaerated solution of NAPQI (0.1 mM) with a known dose of electrons (5.3 μM solvated electrons) followed by time-resolved measurements of the absorbance from 280 to 500 nm at 10 nm intervals (Figure 4.25). Semiquinone imine free radicals were formed by reaction of NAPQI with solvated electrons at diffusion-controlled rates ($k = 10^{10}\ M^{-1}s^{-1}$). Rate constants for the second-order decay of the semiquinone imine radical were obtained by interactive kinetic analysis using a DEC PDP 11T34 computer system.

The rate of approach to equilibrium method was used to determine the one-electron reduction potential of NAPQI.[131,135] Solutions of 0.1 mM NAPQI and 0.1 mM duroquinone were mixed in different proportions and pulsed with electrons. The quinones were present at a combined concentration of 0.1 mM and the ratios of duroquinone/NAPQI used were: 0.2, 0.5, 1.0, 1.25, 2.0, and 5.0. After pulsing, the decay rate of the durosemiquinone radical ($DQ^{-\cdot}$) was measured at 350 nm in the equilibrium reaction shown below.

$$DQ^{-\cdot} + NAPQI \rightleftharpoons DQ + NAPQI^{-\cdot} \qquad \text{Equation 4.2}$$

The initial decay of $DQ^{-\cdot}$ toward equilibrium at different ratios of duroquinone to NAPQI was pseudo-first-order with a rate constant k_{obs} according to Equation 4.3.

$$k_{obs} = k_f[NAPQI] + k_r[DQ] \qquad \text{Equation 4.3}$$

Plotting k_{obs}/[NAPQI] against [DQ]/[NAPQI] (Figure 4.26), and from this determining k_f (intercept) and k_r (slope), the equilibrium constant for Equation 4.2 was calculated using $K_{eq} = k_f/k_r$. The difference in one-electron reduction potential at pH 7.0 (ΔE_7^1) between the NAPQI/$NAPQI^{-\cdot}$ couple and the duroquinone/durosemiquinone reference couple (-244 mV)[136] was closely approximated by Equation 4.4.

$$\Delta E_7^1 = 59 \log K_{eq} \qquad \text{Equation 4.4}$$

Similar methods were used in the calculation of the one-electron reduction potential of NAPQI using the oxygen/superoxide couple as reference. In these experiments 0.1 mM NAPQI solutions were equilibrated with mixtures of oxygen and nitrogen containing up to 80% O_2 giving [NAPQI]/[O_2] ratios ranging from 0.1 to 0.85. The concentration of oxygen was calculated based on the assumption that a solution under 1 atmosphere O_2 would equilibrate to 1.25 mM O_2, and that the concentration was linearly dependent on the partial pressure. The observed first-order rate constant (k_{obs}) was measured at 440 nm by following the increase in acetaminophen radical concentration approaching equilibrium, and plotted as k_{obs}/O_2 versus [NAPQI]/O_2 (figure 4.27). The one-electron reduction potential of NAPQI was calculated from the k_f and k_r values as previously described.

REFERENCES

1. J.A. Miller, Cancer Res., 30:559 (1970).

2. P. Sims, P.L. Grover, A. Swaisland, K. Pal, and A. Hewer, Nature, 252:326 (1974).

3. J. Kapitulnik, P.G. Wislocki, W. Levin, H. Yagi, D.M. Jerina, and A.H. Conney, Cancer Res., 38:354 (1978).

4. K. Handu, and S. Sato, Gann, 67:523 (1976).

5. N.R. Bachur, S.L. Gordon, M.V. Gee, and H. Kon, Proc. Natl. Acad. Sci., USA, 76:954 (1979).

6. E.G. Minnaugh, M.A. Trush, and T.E. Gram, Biochem. Pharmacol., 30:2797 (1981).

7. R.A. Minow, R.S. Benjamin, and J.A. Gottlieb, Cancer Chemother. Rep., 6:195 (1975).

8. S.D. Nelson, J. Med. Chem., 24:753 (1982).

9. J. von Mering, Therap. Monatash., 7:577 (1983).

10. D.M. Woodbury, and E. Fingl, in The Pharmacological Basis of Therapeutics. Edited by L.S. Goodman, and A. Gilman. New York, MacMillam, pp 343-350 (1975).

11. M. Black, Gastroenerology, 78:382 (1980).

12. O. Suhler, and H.U. Zollinger, Z. Clin. Med., 151:1 (1953).

13. T. Murray, and M. Goldberg, Ann. Rev. Med., 26:537 (1975).

14. L.F. Prescott, Br. J. Clin. Pharmacol., 7:453 (1979).

15. E.M. Boyd, and G.M. Bereczky, Br. J. Pharmacol., 26:606 (1966).

16. D.G.D. Davidson, and W.M. Eastham, Br. Med. J., 2:497 (1966).

17. G.N. Volans, J. Int. Med. Res. (suppl. 4), 4:7 (1976).

18. J.S. Thomson, L.F. Prescott, Br. Med. J., 2:506 (1966).

19. D. Maclean, T.J. Peters, R.A.G. Brown, and M. McCarthy, Lancet, 2:849 (1968).

20. P.G. Rose, Br. Med.J., 1:381 (1969).

21. E.J. Will, and A.M. Tomkins, Br. Med. J. 4:430 (1971).

22. A.J. Proudfoot, and N. Wright, Br. Med. J., 3:557 (1970).

23. L.F. Prescott, N. Wright, P. Roscoe, et al., Lancet, 1:516 (1971).

24. J. Cate, R.W. Moriarty, and B.H. Rumack, Patient Care, 13:16 (1979).

25. B.H. Rumack, and H. Matthew, Pediatrics, 55:871 (1975).

26. J.F. Groarke, J.M. Averett, and B.I. Hirschowitz, N. Engl. J. Med., 296:233 (1977).

27. E. Fernandez, and A.C. Brito-Fernandez, N. Engl. J. Med., 296:577 (1977).

28. D.R. Ferguson, S.K. Snyder, and A.J. Cameron, Mayo Clinic Proc., 52:246 (1977).

29. A.G. Noyera, and J.E. Bremner, Pediatrics, 92:832 (1978).

30. J.T. Wilson, V. Kasantikal, R. Harbison, et al., Am. J. Dis. Child, 132:466 (1978).

31. T.D. Boyer, and S.L. Rouff, J. Am. Med. Assoc., 218:440 (1971).

32. I. Cobden, C.O. Record, M.K. Ward, and D.N.S. Ken, Br. Med. J., 284:21 (1982).

33. J.R. Mitchell, S.S. Thorgeirsson, W.Z. Potter, D.J. Jollow, and H. Keiser, Clinical Pharmacol. Ther., 16:676 (1974).

34. W.Z. Potter, S.S. Thorgeirsson, D.J. Jollow, and J.R. Mitchell, Pharmacology, 12:129 (1974).

35. J.R. Mitchell, D.J. Jollow, W.Z. Potter, D.C. Davis, J.R. Gillette, and B.B. Brodie, J. Pharmacol. Exp. Ther., 187:185 (1973).

36. B.B. Brodie, W.D. Reid, A.K. Cho, G. Sipes, G. Krishna, and J.R. Gillette, Proc. Natl. Acad. Sci., USA, 68:160 (1971).

37. D.J. Jollow, J.R. Mitchell, W.Z. Potter, D.C. Davis, J.R. Gillette, and B.B. Brodie, J. Pharmacol. Exp. Ther., 187:195 (1973).

38. W.Z. Potter, D.C. Davis, J.R. Mitchell, D.J. Jollow, J.R. Gillette, and B.B. Brodie, J. Pharmacol. Exp. Ther., 187:203 (1973).

39. J.A. Hinson, S.D. Nelson, and J.R. Mitchell, Mol. Pharmacol., 13:625 (1977).

40. J.R. Mitchell, D.J. Jollow, W.Z. Potter, J.R. Gillette, and B.B. Brodie, J. Pharmacol. Exp. Ther., 187:211 (1973).

41. J.A. Hinson, Rev. Biochem. Toxicol., 2:103 (1980).

42. R. Williams, and M. Davis, Acta Pharmacol. Toxicol., 41:282 (1977).

43. D. Howie, P.I. Adriaenssens, and L.F. Prescott, J. Pharm. Pharmacol., 29:235 (1977).

44. E. Boyland, and L.F. Chasseud, Adv. Enzymol., 32:173 (1969).

45. J. A. Hinson, T.J. Monks, M. Hong, R.J. Highet, and L.R. Pohl, Drug Metab Disp., 10:47 (1982).

46. D.J. Jollow, S.S. Thorgeirsson, W.Z. Potter, M. Hashimoto, and J.R. Mitchell, Pharmacol., 12:251 (1974).

47. W.Z. Potter, D.C. Davis, J.R. Mitcell, D.J. Jollow, J.R. Gillette, and B.B. Brodie, J. Pharmacol. Exp. Ther., 187:203 (1973).

48. J.R. Mitchell, W.Z. Potter, J.A. Hinson, W.R. Snodgrass, J.A. Timbrell, and J.R. Gillette, in Handb. of Exper. Pharmacol.. Edited by J.R. Gillette, and J.R. Mitchell. Springer-Verlag, Berlin/New York, p383 (1975).

49. P.H. Grantham, E.K. Weisburger, and J.H. Weisburger, Biochem. Biophys. Acta, 107:414 (1965).

50. J.A. Hinson, J.R. Mitchell, and D.J. Jollow, Mol. Pharmacol. 11:462 (1975).

51. J.A. Hinson, and J.R. Mitchell, Drug Metab. Dispos., 4:435 (1976).

52. J.A. Miller, and E.C. Miller, in The Jerusalem Symp. on Quant. Chem. and Biochem., Vol I. Edited by E.D. Bergman, and B. Pullman. Israel Acad. Sci. Hum., p237 (1969).

53. K. Healy, I.C. Calder, A.C. Yong, C.A. Crowe, C.C. Funder, K.N. Ham, and J.D. Tange, Xenobiotica, 8:403 (1978).

54. M.W. Gemborys, G.W. Gribble, and G.H. Mudge, J. Med. Chem., 21:649 (1978).

55. J.A. Hinson, L.R. Pohl, and J.R. Gillette, Life Sci., 24:2133 (1979).

56. S.D. Nelson, A,J, Forte, and D.C. Dahlin, Biochem. Parmacol., 29:1617 (1980).

57. G.J. Mulder, J.A. Hinson, and J.R. Gillette, Biochem. Pharmacol., 26:189 (1977).

58. D.J. Miner, and P.T. Kissinger, Biochem. Pharmacol., 28:3285 (1979).

59. I.A. Blair, A.R. Boobis, and D.S. Davies, Tet. Lett., 31:4947 (1980).

60. A.C. Huggett, A.R. Boobis, D.S. Davies, and I.A. Blair, Free Communication 3, BTS Meeting, Kent Sept. 1981.

61. D.C. Dahlin, and S.D. Nelson, J. Med. Chem., 25:885 (1982).

62. D.C. Dahlin, G.T. Miwa, A.Y.H. Lu, and S.D. Nelson, Proc. Natl. Acad. Sci., USA, in print.

63. J.H. Knox, and J. Jarand, J. Chromatog., 149:297 (1978).

64. A. Focella, R.Heslin, and D.Teitel, Can. J. Chem., 50:2025 (1972).

65. R.E. Andrews, C.C. Bond, J. Burnett, A. Saunders, and K. Watson, J. Int. Med. Res. (suppl. 4), 4:34 (1978).

66. M. Davis, D. Labadarios, and R.S. Williams, J. Int. Med. Res. (suppl. 4), 4:40 (1976).

67. S.D. Nelson, D.C. Dahlin, E.J. Rauchman, and G.M. Rosen, Mol. Pharmacol., 20:195 (1981).

68. G. Powis, B.A. Svingen, D.C. Dahlin, and S.D. Nelson, Biochem. Pharmacol., in print.

69. G.M. Rosen, E.J. Rauckman, S.P. Ellington, D.C. Dahlin, and S.D. Nelson, Mol. Pharmacol.,in print.

70. J.A. Holme, D.C. Dahlin, S.D. Nelson, and E. Dybing, Biochem. Pharmacol., in print.

71. A.J. Streeter, D.C. Dahlin, S.D. Nelson, T.A. Baillie, Biochem. Pharmacol., in print.

72. R.J. McMurtry, W.R. Snodgrass, and J.R. Mitchell, Toxicol. Appl. Pharmacol., 46:87 (1978).

73. R.S. Andrews, Sterling Winthrop Laboratories, U.K., personal communication.

74. D.M. Jerina, J.W. Daly, B. Wittkop, P. Zaltzman-Nirenberg, and S. Undenfriend, Biochem., 9:147 (1970).

75. C. Wheeler, Ph.D. Dissertation, University of Washington, Seattle, WA.

76. O. Lowry, N.J. Rosenbrough, A.L. Farr, and R.J. Randall, J. Biol. Chem., 193:165 1951.

77. G.L. Miller, Anal. Chem., 31:964 (1959).

78. A.H. Beckett, in Biological Oxidation of Nitrogen, edited by J.W. Gorrod, Elsevier, Amsterdam, 1978, p 3.

79. J.T. Groves, G.A. McClusky, R.E. White, and M.J. Coon, Biochem. Biophys. Res. Comm., 81:154 (1978).

80. O. Augusto, H.S. Beilan, and P.R. Ortiz de Montellano, J. Biol. Chem., 257:11288 (1982).

81. H.B. Dunford, J.S. Stillman, Coord. Chem. Rev., 19:187 (1976).

82. W.D. Hewson, L.P. Hager, in The Porphyrins, vol. 7,edited by D. Dolphin, Academic Press, New York, 1979, pp 295-332.

83. E.G. Janzen, and J.I.-P. Liu, J. Mag. Res., 9:510 (1973).

84. S.D. Nelson et al., unpublished results.

85. J.A. Hinson, and J.R. Mitchell, Fed. Proc., 39:743 (1980).

86. S.D. Nelson, A.J. Forte, and R.J. McMurtry, Res. Comm. Chem. Pathol. Pharmacol., 22:61 (1978).

87. J.A. Hinson, S.D. Nelson, and J.R. Mitchell, Mol. Pharmacol., 13:625 (1977).

88. E.G. Hrycay, and P.J. O'Brien, Arch. Biochem. Biophys., 153:480 (1972).

89. G.D. Nordblom, R.E. White, and M.J. Coon, Arch. Biochem. Biophys., 175:524 (1976).

90. A.D. Rahimtula, P.J. O'Brien, E.G. Hrycay, J.A. Peterson, and R.W. Eastabrook, Biochem. Biophys. Res. Commmun., 60:695 (1974).

91. R.E. White, and M.J. Coon, Ann. Rev. Biochem., 49:315 (1980).

92. K.G. Paul, inThe Enzymes, vol 8, edited by P.D. Boyer, H. Lardy, and K. Myrback, Academic Press, New York, 1963, pp 227-274.

93. B.W. Griffin, Arch. Biochem. Biophys., 190:850 (1978).

94. E.G. Hrycay, J.-A. Gustafsson, M. Ingelman-Sundberg, and L. Ernster, Biochem. Biophys. Res. Commun., 66:209 (1975).

95. M.J. Coon, R.E. White, and R.C. Blake, in Oxidases and Related Redox Systems, edited by T.E. King, H.S. Mason, and M. Morrison, University Park Press, Baltimore, 1979.

96. D. Dolphin, A. Forman, D.C. Borg, J. Fajer, and R.H. Felton, Proc. Natl. Acad. Sci., USA, 68:614 (1971).

97. R.C. Blake, and M.J. Coon, Fed. Proc., 38:319 (1979).

98. G.A. Hamilton, in Molecular Mechanisms of Oxygen Activation, edited by O. Hayaishi, Academic Press, New York, 1974, pp 405-451.

99. R.P. Mason, in Reviews in Biochemical Toxicology, vol I, edited by E. Hodgson, J.R. Bend, and R.M. Philpot, Elsevier/North Holland, New York, 1979, pp 151-200.

100. A.R. Buckpitt, D.E. Rollins, S.D. Nelson, R.B. Franklin, and J.R. Mitchell, Anal. Biochem., 83:168 (1977).

101. R. Bonnett, F.C. Brown, V.M. Clark, O. Sutherland, and A. Todd, J. Chem. Soc. (Lond.), 2094 (1959).

102. C.R. Fernando, J,C, Calder, and K.M. Ham, J. Med. Chem., 23:1153 (1980).

103. R. Medola, and W.F. Holley, J. Chem. Soc., 105:2073 (1914).

104. G.J. Mulder, J.A. Hinson, and J.R. Gillette, Biochem. Pharmacol., 27:1641 (1978).

105. I.C. Calder, M.J. Creek, P.J. Williams, C.C. Funder, C.R. Green, K.N. Ham, and J.D. Tange, J. Med. Chem., 16:499 (1973).

106. G.B. Corcoran, J.R. Mitchell, Y.N. Vaishnav, and E.C. Horning, Molec. Pharmacol., 18:536 (1980).

107. M.W. Gemborys, G.H. Mudge, and G.W. Gribble, J. Med. Chem., 23:304 (1980).

108. I.C. Calder, S.J. Hart, K. Healey, and K.N. Ham, J. Med. Chem., 24:988 (1981).

109. R. Willstattor, and A. Pfarnenstiel, Ber., 61: 3467 (1939).

110. L. Fieser, and M. Fieser, Reagents for Organic Synthesis, John Wiley and Sons, 1967, pp 1101-1015.

111. K.L. Laidler, Reaction Kinetics, vol I, Pergamon Press, New York, 1963, p 179.

112. E.J. Rosenbaum, Physical Chemistry, Appleton-Century-Crofts, New York, 1970, p 401.

113. T.C. Bruice, Proc. Natl. Acad. Sci., USA, 79:4604 (1982).

114. G.L. Long, and J.D. Wineforder, Anal. Chem., 55:713A (1983).

115. P. Moldeus, Biochem. Pharmacol., 27:2859 (1978).

116. S.D. Nelson, A.J. Forte, Y. Vaishnav, J.R. Mitchell, J.R. Gillette, and J.A. Hinson, Molec. Pharmacol., 19:140 (1981).

117. P. Segler, Methods Cell Biol., 13:29 (1975).

118. B. Sandstrom, Exp. Cell Res. , 37:552 (1965).

119. J.A. Hinson, L.R. Pohl, T.J. Monks, and J.R. Gillette, Life Sci., 29:107 (1981).

120. F. Tietze, Anal. Biochem., 27:502 (1969).

121. J.A. Holme, P.J. Wirth, E. Dybing, and S.S. Thorgeirsson, Acta Pharmacol. Toxicol., 51:87 (1982).

122. J.A. Holme, P.J. Wirth, E. Dybing, and S.S. Thorgeirsson, Acta Pharmacol. Toxicol., 51:96 (1982).

123. N.H. Stacey, L.R. Cantilena, and C.D. Kaassen, Toxicol. Appl. Pharmacol., 53:470 (1980).

124. R. Reiter, and A. Wendel, Biochem. Pharmacol., 32:665 (1983).

125. A. Wendel, S. Feurstein, and K.-H. Konz, Biochem. Pharmacol., 28:2051 (1979).

126. G. Powis, and P.L. Appel, Biochem. Pharmacol., 29:2567 (1980).

127. N.S. Kosower, E.M. Kosower, Int. Rev. Cytol., 54:109 (1978).

128. G.M. Rosen, E.J. Rauchman, and K.W. Hanck, Toxicol. Lett., 1:71 (1977).

129. E.G. Rozantsev, Free Nitroxyl Radicals, Plenum Press, New York, 1970, pp 93-99.

130. G.M. Rosen, E.Finkelstein, and E.J. Rauckman, Arch. Biochem. Biophys., 215:367 (1982).

131. B.A. Swingen, and G. Powis, Arch. Biochem. Biophys., 209:119 (1981).

132. B.H.J. Bielski, and J.M. Gebicki, in Free Radicals in Biology, vol I, edited by W.A. Pryor, Academic Press, New York, 1977, pp 1-51.

133. K.B. Patel, and R.L Wiison, J. Chem. Soc. Lond. Faraday Trans., 69:814 (1973).

134. T. Iyanagi, and I. Yamazaki, Biochem. Biophys. Acta, 172:370 (1969).

135. P. Wardman, and E.P. Clarke, J. Chem. Soc. Lond. Faraday Trans. 1, 72:1377 (1976).

136. G.E. Adams, and P. Wardman, in Free Radicals in Biology, vol III, edited by W.A. Pryor, Academic Press, New York, 1977, pp 53-95.

137. J.S. Bus, and J.E. Gibson, in Reviews in Biochemical Toxicology, vol I, edited by E. Hodgson, J. R. Bend, and R.M. Philpot, Elseier/ North-Holland, New York, 1979, pp 125-150.

138. R.J. McMurtry, personal communication.

139. B.H. Lauterburg, G.B. Corcoran, and J.R. Mitchell, J. Clin. Invest., 71:980 (1983).

140. L.T. Wong, L.W. Whitehorse, G. Solomonraj, and C.J. Paul, Toxicology, 17:297 (1980).

141. G. Bellomo, S.A. Jewell, H. Thor, and S. Orrenius, Proc. Natl. Acad. Sci., USA, 79:6842 (1982).

142. S.A. Jewell, G. Bellomo, H. Thor, S. Orrenius, and M.T. Smith, Science, 217:1257 (1982).

143. D.P. Jones, H. Thor, M.T. Smith, S.A. Jewell, and S. Orrenius, J. Biol. Chem., 258:6390 (1983).

144. A. Wendel, and S. Feuerstein, Biochem. Pharmacol., 30:2513 (1981).

145. K.P. Zeller, in Chemistry of the Quinonoid Compounds, part I, edited by S. Patai, Wiley, New York, 1974, p 231.

146. U. Yasukochi, and B.S.S. Masters, J. Biol. Chem., 251:5337 (1976).

147. A.H. Philips, and R.E. Langdon, J. Biol. Chem., 237:2652 (1962).

148. S.B. West, M.T. Huang, G.T. Miwa, and A.Y.H. Lu, Arch. Biochem. Biophys., 193:42 (1979).

149. G.T. Miwa, S.B. West, M.T. Huang, and A.Y.H. Lu, J. Biol. Chem., 254:5695 (1979).

150. E. Finkelstein, G.M. Rosen, E.J. Rauckman, and J. Paxton, Mol. Pharmacol., 16:676 (1979).

151. G.M. Rosen, E.J. Rauckman, and K.W. Hank, Toxicol. Lett., 1:71 (1977).

VITA

David C. Dahlin was born January 14, 1954 in Seattle, Washington, and is the eldest of four children raised by Clyde and Jean Dahlin. He attended elementary through high school in Montesano, Washington, graduating in 1972. After working one year as a carpenter and laborer, he enrolled at Grays Harbor College where he graduated fifth in his class of 1975. He obtained his Bachelor of Science in Chemistry from Central Washington University in Ellensberg, and entered the Department of Pharmaceutical Sciences at the University of Washington in 1978. Under the guidance of Professor Sidney D. Nelson he completed his studies in 1983, and accepted a position with the Medical Research Division of American Cyanamid in Pearl River, New York.